DYNAMIC PROBABILISTIC RISK ASSESSMENT OF NUCLEAR POWER GENERATION STATIONS

DYNAMIC PROBABILISTIC RISK ASSESSMENT OF NUCLEAR POWER GENERATION STATIONS

By

Mohamed Hamdi Mohamed Elsefy

BSc., M.Sc.

A Thesis Submitted to the School of Graduate Studies in Partial Fulfillment of the Requirements for the Degree

Doctor of Philosophy

Doctor of Philosophy (2021)	McMaster University
(Civil Engineering)	Hamilton, Ontario
TITLE:	Dynamic Probabilistic Risk Assessment of Nuclear Power Generation Stations
AUTHOR:	Mohamed Hamdi Mohamed Elsefy BSc., MSc. (Ain Shams University)
SUPERVISORS:	Dr. Wael El-Dakhakhni Dr. Lydell Wiebe
NUMBER OF PAGES:	xxv, 230

Dedications

To Hamdi Elsefy & Azza Mohamed,

Ahmed & Amira,

Mohamed, Aya & Adam

Abstract

Risk assessment is essential for nuclear power plants (**NPPs**) due to the complex dynamic nature of such systems-of-systems, as well as the devastating impacts of nuclear accidents on the environment, public health, and economy. Lessons learned from the Fukushima nuclear accident demonstrated the importance of enhancing current risk assessment methodologies and developing efficient early warning decision support tools. *Static* probabilistic risk assessment (**PRA**) techniques (e.g., event and fault tree analysis) have been extensively adopted in nuclear applications to ensure NPPs comply with safety regulations. However, numerous studies have highlighted the limitations of static PRA methods such as the lack of considering the dynamic hardware/software/operator interactions inside the NPP and the timing/sequence of events. In response, several *dynamic* probabilistic risk assessment (**DPRA**) methodologies have been developed and continuously evolved over the past four decades to overcome the limitations of static PRA methods. DPRA presents a comprehensive approach to assess the risks associated with complex, dynamic systems. However, current DPRA approaches are faced with challenges associated with the intra/interdependence within/between different NPP complex systems and the massive amount of data that needs to be analyzed and rapidly acted upon.

In response to these limitations of previous work, the main objective of this dissertation is to develop a physics-based DPRA platform and an intelligent data-driven prediction tool for NPP safety enhancement under normal and abnormal operating conditions. The results of this dissertation demonstrate that the developed DPRA platform is capable of simulating the dynamic interaction between different NPP systems and estimating the temporal probability of core damage under different transients with significant analysis advantages from both the

computational time and data storage perspectives. The developed platform can also explicitly account for uncertainties associated with the NPP's physical parameters and operating conditions on the plant's response and probability of its core damage. Furthermore, an intelligent decision support tool, developed based on artificial neural networks (ANN), can significantly improve the safety of NPPs by providing the plant operators with fast and accurate predictions that are specific to such NPP. Such rapid prediction will minimize the need to resort to idealized physics-based simulators to predict the underlying complex physical interactions. Moving forward, the developed ANN model can be trained under plant operational data, plants operating experience database, and data from rare event simulations to consider for example plant ageing with time, operational transients, and rare events in predicting the plant behavior. Such intelligent tool can be key for NPP operators and managers to take rapid and reliable actions under abnormal conditions.

Acknowledgement

I would like to express my sincere appreciation to Dr. Wael El-Dakhakhni, Dr. Lydell Wiebe, Dr. Shinya Nagasaki, Dr. Mohamed Ezzeldin, Dr. Ahmed Yosri, Dr. Ahmed Siam, and Dr. Zoe Li for their continuous help and guidance all the way during my study. A very special thanks to Dr. El-Dakhakhni for his continuous support and encouragement through my research.

Special thanks are due to my brothers, before being friends, in McMaster: Ahmed Yassin, Ahmed Yosri, Ahmed El-Sayed, Ahmed Gondia, Ahmed Salah, Ahmed Ragai, Ayman Farid, Shady Salem, Maysara Ghaith, Mahmoud Madany, Mohamed Gamal, Mohamed Elganzory, Tarek El-Hashimy, and Yassien Salaheldin. I also want to thank my peers and colleagues: Ahmed Ghith, Eric Goforth, Mohamed Khafagy, Feras Alsheet, Mostafa Naiem, Mostafa Medra, Ahmed Ali, Mohamed Abdelnabi, Mostafa Yakout, and Brinda Narayanan.

I owe special thanks to my friends Ahmed Samy, Ayman Hendawy, Amr Abdo, Maged Kamal, Mohamed Abugazia, Mahmoud Eid, Taher El-tayeb, and my sisters before being a friend Aliaa Hamam, Heba Gamal, Laila Ahmed and Shimaa Nassif.

Special thanks are due to my colleagues, in Bruce Power, Tetra Tech, and Next Structural Integrity: Fouad Kelada, Waleed Mekky, Ahmed Ashour, Nader Aly, Sue Chang, Revi Kizhatil, Mohammed Albutainy, Mohamed Hamda, Mohamed Saifelislam, Mazher Burhan, Mostafa Siam, Taher Abu Seer.

Finally, I can find no words to express my sincere gratitude to my family: Hamdi Elsefy, Azza Mohamed, Ahmed Hamdi, Amira Hamdi, Mohamed Sabry, Aya Hamdi, and Adam Mohamed, to whom I would dedicate my work, for their love and unconditional support.

Table of Contents

List of Figures

List of Tables

Acronym List

AI	Artificial Intelligence
ADAPT	Analysis of Dynamic Accident Progression Trees
ADS	Accident Dynamic Simulator
ANN	Artificial Neural Network
APET	Accident Progression Event Trees
CG	Conjugate Gradient Algorithms
CPU	Central Processing Unit
DBA	Design Basis Accidents
DBNs	Dynamic Bayesian Networks
DDET	Discrete Dynamic Event Tree
DDM	Data-Driven Model
DETAM	Dynamic Event Tree Analysis Method
DFM	Dynamic Flowgraph Method
DFT	Dynamic Fault Tree
DPRA	Dynamic Probabilistic Risk Assessment
DSA	Deterministic Safety Assessment
DSS	Decision Support System
DYLAM	Dynamic Logic Analytical Methodology
ESD	Event Sequence Diagram
ET	Event Tree
FT	Fault Tree
GD	Gradient Descent Algorithms

IAEA	International Atomic energy Agency
IDAC	Information, Decision, and Actions in a Crew context
INL	Idaho National Laboratory
I&C	Instrumentation and Control System
LDA	Latent Dirichlet Allocation
Markov-CCMT	Markov/Cell-to-Cell Mapping Technique
MC	Monte Carlo
MCDET	Monte Carlo Dynamic Event Tree
MSE	Mean Squared Error
NPP	Nuclear Power Plant
PCC	Partial Correlation Coefficient
pdf	Probability Density Function
PN	Petri Net
PRA	Probabilistic Risk Assessment
PWR	Pressurized Water Reactor
QN	Quasi-Newton Algorithms
RAVEN	Reactor Analysis and Virtual Control Environment
RPV	Reactor Pressure Vessel
SD	System Dynamics
SCS	Secondary Coolant System
SNL	Sandia National Laboratories
TM	Text Mining

Declaration of Academic Achievement

This dissertation was prepared following the guidelines set by the school of graduate studies at McMaster University for the sandwich thesis format. This dissertation presents the work carried out solely by Mohamed Elsefy, where technical advice and guidance were provided for the whole thesis by Drs. Wael El-Dakhakhni, Lydell Wiebe, Shinya Nagasaki, Mohamed Ezzeldin, Ahmed Yosri, and Ahmed Siam. Four papers were prepared in this dissertation and presented in chapters 2, 3, 4, and 5. The research paper presented in Chapter 3 is already published in *Nuclear Engineering and Technology*, whereas Chapters 2, 4, and 5 have been submitted for publication as journal articles. The original contributions of the author to each paper (Chapter) in this dissertation are outlined below:

Chapter 2: Mohamed El-Sefy, Mohamed Ezzeldin, Wael El-Dakhakhni, Lydell Wiebe, and Shinya Nagasaki. "**Dynamic Probabilistic Risk Assessment of Nuclear Power Plates: State-of-the-Art Review using text Mining.**" Submitted to Nuclear Engineering and Design Journal in February 2021.

Mohamed El-Sefy planned the article, conducted the text mining analysis and prepared the manuscript. The manuscript was then reviewed and edited by Drs. Mohamed Ezzeldin, Wael El-Dakhakhni, Lydell Wiebe, and Shinya Nagasaki.

Chapter 3: Mohamed El-Sefy, Mohamed Ezzeldin, Wael El-Dakhakhni, Lydell Wiebe, and Shinya Nagasaki. 2019. "**System Dynamics Simulation of the**

Thermal Dynamic Processes in Nuclear Power Plants." Nuclear Engineering and Technology Journal, https://doi.org/10.1016/j.net.2019.04.017.

Mohamed El-Sefy envisioned the study and developed a deterministic model to simulate the thermal dynamic processes in nuclear power plants (**NPPs**). The manuscript was reviewed and edited by Drs. Mohamed Ezzeldin, Wael El-Dakhakhni, Lydell Wiebe, and Shinya Nagasaki.

Chapter 4: Mohamed El-Sefy, Ahmed Yosri, Ahmed Siam, Wael El-Dakhakhni, Lydell Wiebe, and Shinya Nagasaki. "**Dynamic Probabilistic Risk Assessment of Core Damage under Different Transients using System Dynamics Simulation Approach.**" Submitted to Nuclear Engineering and Technology Journal in December 2020.

Mohamed El-Sefy developed the DPRA platform described in this article and prepared the manuscript. The manuscript was then reviewed and edited by Drs. Ahmed Yosri, Ahmed Siam, Wael El-Dakhakhni, Lydell Wiebe, and Shinya Nagasaki.

Chapter 5: Mohamed El-Sefy, Ahmed Yosri, Wael El-Dakhakhni, Shinya Nagasaki, and Lydell Wiebe. "**Artificial Neural Network for Predicting Nuclear Power Plant Dynamic Behavior.**" Submitted to Nuclear Engineering and Technology Journal in November 2020.

Mohamed El-Sefy created a data-driven tool for NPP operation decision support using an artificial neural network. Mohamed El-Sefy prepared the

manuscript that was reviewed and edited by Drs. Ahmed Yosri, Wael El-Dakhakhni, Lydell Wiebe, and Shinya Nagasaki.

Chapter 1 : INTRODUCTION

1.1. BACKGROUND AND MOTIVATION

Nations across the globe have been harnessing nuclear energy to fulfill their demands for electrical power. According to the World Nuclear Association, the *Harmony* programme has been established with the aim of adding 1,000 gigawatts by 2050 in order to meet the ever increasing global demand for electricity (World Nuclear Association 2018). Currently, 448 nuclear power reactor units are operational worldwide and provide more than 10% of the global electricity (World Nuclear Association 2019). In addition, around 150 and 57 reactor units are currently under planning and construction, respectively (Canadian Nuclear Association 2019). A nuclear power plant (**NPP**) is a complex system-of-systems that includes the reactor core, secondary cooling, primary heat transport, condenser cooling, shutdown cooling, and emergency core cooling systems, each with its own distinctive functions. All such NPP systems interact dynamically during normal operation to ensure safe and continuous electricity supply. The effective operation and control of a NPP require a full understanding of the component- and system-level behaviors, as well as the dynamic interaction/interdependence between the plant subsystems under normal and abnormal operating conditions. However, accidents attributed to unexpected operation or external hazards can have catastrophic consequences. For example, the Fukushima Daiichi NPP accident resulted in a core meltdown of three nuclear reactor units and a massive release of

radioactive material into the environment (Chino et al. 2011). It is thus more essential now than ever before to ensure the safety of NPPs, as they become more complex, dynamic, and interdependent.

Major catastrophic NPP accidents that took place over the past few decades (e.g., Three Mile Island, Chernobyl, and Fukushima Daiichi) have highlighted the need for risk assessment methodologies. Probabilistic risk assessment (**PRA**) techniques have significantly evolved over the past four decades. Traditionally, PRA has been performed using *static* event and fault tree (**ET/FT**) analysis. Although such methods have been applied successfully in different disciplines (e.g., oil and gas industry, chemical industry), several studies (Aldemir 2013; Amendola and Reina 1981; Hofer et al. 2002a; Hsueh and Mosleh 1996; Mercurio et al. 2009; Siu 1994; Zio 2014) have demonstrated several associated limitations, especially when ET/FT analyses are applied to complex dynamic systems such as NPP. Key limitations include the inability to account for the dynamic interaction between different components, software, and operators (Hu 2005). In NPPs, the uncertain nature of the physical parameters, operating conditions, and accident propagation necessitates conducting the risk assessment within a dynamic stochastic framework in order to efficiently capture the interactions amongst the plant subsystems. As such, *dynamic* PRA (**DPRA**) approaches are desired to consider the dynamic interaction between the different subsystems in NPPs, as well as the dynamic accident propagation.

In the environment of a NPP, operators, decision-makers, and consultants need to consider many aspects to assess the risk associated with the plant operation. A rapid decision support system (**DSS**) can support NPP operators with an early warning to mitigate the risks posed by operational transients and accidents. Lessons learned from the Fukushima nuclear accident demonstrated the necessity of having adequate monitoring systems for pre-accident operation and management processes (IAEA 2015). Strategic NPP decision-making is challenging because of the highly interdependent complex dynamical subsystems within the NPP. Artificial intelligence (**AI**) techniques have been utilized to develop intelligent DSS in many fields, in which a large amount of data is analyzed in order to provide faster and more accurate and effective decisions— creating a possibility to radically empower decision-making within NPP environments (Filip 2008; Phillips-Wren 2013).

1.2. RISK ASSESSMENT OF NUCLEAR POWER PLANTS

PRA techniques are used to assess the risk of NPPs under normal and abnormal operating conditions and when the system is subjected to natural or anthropogenic hazards (CNSC 2014; IAEA 2001). Static ET/FT analysis methods were originally presented within one of the earliest comprehensive PRA platforms, WASH-1400 (U.S. NRC 1975). In NPPs, PRA is a thought process used to estimate three basic NPP risk levels (Hakobyan 2006). Level 1 PRA estimates the risk of severe reactor core damage, in which the plant response is evaluated under different types of postulated initiating events and subsequent accident sequences. These accident scenarios, including both successes and failures (i.e., core damage), can be

represented through ET analysis. On the other hand, FT analysis is used to determine the probability of the system failure based on the logical combination of component and software failures together with human errors. In Level 2 PRA, plant responses to Level 1 PRA are evaluated based on accident sequences that result in core damage and subsequent release of radioactive materials from the containment to the environment. Level 3 PRA estimates the impact of radioactive material releases on the public health and economy. In addition, the use of ET/FT analyses provides a qualitative insight on beyond-design-basis risk scenarios, which can subsequently be used to enhance the NPP design and operation conditions.

Numerous concerns have been raised regarding the capability of static ET/FT analysis methods to adequately account for the time and sequence of events during the nonlinear dynamic components/software/operators interactions (Nejad-Hosseinian 2007). For example, ET/FT analysis methods cannot account for time delays in the activation of safety systems, which may affect the accident propagation. In addition, these methods neglect the feedback mechanisms between NPP physical processes and the system logic (e.g., the behaviors of components and operators) (Hsueh and Mosleh 1996) which result in a highly nonlinear behavior. Furthermore, in static ET/FT, the order of events is prespecified by the analyst (Mandelli et al. 2013b; Zio 2014). This may limit the ability to capture new events that might be overlooked by the analyst (Swaminathan and Smidts 1999a). Thus, the PRA analysis quality, based on ET/FT methods, is entirely analyst dependant (Jankovsky et al. 2018a). Overall, ET/FT analysis methods fail to

reliably evaluate the risk when the dynamic interaction between components, physical plant processes, and operators is of the highest importance. Previous studies (Hu 2005; Mercurio et al. 2009; Nivolianitou et al. 1986; Siu 1994; Zio 2014) have highlighted the importance of considering event times during components/software/operators interactions because the nonlinear dynamic nature of the system parameters may affect the accident propagation. Siu (1994) indicated that PRA limitations can influence the probability of event occurrence, resulting in an unreliable risk assessment. Therefore, limitations of *static* ET/FT methods, combined with recent NPP accidents, have highlighted the need for developing more reliable risk assessment methods to better assure the safety of NPPs.

Amendola and Reina (1981) presented the first step towards the development of a DPRA, which is referred to as *"Event sequences and consequence spectrum."* This approach integrates the states of the system with its physical response in order to investigate the temporal accident sequence and the corresponding probability of occurrence. DPRA of NPPs was subsequently envisioned as the integration of NPP simulation codes (Cojazzi 1996; Smidts 1994) and stochastic processes (Acosta and Siu 1993; Cojazzi 1996; Hofer et al. 2002a; Hsueh and Mosleh 1996; Mandelli et al. 2013b, 2018; Rabiti et al. 2012), in which the stochastic processes include the random failure of subsystems/components (Mandelli et al. 2018) and human intervention with NPP system dynamics (Hu 2005). Accordingly, several DPRA methods have been developed over the past few decades to evaluate the risks within NPPs. These methods represented the event temporal sequence with branching

occurring when a critical variable of the NPP system (e.g., the thermal-dynamic process of the primary loop variables, component states, or operator response) changes (Hsueh and Mosleh 1996). However, recent studies (e.g., Jankovsky et al. 2018; Mandelli et al. 2013, 2017; Manselli et al. 2013; Varuttamaseni 2011) identified new challenges pertaining to the application of DPRA approaches to simulating large complex systems in NPPs including: excessive computational time, massive data to be analyzed, as well as the limited application of DPRA in multi-unit stations, thus highlighting the need to address such challenges to ensure NPP safety (Mandelli et al. 2013b, 2018; Varuttamaseni 2011).

1.3. METHODS AND APPROACHES

As discussed above, extensive research efforts have been conducted to develop effective DPRA methodologies able to consider the dynamic interaction between the different subsystems in NPPs. Such studies provided valuable resources that can be analyzed in order to identify trends in DPRA methodologies and highlight the ongoing evolution and challenges. Text mining provides an efficient quantitative analysis approach that can be used to explore key topics in unstructured datasets (e.g., text). The Latent Dirichlet Allocation (**LDA**) topic modeling and N-Gram text classification are selected in this thesis to identify the main topics related to both DPRA simulation and graphical methodologies, and to identify associated promising methodologies. In addition, a qualitative literature review is performed to investigate the main challenges facing the current DPRA methodologies,

highlighting the necessity of developing a more efficient DPRA platform that can overcome the current limitations of DPRA and enhance the overall safety of NPPs.

The first and key step towards developing a DPRA platform is analyzing the physical response of the plant following an initiating event. The DPRA platform developed in this study is based on physics-based simulation models. System dynamics (**SD**) is a comprehensive modeling technique used to simulate the nonlinear dynamic behavior of complex systems, in which the first-order differential equations governing the system are solved numerically. SD was developed by the mid of 1950s by Jay Forrester (Forrester 1971) to simulate complex social and economic systems. Feedback loops are key in the SD models, and are used to simulate the interdependence between the system components such that the nonlinear dynamical nature of the system can be effectively captured (Sterman 2000). A deterministic SD model is first developed in this study to simulate the thermal dynamic processes inside the pressurized water reactor (**PWR**) subsystems, including the reactor core, primary and secondary cooling systems, hot and cold legs, reactor core inlet and outlet plenums, and steam generator inlet and outlet plenums. The developed model simulates the nonlinear dynamic interactions among these subsystems, in which the PWR subsystem parameters are adopted from the Palo Verde Nuclear Generating Station (Arda 2013). Uncertainties associated with the PWR physical parameters and operating conditions are subsequently considered. Such uncertainties are essential for evaluating the risk associated with design-basis transients. The efficiency of the developed DPRA

platform is demonstrated through assessing its ability to estimate the temporal probability of core damage under different transients.

Finally, AI is adopted to develop an early warning system that can support the plant operators with a fast and accurate DSS. Feed-forward back propagation artificial neural network (**ANN**) is one of the most popular data-driven modeling (**DDM**) tools that rely on AI to learn automatically based on patterns in data. As such, an ANN model is developed in this study based on the responses of a PWR subsystems under 32 different transients. The developed ANN provides an early warning tool that is able to predict the dynamic response of the critical parameters of a PWR system in a quick, reliable and effective manner.

1.4. RESEARCH OBJECTIVES

The main goals of the work in this dissertation are to: *i*) develop an integrated SD platform for the DPRA of NPPs that can aid in enhancing the safety of NPPs by overcoming the limitations of simulating the dynamic interaction among several large complex systems; and, *ii*) develop an intelligent early warning decision tool to aid in the development of effective risk mitigation strategies under abnormal conditions. As such, the following specific objectives are defined:

- Identify main literature topics in DPRA simulation and graphical methodologies that show promise for risk assessment of NPPs, as well as highlight the evolution and development of DPRA methodologies and the main challenges facing the DPRA approach.

- Develop a deterministic model to simulate the dynamic interaction between the different NPP subsystems.
- Develop a DPRA simulation platform that can efficiently simulate the dynamic interaction between large subsystems in NPPs, considering uncertainties in the plant physical parameters and operating conditions.
- Evaluate the temporal probability of reactor core damage under different transients.
- Develop an intelligent DSS for rapid decision making to overcome computational burdens and calibration (using actual plant operational conditions) of physics-based models.

The developed DPRA platform is conducted under the following general assumptions (additional assumptions are highlighted in specific sections where applicable):

- Several parameters are used to describe the physical processes and operating conditions in the considered PWR, in which the nominal values of these parameters were chosen based on those of the Palo Verde Nuclear Generating Station.
- Based on a review of previous studies, twenty-six parameters are assumed to follow a normal distribution, whereas seven parameters are assumed to follow a uniform distribution as a conservative assumption.

- The average fuel temperature is related to the probability of the reactor core damage, where the lower and upper limits of the average fuel temperature are assumed to be 1,600^{o}F [871^{o}C] and 2,600^{o}F [1426^{o}C], respectively.

1.5. THESIS ORGANIZATION

This section summarizes the content of each of the six chapters in this dissertation. **Chapter 1** provides the research need background, overview of SD simulation approach, research objectives, and a description of the thesis organization.

Chapter 2 provides quantitative analysis and qualitative literature review of published articles that discussed the main topics in DPRA methodologies for NPPs. Text mining is utilized to identify the relevant information within 387 articles published in approximately 50 different journals and conferences, providing a quantitative evaluation. LDA topic modeling and N-Gram text classification model are subsequently applied to identify the main topics in DPRA simulation and graphical methodologies. This chapter also qualitatively identifies the main challenges facing the DPRA approach that need to be considered in future studies. The obtained results showed the need to improve or develop new DPRA methodologies in order to enhance the overall safety of NPPs.

Chapter 3 provides the first and key step towards developing an integrated DPRA platform for NPPs. A deterministic model simulating thermal dynamic processes in a PWR is developed to account for the dynamic interactions inside the PWR. SD is utilized to simulate the nonlinear dynamic feedback mechanisms between the different subsystems within the PWR. The developed SD model is

validated using results from other published work. Furthermore, the developed PWR SD model are evaluated under different transients to investigate the dynamic response of the PWR critical parameters.

Chapter 4 presents the newly developed DPRA platform for NPPs. This platform overcomes the limitations of current DPRA methodologies in simulating large complex systems and provides significant advantages from both the time and data storage perspectives. Uncertainties associated with the physical parameters and plant operating conditions are considered while evaluating the temporal probability of core damage under different transients. A global sensitivity analysis is conducted to identify the uncertain PWR input parameters that have a significant impact on the core damage risk.

Chapter 5 discusses the development of an AI-based tool that can rapidly predict the response of critical PWR parameters, and thus serve as an intelligent DSS. An ANN is therefore trained based on the results of several transients and eight different training functions. The results of the ANN are compared to those of the SD model discussed in **Chapters 3 and 4**. The mean squared error and central processing unit time are used to evaluate the performance of the developed ANNs. The developed ANN efficiently predict the dynamic response of the critical PWR parameters, and thus can serve as a rapid early warning tool.

Finally, **Chapter 6** provides a summary of this research, the overall conclusions, and suggestions for future work.

1.6. REFERENCES

Acosta, C., and Siu, N. (1993). "Dynamic event trees in accident sequence analysis: application to steam generator tube rupture." *Reliability Engineering and System Safety*, 41(2), 135–154.

Aldemir, T. (2013). "A survey of dynamic methodologies for probabilistic safety assessment of nuclear power plants." *Annals of Nuclear Energy*, Elsevier Ltd, 52, 113–124.

Amendola, A., and Reina, G. (1981). "Event sequences and consequence spectrum: a methodology for probabilistic transient analysis." *Nuclear Science and Engineering*, 77, 297–315.

Arda, S. (2013). "Implementing a Nuclear Power Plant Model for Evaluating Load-Following Capability on a small Grid." MASc Thesis, Arizona State University.

Canadian Nuclear Association. (2019). *The Canadian Nuclear Factbook*.

Chino, M., Nakayama, H., Nagai, H., Terada, H., Katata, G., and Yamazawa, H. (2011). "Preliminary Estimation of Release Amounts of 131 I and 137 Cs Accidentally Discharged from the Fukushima Daiichi Nuclear Power Plant into the Atmosphere." *Journal of Nuclear Science and Technology*, 48(7), 1129–1134.

CNSC. (2014). *Safety Analysis: Probabilistic Safety Assessment (PSA) for*

Nuclear Power Plants. *REGDOC-2.4.2*, Canadian Nuclear Safety Commission.

Cojazzi, G. (1996). "The DYLAM approach for the dynamic reliability analysis of systems." *Reliability Engineering and System Safety*, 52(3 SPEC. ISS.), 279–296.

El-Sefy, M., Ezzeldin, M., El-Dakhakhni, W., Wiebe, L., and Nagasaki, S. (2019). "System Dynamics Simulation of the Thermal Dynamic Processes in Nuclear Power Plants." *Nuclear Engineering and Technology*, Elsevier Ltd, 51(6), 1540–1553.

Filip, F. G. (2008). "Decision support and control for large-scale complex systems." *Annual Reviews in Control*, 32, 61–70.

Forrester, J. (1971). "Counterintuitive Behavior of Social Systems." *MIT Technology Review*, 73 (3), 52–68.

Hakobyan, A. P. (2006). "Severe accident analysis using dynamic accident progression event trees." Ph.D. Thesis, The Ohio State University.

Hofer, E., Kloos, M., Krzykacz-Hausmann, B., Peschke, J., and Sonnenkalb, M. (2002). "Dynamic event trees for probabilistic safety analysis." *EUROSAFE Forum 2002: convergence of nuclear safety practices in Europe Papers, Germany*.

Hsueh, K. S., and Mosleh, A. (1996). "The development and application of the

accident dynamic simulator for dynamic probabilistic risk assessment of nuclear power plants." *Reliability Engineering and System Safety*, 52, 297–314.

Hu, Y. (2005). "A Guided Simulation Methodology for Dynamic Probabilistic Risk Assessment of Complex Systems." Ph.D. Thesis. University of Maryland.

IAEA. (2001). *Applications of Probabilistic Safety Assessment (PSA) for Nuclear Power Plants, IAEA-TECDOC-1200. International Atomic Energy Agency*.

IAEA. (2015). *Accident Monitoring Systems for Nuclear Power Plants, IAEA Nuclear Energy series NP-T-3.16. International Atomic Energy Agency*.

Jankovsky, Z. K., Denman, M. R., and Aldemir, T. (2018). "Dynamic event tree analysis with the SAS4A/SASSYS-1 safety analysis code." *Annals of Nuclear Energy*, Elsevier Ltd, 115, 55–72.

Mandelli, D., Maljovec, D., Alfonsi, A., Parisi, C., Talbot, P., Cogliati, J., Smith, C., and Rabiti, C. (2018). "Mining data in a dynamic PRA framework." *Progress in Nuclear Energy*, Elsevier, 108, 99–110.

Mandelli, D., Parisi, C., Alfonsi, A., Maljovec, D., Germain, S. S., Boring, R., Ewing, S., Smith, C., and Rabiti, C. (2017). "Dynamic PRA of a Multi-Unit Plant." *International Topical Meeting on Probabilistic Safety Assessment (PSA 2017)*.

Mandelli, D., Smith, C., Rabiti, C., Alfonsi, A., Youngblood, R., Pascucci, V., Wang, B., Maljovec, D., Bremer, P. T., Aldemir, T., Yilmaz, A., and Zamalieva, D. (2013a). "Dynamic PRA: An Overview of New Algorithms to Generate, Analyze and Visualize Data." *Transactions of the American Nuclear Society*.

Mandelli, D., Yilmaz, A., Aldemir, T., Metzroth, K., and Denning, R. (2013b). "Scenario clustering and dynamic probabilistic risk assessment." *Reliability Engineering and System Safety*, Elsevier, 115, 146–160.

Mercurio, D., Podofillini, L., Zio, E., and Dang, V. N. (2009). "Identification and classification of dynamic event tree scenarios via possibilistic clustering: Application to a steam generator tube rupture event." *Accident Analysis and Prevention*, 41, 1180–1191.

Nejad-Hosseinian, S. H. (2007). "Automatic Generation of Generalized Event Sequence Diagrams for Guiding Simulation Based Dynamic Probabilistic Risk Assessment of Complex Systems." Ph.D. Thesis. University of Maryland.

Nivolianitou, Z., Amendola, A., and Reina, G. (1986). "Reliability analysis of chemical processes by the DYLAM approach." *Reliability Engineering*, 14, 163–182.

Phillips-Wren, G. (2013). *Intelligent Decision Support Systems. In Multicriteria Decision Aid and Artificial Intelligence: Links, Theory and Applications;*,

Wiley-Blackwell: Hoboken, NJ, USA.

Rabiti, C., Alfonsi, A., Mandelli, D., Cogliati, J., and Martineau, R. (2012). "RAVEN as Control Logic and Probabilistic Risk Assessment Driver for RELAP-7." *ANS Winter Meeting*.

Siu, N. (1994). "Risk assessment for dynamic systems: An overview." *Reliability Engineering and System Safety*, 43, 43–73.

Smidts, C. (1994). "Probabilistic dynamics: A comparison between continuous event trees and a discrete event tree model." *Reliability Engineering and System Safety*, 44, 189–206.

Sterman, J. (2000). *Business Dynamics: Systems Thinking and Modeling for a Complex World*. Boston: Irwin/McGraw-Hill.

Swaminathan, S., and Smidts, C. (1999). "The Event Sequence Diagram framework for dynamic Probabilistic Risk Assessment." *Reliability Engineering & System Safety*, 63, 73–90.

U.S. NRC. (1975). *Reactor Safety Study: An Assessment of Accident Risks in U.S. Commercial Nuclear Power Plants, WASH-1400 (NUREG-75/014)*.

Varuttamaseni, A. (2011). "Bayesian Network Representing System Dynamics in Risk Analysis of Nuclear Systems." Ph.D. Thesis, University of Michigan.

World Nuclear Association. (2018). "The Harmony programme." <http://world-nuclear.org/harmony>.

World Nuclear Association. (2019). “Nuclear Power in the World Today.” <http://www.world-nuclear.org/information-library/current-and-future-generation/nuclear-power-in-the-world-today.aspx>.

Zio, E. (2014). “Integrated deterministic and probabilistic safety assessment: Concepts, challenges, research directions.” *Nuclear Engineering and Design*, Elsevier B.V., 280, 413–419.

Chapter 2 : Dynamic Probabilistic Risk Assessment of Nuclear Power Plants: State-of-the-Art Review using Text Mining

ABSTRACT

Serious nuclear power plant (NPP) accidents, such as the 2011 Fukushima Daiichi nuclear accident, have highlighted the need for advancement of relevant risk assessment methodologies. NPP risk assessment approaches have been evolving for more than four decades, with recent research focusing on *dynamic* probabilistic risk assessment (DPRA) of NPPs to overcome the limitations of probabilistic risk assessment (PRA) methods that use *static* event and fault tree analysis methods. DPRA considers the dynamic aspect of NPP physical behavior, the interaction between different systems and the operating crew responses, and the stochastic dynamic behavior of cascade failures in NPPs. In this respect, the current study utilizes text mining (a class of data mining) to analyze NPP DPRA-related articles published since 1981. Following the data collection and preparation, Latent Dirichlet Allocation topic modeling is utilized to identify and categorize published articles in terms of their key topics. The N-Gram text classification model is also performed, providing a visual network to the key topics in published articles. Finally, a qualitative survey of the DPRA methodologies, as well as the challenges of DPRA, is presented. The aim of this study is to identify trends in DPRA methodologies related to NPP safety and highlight their evolution and ongoing challenges. The study also identifies DPRA methodologies that are used in the

greatest numbers of published articles on risk assessment of NPP and that are most promising for DPRA of NPPs, and establishes a state of the practice survey of how laboratories/universities/organizations have been developing relevant risk assessment tools. The overarching goal of this study is to guide future DPRA methodology developments in order to enhance the safety of NPPs under dynamic cascade (systemic) risks.

Keywords: Nuclear Power Plant; Dynamic Probabilistic Risk Assessment; Text Mining; Latent Dirichlet Allocation; N-Gram.

2.1. INTRODUCTION

Major investment plans to construct new nuclear power infrastructure are undergoing across the world in order to meet the increasing demands for sustainable energy. In this respect, the Harmony program was launched to expand nuclear energy to provide at least 25% of global electricity by 2050 as part of a reliable and clean low-carbon mix (World Nuclear Association 2018). Globally, around 150 and 57 nuclear reactors are currently in their planning and construction stages, respectively (Canadian Nuclear Association 2019). Considering this significant increase and the number of current plants, the safety of nuclear power plants (**NPPs**) during normal and abnormal operating conditions is key to ensure sustainable power production. A NPP is a complex system-of-systems (El-Sefy et al. 2019) that contains a large number of interdependent components and systems, each with its own distinctive functions, that interact to operate as designed. Such component/system interdependence aims at controlling the reactor power, cooling the reactor core, and containing radioactivity to ensure the safety of the plant while generating electricity.

Natural (e.g., flood and earthquake) or anthropogenic (e.g., fire and human errors) hazards can have severe impacts on the operability and safety of NPPs. In 2011, tsunami waves as high as 14-15 m, caused by the Tōhoku earthquake, hit the Fukushima Daiichi NPP (Yukiya Amano 2015), resulting in eventual core meltdown in three reactor units and the release of a massive amount of radioactive materials. In 2012, three nuclear reactors (i.e., Nine Mile Point 1, Indian Point 3,

and Salem Unit 1 nuclear stations) were shut down by the Nuclear Regulatory Commission during Hurricane Sandy (Bucci et al. 2013). Such hazard realizations demonstrated the importance of the ongoing research efforts (Amin et al. 2018; El-Sefy et al. 2019; Kim et al. 2017; Mandelli et al. 2017b; Rabiti et al. 2014) to enhance traditional risk assessment methodologies and to develop more capable ones.

Prior to 1975, the U.S. nuclear regulations for the design and operation of NPPs were based on a deterministic safety assessment (**DSA**) approach to ensure that all needed functions would be safely accomplished during both normal and abnormal operations. The DSA approach was mainly utilized to ensure that the *defense-in-depth* approach is implemented by analyzing the plant response under pre-determined operational and accident conditions. Several approaches have been developed for the DSA of NPPs (IAEA 2009); initially, a conservative approach was used to take into account the uncertainties in analyzing anticipated operational occurrences and design basis accidents (**DBA**) due to the lack of data and limited understanding of physical phenomena. Subsequently, the Best Estimate Plus Uncertainty approach was considered more realistic as more experimental data became available. DSA approaches provide a high level of confidence in the design of NPP components under normal operation, DBA, and beyond DBA (CNSC 2017). However, as the probability that a component may malfunction always exists, introducing the probabilistic risk assessment (**PRA**) approach in the context of NPP became necessary.

In 1975, the US reactor safety study (*WASH-1400* (U.S. NRC 1975)) introduced the PRA approach for NPPs by using static event and fault tree (**ETs/FTs**) analysis techniques. PRA quantifies the frequencies of low-probability high-consequence accidents, including the frequency of core damage (Level 1-PRA), the frequency of radioactive releases from the containment (Level 2-PRA), and the risk to off-site public health and environment (Level 3-PRA) (IAEA 2010a). However, numerous concerns have been raised regarding the capability of PRA to account for the interdependence between the different NPP components (e.g., hardware and software and their operators) considering their overall stochastic and time-dependant (dynamic) behaviors (Aldemir 2013). Specifically, static analysis techniques typically do not consider the feedback mechanism between NPP system dynamics (e.g., physics of the systems such as temperatures, pressures, flow, etc.) and the system logic (e.g., the behavior of the components/operators) (Amendola and Reina 1981; Nivolianitou et al. 1986), since the analyses of NPP behavior and system response are performed separately (Hsueh and Mosleh 1996). In addition, static ETs are propagated following a so-called "*effect line where branching points are prescribed by order of safety system demands at set points* (Hofer et al. 2002a)" without any consideration of event propagation with time (Mercurio et al. 2009; Zio 2014). The evolution of system dynamic parameters with time may affect the probability of an event and may influence the accident sequence (Siu 1994). In this respect, the order of events is pre-determined by the analyst (Mandelli et al. 2013b; Zio 2014), based on separate thermal-hydraulic calculations. Thus, the quality and

outcome of the PRA analysis are entirely dependant on the analyst developing the event tree to reflect realistic scenarios (Jankovsky et al. 2018a). In addition, static ETs are not capable of capturing new events that might be overlooked by the analyst (Swaminathan and Smidts 1999a). In fact, Siu (1994) indicated that such PRA limitations can result in an inadequate or erroneous NPP risk assessment and can influence the computed probability of event occurrence. Also, Hu (2005) indicated that static ET/FT methods could not enumerate all risk scenarios for the NPP system with complex interactions between components, software operations, and humans. In order to overcome these limitations of the static ET/FT analysis techniques, the notion of a dynamic PRA (**DPRA**) approach has been identified.

The DPRA approach has been developed to consider the dynamic interaction between different systems in NPPs and the temporal propagation of failures within a probabilistic framework. The DPRA of NPPs integrates both NPP simulation codes, including plant system dynamics/software/human interactions (Cojazzi 1996; Smidts 1994) with a stochastic process (Acosta and Siu 1993; Cojazzi 1996; Hofer et al. 2002a; Hsueh and Mosleh 1996; Mandelli et al. 2013b, 2018; Rabiti et al. 2012). Several simulation codes have been used to predict the response of NPPs as part of a dynamic risk assessment. These include RELAP (U.S. NRC 1995) and MELCOR (Gauntt et al. 2000) codes used to simulate the thermal-hydraulic behavior of the plant, while the stochastic process includes models of random system/component failure (Mandelli et al. 2018) and human intervention with NPP system dynamics (Hu 2005). DPRA has been developed to capture event sequences

as a function of time because the branching occurs at a time when any critical variable of the NPP systems (e.g., the thermal-dynamic process of the primary loop variables, component states, and operator response) changes (Hsueh and Mosleh 1996). Specifically, in DPRA, scenarios within an dynamic event tree are developed after triggering a single initiating event and, when a system parameter exceeds a threshold, branching occurs based on the possible outcomes of the system/component responses (Kunsman et al. 2008). Branching thus can create two different scenarios for system evolution, each of which has its own criteria as a function of time.

Several research studies have been focused on DPRA approaches, especially following the Fukushima nuclear accident in 2011. Text mining (**TM**) is utilized in the current study as an objective means to identify the different DPRA methodologies that have been developed in the field of nuclear safety. TM is a subclass of data mining that is used in several research fields to explore key topics within scientific publications (Lazard et al. 2015; Nassirtoussi et al. 2014). TM deals with unstructured or semi-structured data like HTML files, emails, and full-text documents (Salloum et al. 2018). Latent Dirichlet Allocation (**LDA**) is a widely used statistical analysis technique, proposed by Blei et al. (2003) and used in different fields (Tang et al. 2014), including social science (Koltcov et al. 2014), software engineering (Campbell et al. 2015), business (Maskeri et al. 2008), medical science (Paul and Dredze 2011), structural engineering (Ezzeldin and El-Dakhakhni 2019), geography (Yin et al. 2011) and political science (Greene and

Cross 2015), to find relationships among text documents and subsequently extract their key topics.

The goal of this study is to present a thorough survey of how laboratories/universities/organizations have been developing relevant risk assessment tools and to identify recent DPRA methodologies that show promise for risk assessment of NPPs. This study also aims at highlighting and understanding the key challenges facing the developed DPRA methodologies. Identifying DPRA challenges is a crucial step toward exploring new research streams that need to be addressed in future studies. In this respect, TM analysis is performed on published articles to identify such methods and their applications within the nuclear power field. The considered dataset represents 387 articles published in approximately 50 different journals and conferences from 1981 to 2019. Afterward, such articles are analyzed to provide a visual representation of the DPRA research topic landscape, using the LDA and N-Gram text classification modeling techniques. Finally, a qualitative literature review is performed to present an overview of the concepts of DPRA methods and their point of application, as well as to investigate the main challenges facing the DPRA approach.

2.2. TEXT MINING OF THE DYNAMIC PROBABILISTIC RISK ASSESSMENT RESEARCH DATABASE

2.2.1. DATA COLLECTION AND PREPROCESSING

This section provides a quantitative literature analysis, based on TM, to identify key nuclear DPRA topics in the relevant literature. As shown in Figure 2-1, in the first step, published articles are collected from Web of Science (2020), Google Scholar (2020), and Engineering Village (2020). Articles are collected using the following criteria: *i*) journal and conference articles published from 1981 to 2019; *ii*) articles with abstracts that contain technical information; and *iii*) articles with relevant keywords (e.g., NPP and DPRA methods). During data collection, article titles and abstracts are used for the analysis as they contain the research problem, the overall objective of the study, the approach/method/software used in the study, and the main findings as a result of the study (Gatti et al. 2015; Griffiths and Steyvers 2004). A total of 387 articles is collected for dataset A that is subsequently analyzed to explore DPRA methods; however, such a dataset does not provide clear topics for DPRA methods, as will be discussed later. As such, a search is performed using the following keywords: NPP, dynamic probabilistic risk assessment, DPRA simulation methodologies or DPRA graphical methodologies. A total of 223 and 164 articles are collected for DPRA simulation (*dataset 1*) and graphical (*dataset 2*) methods, respectively. Figure 2-2 shows a growing trend in the number of published articles related to DPRA methodologies of NPP with approximately 50%

of the articles being published since 2011. However, with only 387 relevant articles in 40 years, there is an urgent need to make significant progress in the field of DPRA in order to enhance the safety of nuclear power. As shown in Figure 2-3 and Figure 2-4, the majority of articles are published in *Reliability Engineering and System Safety* Journal, *International Topical Meeting on Probabilistic Safety Assessment and Analysis*, and *International Conference on Probabilistic Assessment and Management*. The high number of journals and conferences indicates that the development of DPRA of NPPs is spread through a wide variety of sources and is still a subject of ongoing study.

The *second* step is focused on data cleaning, which is essential to avoid any linguistic noise that can have a negative impact on the statistical analysis within the context of TM (Salloum et al. 2018). The linguistic noise is due to common words (e.g., the, of, and, for), punctuation, variation in word case types (e.g., NUCLEAR and nuclear) and word forms (e.g., assess and assessment). The data cleaning step consists of the following sub-steps: *i*) tokenization, where the abstracts are separated into tokens (i.e., individual words); *ii*) treatment, where the datasets are treated to remove all common words (e.g., the, of, are, it) and un-needed characters (e.g., tags, punctuation, non-alphabetic characters); *iii*) transformation, where all characters are converted to a lowercase format; *iv*) Lemmatizing/Stemming, where all words are returned to their roots/stem based on the Porter stemming algorithm (Khoury and Sapsford 2016); and *v*) cleaning, where all tokens with more than 25 or less than four characters are removed. Figure 2-5 shows the raw and clean

datasets, where the size of each word is in proportion to its probability of occurrence. As can be seen in Figure 2-5, while the raw dataset contains several words with high frequency (e.g., of, and, for, the), the clean dataset has several high-frequency words that are related to nuclear engineering research (e.g., nuclear, dynamic, system, probabilistic), which demonstrates the key importance of these preprocessing steps in enhancing the dataset quality for meaningful analyses. There are many topic modeling techniques presented in the literature, but the LDA model is considered one of the most effective techniques (Blei et al. 2003), as will be shown next. Following the LDA model, the N-Gram text classification model (Violos et al. 2018) is utilized in the current study for data classification and visualization.

2.2.2. LATENT DIRICHLET ALLOCATION MODEL DESCRIPTION

The main concept of the LDA model is that key topics can be identified based on the probability of co-occurrence of words within the same document. Thus, words with the highest probabilities in each topic provide a good indication of that topic. The LDA model is a generative model that simulates each document as a mixture of topics, and subsequently, the Gibbs sampling algorithm evaluates the probability of each word appearing in each given topic. Based on these topics, LDA generates a concise representation of a document (Alghamdi and Alfalqi 2015). In a simple way, the LDA model initially assumes a collection of K latent topics, where each topic contains a distribution of words (ψ_k) that is estimated from a Dirichlet distribution β. Given the K topics, each document ($d \in \{1,..., D\}$) is analyzed by

sampling a topic distribution in a document, θ_d, over K topics, where the multinomial distribution of topics in a document, θ_d, is estimated from a Dirichlet distribution α. Then, for each word i in the document, the LDA model allocates a certain topic, Z_{di}, that belongs to K (i.e., $Z_{di} \in \{1,..., K\}$) based on θ_d and subsequently w_{di} is selected based on multinomial distribution ψ_{Zdi}. LDA technique utilizes several algorithms to estimate the word distribution (ψ) and the document topic distribution (θ). The current study uses the Gibbs sampling algorithm in the sense that key topics can be predicted, regardless of the algorithm that is used (Hofmann and Chisholm 2016). Full details of both the Dirichlet and multinomial distributions can be found in Minka (2000) and Correa (2001), respectively. As indicated earlier, the LDA model requires values for the hyperparameters β and α that control both ψ_k *and* θ_d. According to Griffiths and Steyvers (2004), large β and α values could lead to a uniform topic distribution, while small values of β and α provide sparser topic distribution for the dataset under investigation. In this respect, this study utilizes small values for the hyperparameters β = 0.01 and α = 0.125 (Griffiths and Steyvers 2004).

The optimum number of topics (K) is another challenging step in the topic modeling of unstructured document datasets. Perplexity is a commonly used statistical measure to assess how well a probability model predicts a dataset (Blei et al. 2003). In this regard, for a given k topic initiated by the LDA model, the theoretical word distributions are compared to the actual topic mixtures or distribution of words in the actual documents. According to Zhao et al. (2015), an

iterative approach can be used to determine the number of topics for the dataset, based on the LDA model with minimum perplexity. To do this, datasets A, 1, and 2 are randomly divided into 90% and 10% for training and testing, respectively.

2.2.3. WORD CO-OCCURRENCE NETWORK

A visual representation of data facilitates gaining insights and making better data-driven decisions. In this regard, another text classification method has been used in the current study based on the N-Gram graph representation model (Violos et al. 2018), in which the R code (Silge and Robinson 2019) is utilized to create an alternative representation model for DPRA datasets classification based on TF-IDF (term frequency-inverse document frequency) algorithm. This algorithm is used to assign importance to the words in a text, in which term frequency is used to estimate the frequency of a word in a document, while inverse document frequency represents the ratio between the total number of documents and the number of documents that contain a word. Full details about this algorithm can be found in Qaiser et al. (2018). In its most basic form, the N-Gram model is a contiguous sequence of *n* items from a given sample of text or speech. These items can be letters, words, syllables, or base pairs based on the application. The N-Gram model classification model has the advantages of providing a well-structured representation of data using directed networks, in which words are represented as nodes, while directed links are used to show the sequence of these words within the text. In addition, the frequency of adjacent words is represented by weights on the links between such words.

2.3. TEXT MINING RESULTS FOR DPRA OF NPPS

2.3.1. RESULTS OF THE LDA MODEL

The LDA model's primary outcomes include the probability of word *w* in topic *k*, ψ_{kw}, and distribution of words in each topic *k*, ψ_k. Based on these results, the group of words with the highest probabilities are linked to a corresponding research topic. Figure 2-6, Figure 2-7, and Figure 2-8 show the key topics presented in the literature based on the LDA model results of dataset A, 1, and 2, respectively. As shown in the figures, the font size is directly proportional to the word frequency and only words with high frequencies are shown to facilitate the identification of each key topic through these words. It should be noted that certain words such as "reliability, analysis, system, results, using" have a high co-occurrence frequency between different topics. This could contribute to two methods mentioned in the same topic "i.e., same word cloud" because LDA topic modeling tends to collect the words with a high frequency of co-occurrence in the same topic. In this regard, these common words are excluded during LDA modeling of dataset 1 to ensure that each topic is represented in a particular word cloud. Finally, topic titles are identified by the authors after inspecting the keywords comprising each word cloud.

As can be seen in Figure 2-6, the LDA analysis of dataset A provides 11 different topics, where 5 topics are considered as general topics related to DPRA, such as Topic No.1: DPRA, Topic No. 3: general topic, and Topic 11: Nuclear Power Plant. Therefore, the results of the LDA model for dataset A do not provide

a comprehensive list of topics for DPRA methods. Instead, LDA analysis of datasets 1 and 2 provides 9 and 7 topics for DPRA simulation and graphical methods, respectively, as discussed below.

The LDA model results for dataset 1 are shown in Figure 2-7. The words "event, tree, dynamic, discrete, continuous, comparison" in Topic No. 1, are mostly related to the DPRA simulation approaches including discrete dynamic event tree (**DDET**) and continuous event tree (**CET**). Similarly, the words "application, event, tree, dynamic, generate", "methodology, plant, safety, dynamic, system, dylam, process", and "control, markov, model, scenario, learn, ccmt", in Topics No. 2, 3 and 4 are typically connected to the DET, DYLAM and Markov/CCMT methods, respectively. Also, the words "adsidac, study, dynamic, pra, behavior" in Topic No. 5 are frequently used in the ADS-IDAC methodology, while "raven, code, relap5-3d" in Topic No. 8 are frequently used in RAVEN code. In summary, LDA results have shown seven topics (i.e., topics 2 to 8) related to DPRA simulation methodologies, while topic 1 is related to DPRA simulation approaches, as presented in Figure 2-7. Moreover, Topic No. 9 present one of the most frequent applications of DPRA simulation methods in the nuclear engineering field related to simulating the crew/operator's response as presented in the words "operator, model, cognitive, response, crew, simulation, accident", besides other applications are mentioned within topics 2 and 8, as presented in the words "rupture, steam, tube", and "flood, water, station, blackout", respectively.

The LDA model results for dataset 2 are shown in Figure 2-8. The words

"*monitor*, *reliability*, *go-flow*, *methodology*" in Topic No. 1 are mostly related to the Go-flow method. Similarly, the words "*methodology*, *dynamic*, *flowgraph*, *model*" in Topic No. 4 are typically connected to the dynamic flowgraph method, while "*dynamic*, *network*, *risk*, *Bayesian*" in Topic No. 6 are frequently used in the dynamic Bayesian network (**DBN**) methodology. In summary, LDA results have shown *six* topics (i.e., topics 1 to 6) related to DPRA graphical methodologies, as presented in Figure 2-8. Moreover, Figure 2-8 shows that the LDA can identify some general topics that are frequently used in technical writing. For example, the words "*safety*, *system*, *analysis*, *application*, *software*, *method*" in Topic No. 7 are considered as general words that are used frequently within several scientific research fields. Figure 2-6, Figure 2-7, and Figure 2-8 also show the sensitivity of the perplexity to the number of topics for each dataset, in which the minimum perplexity values are attained at K equals 11, 9, and 7 for datasets A, 1, and 2, respectively. Therefore, the current study utilized the same K values in presenting key topics in datasets A, 1, and 2. In general, the results of the LDA analysis of datasets 1 and 2 show 7 and 6 technical topics for DPRA simulation and graphical methods, respectively. Figure 2-7 shows that DET, DYLAM, Markov/CCMT, ASD-IDAC, Monte Carlo, ADAPT, and RAVEN are the most common topics related to DPRA simulation methods, while topics of go-flow, Petri-net (**PN**), dynamic fault tree (**DFT**), dynamic flowgraph (**DFM**), event sequence diagram (**ESD**), and Bayesian network (**BN**) are the most common topics related to DPRA graphical methods, as shown in Figure 2-8.

2.3.2. RESULTS OF THE N-GRAM MODEL

The N-gram weighted directed network was the second text classification methods used in the current study to investigate the literature in the field of DPRA of NPPs. Using this classification method, Figure 2-9 and Figure 2-10 represent the most frequent words in datasets 1 and 2 as a sequence of separated words through a directed network. In addition, links connecting words with high frequencies, relative to other words, have higher weights represented by bold arrows in Figure 2-9 and Figure 2-10. For example, Figure 2-9 and Figure 2-10 show a contiguous sequence of the most frequent words in the DPRA simulation and graphical methods, respectively. It is clear from Figure 2-9 that DET, DYLAM, ASD-IDAC, MCDET, RAVEN, Markov-CCMT, and ADAPT are the main topics in the field of DPRA simulation methods. Also, the word sequences *crew-response*, *operator action*/*response*, *operating-crew*, and *human-performance* show that the operator action has been investigated through the different DPRA simulation methods. Besides the word sequence station-blackout, steam-generator-tube-rupture represent applications of DPRA in NPPs. On the other hand, go-flow, dynamic flowgraph, event sequence diagram, Petri-net, Bayesian network, and dynamic fault tree are the main topics in the field of DPRA graphical methods, as shown in Figure 2-10. As can be demonstrated from Figure 2-7 through Figure 2-10, several DPRA simulation and graphical methods have been developed in the nuclear engineering field. Thus, the following section presents the different DPRA methods which are extracted from the LDA and N-Gram analyses of DPRA datasets 1 and 2.

2.4. DPRA SIMULATION METHODS

The LDA statistical analysis technique identified eight main topics related to DPRA simulation approaches/methods. Figure 2-11a and Figure 2-11b present the rate of publications in DPRA simulation methods and the cumulative number of publications for each DPRA simulation methodology, respectively. As shown in this figure, some methodologies have a significant contribution to the number of publications with an increasing growth rate in the number of publications, while other methodologies have a stable or decreasing trend in the number of publications. As shown in Figure 2-2 and Figure 2-11b, the rate of new publications increased after 2005 and 2011. In the first phase, between 2005 and 2011, ADAPT was developed around 2006 and contributed to new publications related to DPRA simulation method. In addition, the rate of new publications related to ADS-IDAC and DET increased during this phase compared to other DPRA simulation methods. In the second phase, between 2011 and 2019, RAVEN was developed as a new DPRA simulation method and significantly contributed to a high number of publications during this phase. In addition, the rate of publications related to DET, MC, and ADAPT increased during this phase compared to the first phase. It should be noted that the ADS-IDAC simulation methodology made a significant contribution to the number of published articles with 20% of the published articles related to DPRA simulation methodologies over the last 23 years. Also, the number of articles written using ADAPT and RAVEN during the last decade indicates the promising start for these new DPRA simulation methodologies for NPPs: ADAPT

and RAVEN have contributed to 12% and 16% of the published articles related to DPRA simulation methodologies over the last decade. On the other hand, the DYLAM simulation methodology has had a fixed number of publications since the mid-1990s due to the development of other DPRA simulation methodologies.

Finally, it should be noted that an R code is developed to identify the methodology implemented in each article and check the overlap between different methodologies. In this respect, seven research studies in dataset 1 contained two different methodologies in the same articles, particularly for ADAPT and RAVEN, as well as Monte Calro and Markov simulation methodologies. These articles are categorized twice based on the two methodologies that are mentioned in the article. The rest of the published articles in dataset 1 that are not shown in Figure 2-11b are related to the DPRA approach without referring to any of the DPRA simulation methodologies. The following sub-sections include a qualitative literature review of these topics to investigate their development.

2.4.1. TOPIC 1: DISCRETE DYNAMIC EVENT TREE AND CONTINUOUS EVENT TREE

There are two primary simulation approaches for DPRA of NPPs, including DDET and CET (known as the Monte Carlo simulation approach). DDET provides a basis for discrete-time DPRA simulation methods that integrate the physical response of NPPs, the logic of the system, and the operator actions to generate dynamic event trees, in which branching occurs at discrete points in time. A DDET consists of

three main parts that are integrated to create the DPRA of NPPs: i) model of the NPP physical and control processes; ii) model of the components and crew responses; and iii) a scheduler to control branching points. Unlike DDET, CET allows events to occur randomly at any time. It should be noted that the majority of DPRA simulation methods are related to the discrete-time DPRA method, while Monte Carlo and RAVEN have both capabilities to be applied for discrete and continuous DPRA of NPPs. DET is the most popular method to apply the DDET approach and is considered the basis for existing discrete-time DPRA simulation methods, including DYLAM, Markov/CCMT, ADS-IDAC, MCDET, and ADAPT. As can be seen in Figure 2-11b, DDET, through its discrete-time DPRA simulation methodologies, has contributed to a substantial number of published articles related to DPRA simulation methods, and thus DDET is considered the most common approach for DPRA simulation methods.

2.4.2. TOPIC 2: DYNAMIC EVENT TREE (DET)

Unlike static ETs, DETs consider timing and sequence of system responses through a scheduler that controls the timing and branching of the event tree and thus saving the information about the system states at all branching points (Chang et al. 2003). In DET, after the first scenario associated with a branch is completed, the simulation returns to the previous branching point and subsequently, the saved system state is restored to start a new scenario. As such, the temporal progression and sequence of system responses after an initiating event in dynamic event trees are determined by a time-dependent model of system evolution and branching conditions selected by

the analyst (Aldemir 2013). Branching nodes are allowed to occur at random, representing discrete points in time (Acosta and Siu 1991) when a system or operator action is called for. As such, the length of the time step has a significant influence on the accuracy of the analysis (Hu 2005). The procedural evolution of the DET approach is demonstrated in Chang et al. (2003). In general, this approach was established to consider all possible combinations of system states at branching points, where each branch represents a new stochastic event.

2.4.3. TOPIC 3: THE DYNAMIC LOGIC ANALYTICAL METHODOLOGY (DYLAM)

DYLAM is a simulation software developed by the Joint European Center at Ispra, Italy, in the mid-1980s (Aldemir 2013). DYLAM was the most common simulation methodology until the mid 1990s, as shown in Figure 2-11a. DYLAM was developed by integrating the time dimension into the logical analytical methodology modeling technique (Cacciabue et al. 1986; Cojazzi 1996; Nivolianitou et al. 1986) in order to create a tool that couples the probabilistic and dynamic behavior of the system. Specifically, DYLAM considers the dynamic aspect generated from the interaction between time-dependent physical parameters of components, control and safety systems, and human actions, in which the probability of an undesirable event is estimated by summing the probabilities of contributing scenarios (i.e., branches) (Aldemir 2013). As a first step, the information regarding the physical system under investigation is contained within

the system simulator (Cojazzi 1996; Kunsman et al. 2008) developed by the analyst (Cojazzi 1996). The system simulator is constructed by linking different models to represent the physical systems, where the active components are modeled to have different operating states (nominal, failed on, failed off, stuck, etc.). Once the system simulator is linked to DYLAM, DYLAM assigns a stochastic transitions in the component states or initial states to each tree branch in order to drive the simulation, considering the logical states time-history of system components (Cojazzi 1996; Kunsman et al. 2008). DYLAM starts at time t = 0 and a user-defined initial condition for the system. At the end of each time step, the system simulator is used to examine the change in the system dynamic variables to determine whether or not to generate a new branch. If DYLAM creates a new branch, all the information about component states is stored when a new branching point occurs. After analyzing an initial scenario, DYLAM returns to the last branching point and retrieves all the stored data about component states at that time in order to start a new scenario. DYLAM then repeats the previous process to identify all the possible accident scenarios. For each path, a time-dependent probability is determined, while the probability of occurrence of a top event is calculated by summing the probabilities of all scenarios resulting in the top event (Aldemir 2013; Cojazzi 1996; Kunsman et al. 2008).

DYLAM has several alternatives that use different branching logic with more emphasis on the modeling of human-system interactions. An extension of DYLAM called the dynamic event tree analysis (DETAM) (Acosta and Siu 1993) was

developed to deal with the limitations of DYLAM in dealing with the dynamic NPP behavior and its crew following the initiation of an event. The DETAM is a simulation tool that is capable of modeling both the stochastic variations in the component states and the operator states (i.e., defined by the crew's diagnosis states, quality states, and planning states) (Cojazzi 1996). This tool considers the interdependence between component states, system's dynamic responses, and the crew actions during the accident scenario.

2.4.4. TOPIC 4: MARKOV/CELL-TO-CELL MAPPING TECHNIQUE (MARKOV-CCMT)

Markov-CCMT is a combination between the discrete-state Markov process and the Cell-to-Cell mapping technique (e.g., a systematic technique to present the linear and non-linear dynamic characteristics of the system in discrete-time and discretized system state space (Mandelli 2008)). Markov-CCMT provides an efficient modeling technique to address the reliability of the digital Instrumentation and Control (**I&C**) system by considering the dynamic interactions between different components comprising the digital I&C system, and between this system and the control NPP physical processes (Aldemir et al. 2009).

The Markov/CCMT technique was utilized in a recent study to investigate the steam generator digital water level control system inside a pressurized water reactor (**PWR**) (Gomes and Saldanha 2013). The obtained results showed the possible failure scenarios that can occur due to the dynamic interactions between the I&C

system, the controlled process, and the various subsystems of the digital system. Recently, Markov/CCMT was utilized in (Li et al. 2017) to assess the dynamic reliability of the main and startup feedwater control system inside a NPP. The results demonstrated the efficiency of Markov/CCMT compared to static ET/FT methods.

2.4.5. TOPIC 5: ACCIDENT DYNAMIC SIMULATOR (ADS)

The ADS has been extensively used to perform the dynamic risk assessment of NPPs starting from 1996, as shown in Figure 2-11a. The ADS was developed at the University of Maryland (Chang and Mosleh 2007a; Hsueh and Mosleh 1996) for the dynamic simulation of Level 1-PRA, especially for large-scale dynamic accident sequences (Hsueh and Mosleh 1996). The ADS exhibited significant improvement when being integrated with human reliability analysis and RELAP within dynamic risk analysis (Mercurio et al. 2009), in which the DDET is utilized to generate time-dependent scenarios following initiating events in NPPs by predicting the changes in both the component and crew responses during the accident sequences. Hsueh and Mosleh (1996) explained the ADS strategy to be based on "*breaking down the accident analysis model into different parts according to the nature of the processes involved, simplifying each part while retaining its essential features, and developing integration rules for full-scale application* (Hsueh and Mosleh 1996)". In addition, the ADS has been developed to simulate the variations in the crew responses during NPP transient and/or accident events by integrating the Information, Decision, and Actions in a Crew context (**IDAC**)

within a cognitive model. IDAC provides a significant contribution in simulating the operator performance to include three main categories of operators, namely *"decision-maker, action maker, and consultant* (Chang and Mosleh 2007b)*"*.

2.4.6. TOPIC 6: MONTE CARLO SIMULATION METHOD

Unlike the DDET, Monte Carlo (**MC**) simulation allows events to occur at any time (e.g., represent a continuous event tree) and is insensitive to the size and complexity of the system (Hu 2005). It can also include any modeling assumptions such as the non-fixed failure rate assumption, interaction between components and process dynamics, and random delays. While the MC simulation method can result in an inadequate representation of rare events, this can be addressed by integrating appropriate biasing techniques. Additionally, this method provides the probability of reaching a specific end state (i.e., reactor core damage) without collecting detailed information related to scenarios that lead to this end state (Varuttamaseni 2011).

The MC dynamic event tree (**MCDET**) simulation combines the dynamic event tree and the MC simulation method to generate a discrete-time DPRA simulation method, in which MCDET can be integrated with severe accident analysis code MELCOR. The MCDET method, developed at Gesellschaft für Anlagen und Reacktorsicherheit, aimed at achieving a realistic simulation of a dynamic system (Hofer et al. 2002a), and contributed to approximately 60% of published papers related to MC method. This method generates a discrete DET to estimate the response of dynamic parameters and probabilities along branches for

each random event generated by MC simulation. Kloos and Peschke (2007) integrated MCDET with a Crew module to simulate the crew interactions with the plant model, including the operator's knowledge and communications, ergonomics and stress. Pan et al. (2017) also utilized MCDET to investigate the behavior of the level control dynamic system and the emergency standby power system due to different aging components. The results demonstrated that MCDET provides adequate modelling of sequences with low probabilities of occurrence.

2.4.7. TOPIC 7: ANALYSIS OF DYNAMIC ACCIDENT PROGRESSION TREES (ADAPT)

ADAPT is a system software developed at Ohio State University under a Sandia National Laboratories (**SNL**) research project in 2006 (Kunsman et al. 2008). ADAPT has been developed to generate automated accident progression event trees (**APET**) based on the DET concept for different types of reactors (Jankovsky et al. 2018b) and has evolved for over 14 years, as shown in Figure 2-11a. Initially, the APET approach was used to quantify the accident progression and containment responses for Levels 2 and 3 PRAs (U.S. NRC 1990). However, APET has some drawbacks, as described by Hakobyan et al. (2008). For example, the APET approach is relatively computationally expensive (Hakobyan et al. 2006) while being a static approach, similar to the ET analysis, but with explicit modeling of the physical behavior (Hakobyan et al. 2008). ADAPT is used to overcome the limitations of the APET approach by coupling the dynamic behavior of NPPs

(MELCOR, RELAP, SAS4A) with the modeling of stochastic system evolution for dynamic risk assessment of nuclear processes. ADAPT is similar to other DET techniques, in which the system code determines the path of the accident sequence within a probabilistic context. ADAPT has a significant advantage of running all the branching scenarios in parallel to create the event tree (Hakobyan 2006). ADAPT is capable of considering the aleatory uncertainties associated with the behavior of active (e.g., pump, valve) and passive (e.g., pipes, containment) components, while also considering the epistemic uncertainty associated with system parameters (e.g., heat transfer coefficient, coolant flow) (Aldemir 2013; Hakobyan et al. 2008). Furthermore, ADAPT can be used for Level 1 PRA and for the analysis of any complex system that can be abstracted as an event tree.

2.4.8. TOPIC 8: REACTOR ANALYSIS AND VIRTUAL CONTROL ENVIRONMENT (RAVEN)

Developed in 2012 at the Idaho National Laboratory (**INL**), RAVEN performs probabilistic analysis considering the dynamic response of NPPs through providing dynamic risk analysis capabilities to the thermal-hydraulic simulator RELAP-7. As shown in Figure 2-11a, RAVEN has attached significant interest during the last seven years because of its flexibility in terms of its interface abilities with other code (Rabiti et al. 2014).

The first version of RAVEN (i.e., coded in python) focused on developing a DPRA, in which RAVEN was coupled with RELAP-7 thermal-hydraulic simulator

to derive NPP system control logic that is dictated by: *i*) NPP control logic; *ii*) crew actions; and *iii*) the stochastic behavior of components and human actions (Mandelli et al. 2014; Rabiti et al. 2012). Since then, INL has extended the capabilities of RAVEN to be coupled with RELAP5-3D and BISON fuel behavior code (Williamson et al. 2012). In RAVEN, the stochastic behavior of the system is implemented by MC and DET analysis methodologies (Mandelli et al. 2017b; Rabiti et al. 2012). RAVEN is used to perform parametric and probabilistic analyses based on the response of a complex system (Alfonsi et al. 2014). RAVEN is comprised of a Control Logic System, Graphical User Interface, and a Probabilistic and Parametric framework as summarized by Alfonsi et al. (2013) and Rabiti et al. (2013).

2.5. DPRA GRAPHICAL METHODS

The LDA statistical analysis technique identified six topics related to DPRA graphical methods. Figure 2-12a and Figure 2-12b show the rate of publications in DPRA graphical methods and the cumulative number of publications for each DPRA graphical methodologies, respectively. As can be seen in Figure 2-12a, the dynamic flowgraph method contributed to approximately 32% of the published articles related to the DPRA graphical interface methods since 1995. PNs also account for a significant proportion of publications, with approximately 25% of the published paper related to DPRA graphical interface methods. Moreover, the number of articles published using DBNs indicate that this graphical method is promising for DPRA of NPPs. Specifically, as shown in Figure 2-2 and Figure

2-12b, the rate of new publications increased after 2005 and 2011. In the first phase, between 2005 and 2011, the rate of new publications related to DFM increased during this phase compared to other DPRA graphical methods. In the second phase, between 2011 and 2019, DBN was developed as a new DPRA graphical method and significantly contributed to a high number of publications during this phase. In addition, the rate of publications related to Go-Flow, PN, and DFM increased during this phase compared to the first phase. On the other hand, ESD publication showed a decreasing trend over the last decade with limited articles compared to other DPRA graphical interface methods. Finally, it should be noted that an R code is developed to identify the methodology implemented in each article and check the overlap between different methodologies. In this respect, six research studies in dataset 2 contained two different methodologies in the same articles, particularly for Petri Net and Bayesian Network, as well as Go-Flow and Bayesian Network graphical methodologies. These articles are categorized twice based on the two methodologies that are mentioned in the article. The following sub-sections include a qualitative literature review of these topics to investigate their development.

2.5.1. TOPIC 1: GO-FLOW

The Go-Flow methodology was presented in 1985 as a reliability analysis method (Matsuoka and Kobayashi 1985, 1987) with a large proportion of published articles, as shown in Figure 2-12a; however, the contribution of this methodology to the DPRA graphical methods decreased after developing the dynamic flowgraph method (Topic 4) at the beginning of the 1990s. The Go-Flow methodology is a

success-oriented system analysis technique used to evaluate the reliability and availability of dynamic systems (Matsuoka 1988). As a key step, the Go-Flow chart is developed to represent the function of operators/components/systems in addition to the majority of the operating system conditions (Takeshi 2010). A recent research study integrated the Go-Flow methodology with the DBN (Topic 6) for uncertainty analysis for the auxiliary power system of a NPP under different input for the operator action, in which the results showed an enhancement in the reliability evaluation of the Go-flow methodology, providing the operators with valuable risk information for the safe operation of NPPs (Ren et al. 2017). Another recent study utilized the Go-Flow methodology for the risk assessment of the auxiliary feedwater system in a PWR (Xinyu et al. 2017).

2.5.2. TOPIC 2: PETRI NETS (PNS)

In 1987, Leveson and Stolzy (1987) explored the ability to use time Petri net modeling in the design and analysis of safety-critical dynamic systems. Petri net is a graphical and mathematical modeling tool that can set up algebraic equations that describe the characteristics of many systems. A Petri net contains places (i.e., possible states of the system), transitions (i.e., events or actions that may occur and have an influence on the state of the system), and arcs that connect places and transitions. Places in PN may contain a number of tokens (i.e., conditions or input data related to the place), in which tokens are used to simulate the dynamic, concurrent, and asynchronous activities of systems. Many extensions of Petri nets have been developed, including deterministic PNs (Tomek et al. 1994), stochastic

PNs (Murata 1989), colored PNs (Cho et al. 1996) and hybrid PNs (David and Alla 2004). Colored PNs were utilized to analyze the critical safety of several systems after the shutdown of a Korean NPP (Cho et al. 1996). In a different study, PNs were utilized to model the dynamic process of the emergency management system within the Khaskovo NPP (Tavana 2008).

2.5.3. TOPIC 3: DYNAMIC FAULT TREE (DFT)

The DFT approach was developed by Dugan (1991) to overcome the limitation of static FTs by adding additional dynamic gates to model the complex dynamic interactions. Specifically, this approach is an extension of FTs that can capture the dynamic features of complex systems, in which Markov analysis is utilized to solve dynamic gates such as the priority-AND gate, sequence-enforcing gate, the standby or spare gate, and the functional dependency gate (Dugan et al. 1992). Several software packages such as DITree and later Galileo have been developed at the University of Virginia to solve DFT (Dugan 2000; Dugan et al. 2000). Another DFT method was proposed by Cepin (Cepin 2001; Cepin and Mavko 2002) to extend the classical FTs with time requirements in a way that reduces the system unavailability and assesses the actual time-dependent risk profile. Both DFT methods have limited dynamic characteristics; these approaches are not capable of dealing with the full spectrum of dynamic system features (Hu 2005). As such, the dynamic interaction between different components/systems and the process parameters are not easily captured by DFT methods (Nejad-Hosseinian 2007).

2.5.4. TOPIC 4: DYNAMIC FLOWGRAPH METHOD (DFM)

DFM is considered one of the most important DPRA graphical methods to assess the safety/reliability of NPPs. This method was developed in the early 1990s (Garrett et al. 1993) based on the logic flowgraph method but with dynamic characteristics. The DFM is a directed graph that is analyzed at discrete time steps (Karanta 2013). This method is used to model the logical and dynamic behavior of complex systems, including the interdependence between system parameters such as hardware, software and operator actions. DFM models contain vertices and edges to represent the system, in which vertices represent the components and variables, while edges represent the interaction between such vertices (Tyrväinen 2013). The DFM models were developed in terms of cause and effect relationships between the physical variables and the states of control systems. This method can be used to identify the root cause of a top event or to trace event propagation in time (Karanta 2013). For example, DFM has been applied to assess the digital I&C system for the feedwater control system through different scenarios, such as the failure of the main computer or the main feedwater control valve (Yin et al. 2013). The obtained results demonstrated the ability of DFM to find the roots (i.e., initial events) that lead to the top event.

2.5.5. TOPIC 5: EXTENDED EVENT SEQUENCE DIAGRAM

In 1999, Swaminathan and Smidts (1999a) proposed a mathematical model to extend the event sequence diagrams to allow for modeling of dynamic scenarios.

Static Event Sequence Diagram (**ESD**) is a graphical method used to present both the success and failure scenarios starting from an initial event to a final state. The main breakthrough in ESD occurred when Swaminathan and Smidts (1999a; b; c) extended the static ESD to capture dynamic phenomena such as time conditions, physical conditions, competing events, synchronizations, concurrent independent processes, mutually exclusive processes, and cyclic scenarios. However, the Extended ESD has not been fully developed, as Xie et al. (2010) showed some limitations in the proposed icons that can affect the modeling of many dynamic scenarios.

2.5.6. TOPIC 6: DYNAMIC BAYESIAN NETWORKS (DBNS)

DBNs are probabilistic networks based on graph theory and can be considered as one of the most promising modeling techniques utilized to assess the reliability and safety of dynamic systems recently (Boudali and Dugan 2005; Langseth and Portinale 2007; Mahadevan et al. 2001). According to Weber et al. (2012), *Reliability Engineering and System Safety* published a significant number of articles related to DBNs and their applications to risk analysis between 1999 and 2009. Although this modeling technique can add value to the NPP monitoring processes, the application of DBNs to investigate the safety of dynamic NPP systems is still limited (Jones et al. 2016).

DBNs are a graphical method that contains a set of nodes, representing random variables that can change with time, and directed links between these nodes, representing temporal probabilistic dependencies between the connected variables.

DBNs allow the modeling of random variables and investigation of their influence on the future distribution of other variables (Weber and Jouffe 2006). For example, Varuttamaseni (2011) integrated DBNs with reactor transient code to evaluate the time-dependent core damage frequency following a loss-of-feedwater accident. A combination of discrete DET (implemented through ADAPT), MELCOR, and BN techniques were also integrated to provide a new risk-informed accident management framework for NPP diagnostic support (Groth et al. 2014). In a different study, Jones et al. (2016) investigated the viability of the developed framework through DBNs. The developed DBN was utilized to investigate the conditions of observed power plant parameters that could lead to transient overpower and loss of flow accidents. Based on this framework, Groth et al. (2018) developed a prototype model to analyze and investigate the generic sodium fast reactor states following the loss of flow and earthquake-induced overpower transients. Another recent application utilized DBNs to assess two critical systems, namely the fire alarm system and the steam generator system (Amin et al. 2018).

2.6. CURRENT CHALLENGES AND FUTURE RESEARCH ROADMAP

DPRA methodologies have been extensively utilized to investigate the crew behavior and the dynamic response of NPP systems following an internal event such as loss-of-feedwater, station blackout, and shutdown of the safety system. Although numerous papers related to DPRA of NPPs have been published in journals and conference proceedings, some key challenges still need to be addressed. DPRA methodologies adopting dynamic event trees provide extensive

information associated with all the possible accident-sequence scenarios since each branch contains evolution over time of a large number of system variables, and therefore can generate a large number of branches (Mandelli et al. 2013a). In this respect, DPRA methodologies are computationally expensive and memory-intensive with a storage requirement of gigabytes or higher (Mandelli et al. 2018), and can be challenging to organize and interpret the underlying data toward identifying scenario evolutions and the primary risk contributors for each initiating event (Zio 2009). In addition, such a large amount of information can lead to complexity in extracting useful information and provide an insufficient estimate for the risk and its associated uncertainty (Mandelli et al. 2013b). As a result of these challenges, to date, DPRA methodologies have only been used to simulate critical situations for small subsystems, when the interactions between the process variable and the control systems are important or when operator actions need to be explicitly modeled; these methodologies have limited applications in the risk assessment of large/complex systems (Varuttamaseni 2011). Moreover, the Fukushima nuclear accident demonstrated the importance of quantifying the risk of multi-unit NPPs; however, only a limited number of studies have analyzed the risk associated with the dynamic interaction between multiple units under normal and abnormal events (Mandelli et al. 2017b).

The rate of publications on DPRA of NPPs has grown rapidly due to the importance and the promising potential of DPRA approaches. DPRA methodologies experienced major evolution over four decades to continuously

enhance and improve the overall safety of NPPs. Some of these methodologies are still being developed and improved at laboratories, universities, and organizations. In addition, some of the key challenges mentioned above are currently under investigation. In this regard, the current study presents a set of research streams that need to be considered in future studies. This study demonstrates the importance of improving and/or developing DPRA tools that are capable of simulating large subsystems within NPPs. Such complex and interdependent subsystems need to be precisely simulated to consider all the scenarios that may occur during the operation of NPPs. In addition, multi-unit risk is an important issue in several countries and needs to be addressed comprehensively since the majority of NPPs contain more than one reactor unit (Kumar et al. 2015). Thus, multi-unit DPRA of NPPs is a crucial research stream that requires several studies to assess the safety of NPPs under normal or abnormal operating conditions (Mandelli et al. 2017b). Moreover, several algorithms (e.g., regression models, artificial neural networks, cluster analysis, machine learning) have been developed recently to analyze large amounts of information; these methods/algorithms can be used for data mining of DPRA data to extract useful information from large data sets. This study also recommends the importance of continuous funding for researchers, universities, and laboratories to support the developed work in DPRA methodologies. Recent DPRA methodologies (e.g., RAVEN, ADAPT, DBNs) have shown great potential in DPRA of NPPs; these methodologies are under development, and it is recommended to consider the challenges mentioned above in their future

development efforts.

2.7. CONCLUSIONS

NPPs are complex dynamic systems-of-systems because of their internal interdependence and their connectivity to other external systems. Previous research studies have been conducted to develop DPRA methodologies that take into account the dynamic interactions between hardware, software, and operator actions. In this respect, a total of 387 articles published in 50 different journals and conferences from 1981 to 2019 was analyzed in the current study using text mining to identify the key topics in the field of DPRA of NPP. The LDA topic modeling was used to identify and categorize published articles in terms of their topics. An N-Gram classification model was also developed, providing visual networks to evaluate the DPRA research topics. Afterward, quantitative measures were performed to estimate the temporal distribution of these topics over four decades. Based on such quantitative analyses, a qualitative literature review was presented to show several DPRA simulation/graphical methods and their corresponding applications within the nuclear engineering field, in addition to investigate the main challenges facing the current DPRA approach.

The analysis results identified eight topics related to the DPRA simulation approaches/methodologies and six related to graphical methodologies. LDA results demonstrated that the discrete dynamic event tree is one of the most common approaches for DPRA simulation methodologies. In addition, RAVEN, ADAPT, and DBNs all showed a growing trend among recent publications related to DPRA.

Furthermore, the results showed the significant impact of both ADS-IDAC and DFM in publications on DPRA simulation and graphical methods, respectively. In addition, the quantitative analysis showed several applications of DPRA simulation methodologies related to station blackout, fire, flood, steam generator tube rupture, and operator actions.

Text mining analysis and quantitative literature review presented in the current study demonstrates the impact of DPRA methodologies in enhancing the safety of NPPs by overcoming the limitation of static PRA. Several universities, laboratories, and organizations are continually working on improving and/or developing DPRA methodologies for NPPs. However, the qualitative literature review of DPRA methodologies has highlighted specific challenges in simulating large/complex systems and analyzing massive data for a considerable number of scenarios, highlighting the necessity of developing a more efficient DPRA platform that can overcome the current limitations of DPRA and enhance the overall safety of NPPs. Further research is required to address DPRA-related challenges, such as simulating several subsystems, considering the dynamic interaction among multi-units, and analyzing the large value of DPRA-data in order to improve our understanding of DPRA of NPPs.

2.8. ACKNOWLEDGMENTS

The financial support for the study was provided through the Canadian Nuclear Energy Infrastructure Resilience under Seismic Systemic Risk (CaNRisk) – Collaborative Research and Training Experience (CREATE) program of the

Natural Science and Engineering Research Council (NSERC) of Canada. Additional support through the INViSiONLab and the INTERFACE Institute is also acknowledged.

2.9. NOTATION

The following symbols are used in this paper:

D	=	Number of documents;
d	=	Index of documents, ($d \in \{1,..., D\}$);
K	=	Number of topics;
k	=	Index of topics, ($k \in \{1,..., K\}$);
w_{di}	=	Word i in document d;
Z_{di}	=	Topic assignment for word w_{di} from document d;
θ	=	Topic distribution;
θ_d	=	Multinomial distribution of topics in a document d;
α	=	Dirichlet prior on the per-document topic distributions;
β	=	Dirichlet prior on the per-topic word distributions;
ψ	=	Word distribution;
ψ_k	=	Distribution of words in topic k;
ψ_{kw}	=	Probability of word w in topic k; and
ψ_{Zdi}	=	Multinomial distribution of topic assignment for word w_{di} from document d.

2.10. REFERENCES

Acosta, C. G., and Siu, N. (1991). "Dynamic Event Tree Analysis Method (DETAM) for Accident Sequence Analysis." Ph.D. Thesis. Massachusetts Institute of Technology.

Acosta, C., and Siu, N. (1993). "Dynamic event trees in accident sequence analysis: application to steam generator tube rupture." *Reliability Engineering and System Safety*, 41(2), 135–154.

Aldemir, T. (2013). "A survey of dynamic methodologies for probabilistic safety assessment of nuclear power plants." *Annals of Nuclear Energy*, Elsevier Ltd, 52, 113–124.

Aldemir, T., Guarro, S., Kirschenbaum, J., Mandelli, D., Mangan, L. A., Bucci, P., Yau, M., Johnson, B., Elks, C., Ekici, E., Stovsky, M. P., Miller, D. W., Sun, X., Arndt, S. A., Nguyen, Q., and Dion, J. (2009). *A Benchmark Implementation of Two Dynamic Methodologies for the Reliability Modeling of Digital*. NUREG/CR-6985, U.S. Nuclear Regulatory Commission, Washington D.C.

Alfonsi, A., Rabiti, C., Mandelli, D., Cogliati, J. J., and Kinoshita, R. A. (2013). "Raven As a Tool for Dynamic Probabilistic Risk Assessment: Software Overview." *International Conference on Mathematics and Computational Methods Applied to Nuclear Science& Engineering (M&C 2013)*.

Alfonsi, A., Rabiti, C., Mandelli, D., Cogliati, J., Kinoshita, R., and Naviglio, A. (2014). "RAVEN and Dynamic Probabilistic Risk Assessment: Software

Overview." *Proceedings of ESREL European Safety and Reliability Conference*, 759–766.

Alghamdi, R., and Alfalqi, K. (2015). "A Survey of Topic Modeling in Text Mining." *International Journal of Advanced Computer Science and Applications*, 6(1), 147–153.

Amendola, A., and Reina, G. (1981). "Event sequences and consequence spectrum: a methodology for probabilistic transient analysis." *Nuclear Science and Engineering*, 77, 297–315.

Amin, M. T., Khan, F., and Imtiaz, S. (2018). "Dynamic Availability Assessment of Safety Critical Systems Using a Dynamic Bayesian Network." *Reliability Engineering and System Safety*, Elsevier Ltd.

Blei, D. M., Ng, A. Y., and Jordan, M. I. (2003). "Latent Dirichlet Allocation." *Journal of Machine Learning Research*, 3, 993–1022.

Boudali, H., and Dugan, J. B. (2005). "A discrete-time Bayesian network reliability modeling and analysis framework." *Reliability Engineering and System Safety*, 87, 337–349.

Bucci, S. P., Inserra, D., Lesser, J., Mayer, M. A., Slattery, B., Spencer, J., and Tubb, K. (2013). *After Hurricane Sandy: Time to Learn and Implement the Lessons in Preparedness, Response, and Resilience*. The Heritage Foundation Emergency Preparedness Working Group. 144.

Cacciabue, P. C., Amendola, A., and Cojazzi, G. (1986). "Dynamic Logical Analytical Methodology Versus Fault Tree: The Case Study of the Auxiliary

Feedwater System of a Nuclear Power Plant." *Nuclear Technology*, 74(2), 195–208.

Campbell, J. C., Hindle, A., and Stroulia, E. (2015). "Latent Dirichlet Allocation: Extracting Topics from Software Engineering Data." *In The art and science of analyzing software data*, 139–159.

Canadian Nuclear Association. (2019). *The Canadian Nuclear Factbook*.

Cepin, M. (2001). "Dynamic fault tree as an extension of standard fault tree." *Transactions of the American Nuclear Society*, ANS,USA.

Cepin, M., and Mavko, B. (2002). "A dynamic fault tree." *Reliability Engineering and System Safety*, 75, 83–91.

Chang, Y. H. J., and Mosleh, A. (2007a). "Cognitive modeling and dynamic probabilistic simulation of operating crew response to complex system accidents. Part 2: IDAC performance influencing factors model." *Reliability Engineering and System Safety*, 92(8), 1014–1040.

Chang, Y. H. J., and Mosleh, A. (2007b). "Cognitive modeling and dynamic probabilistic simulation of operating crew response to complex system accidents Part 1: Overview of the IDAC Model." *Reliability Engineering & System Safety*, 92, 997–1013.

Chang, Y. H., Mosleh, A., and Dang, V. N. (2003). *Development of Dynamic Probabilistic Safety Assessment: the Accident Dynamic Simulator (ADS) Tool*. *University of Maryland*.

Cho, S. M., Hong, H. S., and Cha, S. D. (1996). "Safety Analysis Using Coloured

Petri Nets." *Proceedings of the Asia Pacific Software Engineering Conference (APSEC 1996)*, 176–193.

CNSC. (2017). "Probabilistic safety assessment: A tool to estimate risk and drive safety improvement at nuclear power plants." <http://nuclearsafety.gc.ca/eng/resources/educational-resources/feature-articles/probabilistic-safety-assessment.cfm>.

Cojazzi, G. (1996). "The DYLAM approach for the dynamic reliability analysis of systems." *Reliability Engineering and System Safety*, 52(3 SPEC. ISS.), 279–296.

Correa, J. (2001). "Interval estimation of the parameters of the multinomial distribution." *Statistics on the Internet.*, 1–9.

David, R., and Alla, H. (2004). *Discrete, Continuous, and Hybrid Petri Nets*. Springer-Verlag, Berlin, Heidelberg, Germany.

Dugan, J. B. (1991). "Automated-Analysis Of Phased-Mission Reliability." *IEEE Transactions on Reliability*, 40(1).

Dugan, J. B. (2000). "A tool for dynamic fault tree analysis." *Computer Performance Evaluation, Proceedings, 1786*, 328–331.

Dugan, J. B., Bavuso, S. J., and Boyd, M. A. (1992). "Dynamic Fault-Tree Models for Fault-Tolerant Computer Systems." *IEEE Transactions on Reliability*, 41(3), 363–377.

Dugan, J. B., Sullivan, K. J., and Coppit, D. (2000). "Developing a Low-Cost High-Quality Software Tool for Dynamic Fault-Tree Analysis." *IEEE*

Transactions on Reliability, 49(1), 49–59.

El-Sefy, M., Ezzeldin, M., El-Dakhakhni, W., Wiebe, L., and Nagasaki, S. (2019). "System Dynamics Simulation of the Thermal Dynamic Processes in Nuclear Power Plants." *Nuclear Engineering and Technology*, Elsevier Ltd, 51(6), 1540–1553.

Engineering Village. (2020). <https://www.engineeringvillage.com/home.url>.

Ezzeldin, M., and El-Dakhakhni, W. (2019). "Metaresearching Structural Engineering Using Text Mining Trend Identifications and Knowledge Gap Discoveries." *Journal of Structural Engineering*.

Garrett, C. J., Guarro, S. B., and Apostolakis, G. E. (1993). "Assessing digital control system dependability using the dynamic flowgraph methodology." *American Nuclear Society 1993 Winter Meeting*.

Gatti, C. J., Brooks, J. D., and Nurre, S. G. (2015). *A historical analysis of the field of OR/MS using topic models*. arXiv:1510.05154.

Gauntt, R.O., Cole, R., Erickson, C. M., Gido, R. G., Gasser, R. D., Rodriguez, S. B., and Young, M. F. (2000). *MELCOR Computer Code Manuals*.

Gomes, I. B., and Saldanha, P. L. C. (2013). "A Cell-to-Cell Markovian Model for the Reliability of a Digital Control System of a Steam Generator." *International Nuclear Atlantic Conference - INAC 2013*.

Google Scholar. (2020). <https://scholar.google.com/>.

Greene, D., and Cross, J. P. (2015). "Unveiling the Political Agenda of the European Parliament Plenary : A Topical Analysis." *Proceedings of the ACM*

web science conference. ACM.

Griffiths, T. L., and Steyvers, M. (2004). "Finding scientific topics." *Proceedings of the National Academy of Sciences*, 101(suppl. 1), 5228–5235.

Groth, K. M., Denman, M. R., Cardoni, J. N., and Wheeler, T. A. (2014). "'Smart Procedures': Using dynamic PRA to develop dynamic, context- specific severe accident management guidelines (SAMGs)." *Probabilistic Safety Assessment and Management PSAM 12*.

Groth, K. M., Denman, M. R., Darling, M. C., Jones, T. B., and Luger, G. F. (2018). "Building and using dynamic risk-informed diagnosis procedures for complex system accidents." *Journal of Risk and Reliability*.

Hakobyan, A., Aldemir, T., Denning, R., Dunagan, S., Kunsman, D., Rutt, B., and Catalyurek, U. (2008). "Dynamic generation of accident progression event trees." *Nuclear Engineering and Design*, 238, 3457–3467.

Hakobyan, A., Denning, R., Aldemir, T., Dunagan, S., and Kunsman, D. (2006). "A Methodology for Generating Dynamic Accident Progression Event Trees for Level-2 PRA." *ANS Topical Meeting on Reactor Physics*, 1–9.

Hakobyan, A. P. (2006). "Severe accident analysis using dynamic accident progression event trees." Ph.D. Thesis, The Ohio State University.

Hofer, E., Kloos, M., Krzykacz-Hausmann, B., Peschke, J., and Sonnenkalb, M. (2002). "Dynamic event trees for probabilistic safety analysis." *EUROSAFE Forum 2002: convergence of nuclear safety practices in Europe Papers, Germany*.

Hofmann, M., and Chisholm, A. (2016). *Text Mining and Visualization: Case Studies Using Open-source Tools*. CRC Press.

Hsueh, K. S., and Mosleh, A. (1996). "The development and application of the accident dynamic simulator for dynamic probabilistic risk assessment of nuclear power plants." *Reliability Engineering and System Safety*, 52, 297–314.

Hu, Y. (2005). "A Guided Simulation Methodology for Dynamic Probabilistic Risk Assessment of Complex Systems." Ph.D. Thesis. University of Maryland.

IAEA. (2009). *Deterministic Safety Analysis for Nuclear Power Plants*. *International Atomic Energy Agency*.

IAEA. (2010). *Development and Application of Level 2 Probabilistic Safety Assessment for Nuclear Power Plants*.

Jankovsky, Z. K., Denman, M. R., and Aldemir, T. (2018a). "Dynamic event tree analysis with the SAS4A/SASSYS-1 safety analysis code." *Annals of Nuclear Energy*, Elsevier Ltd, 115, 55–72.

Jankovsky, Z. K., Haskin, T., and Denman, M. (2018b). *How to ADAPT*. Sandia National Laboratories.

Jones, T. B., Darling, M. C., Groth, K. M., Denman, M. R., and Luger, G. F. (2016). "A Dynamic Bayesian Network for Diagnosing Nuclear Power Plant Accidents." *The 29th International Florida Artificial Intelligence Research Society Conference*, 179–184.

Karanta, I. (2013). “Implementing dynamic flowgraph methodology models with logic programs.” *Journal of Risk and Reliability*, 227(3), 302–314.

Khoury, R., and Sapsford, F. (2016). “Latin word stemming using Wiktionary.” *Digital Scholarship in the Humanities*, 31(2), 368–373.

Kim, I. S., Jang, M., and Kim, S. R. (2017). “Holistic Approach to Multi-Unit Site Risk Assessment: Status and Issues.” *Nuclear Engineering and Technology*, Elsevier B.V, 49, 286–294.

Kloos, M., and Peschke, J. (2007). “Consideration of human actions in combination with the probabilistic dynamics method MCDET.” *European Safety and Reliability Conference*.

Koltcov, S., Koltsova, O., and Nikolenko, S. (2014). “Latent Dirichlet Allocation : Stability and Applications to Studies of User-Generated Content.”

Kumar, C. S., Hassija, V., Velusamy, K., and Balasubramaniyan, V. (2015). “Integrated risk assessment for multi-unit NPP sites - A comparison.” *Nuclear Engineering and Design*, Elsevier B.V., 293, 53–62.

Kunsman, D. M., Dunagan, S., Aldemir, T., Denning, R., Hakobyan, A., Metzroth, K., Catalyurek, U., and Rutt, B. (2008). *Development and Application of the Dynamic System Doctor to Nuclear Reactor Probabilistic Risk Assessments*. Sandia National Laboratories.

Langseth, H., and Portinale, L. (2007). “Bayesian networks in reliability.” *Reliability Engineering and System Safety*, 92, 92–108.

Lazard, A. J., Scheinfeld, E., Bernhardt, J. M., Wilcox, G. B., and Suran, M.

(2015). “Detecting themes of public concern: A text mining analysis of the Centers for Disease Control and Prevention’s Ebola live Twitter chat.” *American Journal of Infection Control*, Elsevier Inc, 43(10), 1109–1111.

Leveson, N. G., and Stolzy, J. L. (1987). “Safety Analysis Using Petr Nets.” *IEEE Transactions on Software Engineering*, SE-13(3), 386–397.

Li, W., Gu, D., and Zhang, H. (2017). “MARKOV/CCMT Dynamic Reliability Analysis of the Main and Startup Feedwater Control System in Nuclear Power Plant.” *Proceedings of the 2017 25th International Conference on Nuclear Engineering, ICONE25*.

Mahadevan, S., Zhang, R., and Smith, N. (2001). “Bayesian networks for system reliability reassessment.” *Structural Safety*, 23, 231–251.

Mandelli, D. (2008). “Reliability Modeling of Digital Control Systems Using the Markov/Cell-to-Cell Mapping Technique.” M.Sc. Thesis. The Ohio State University.

Mandelli, D., Maljovec, D., Alfonsi, A., Parisi, C., Talbot, P., Cogliati, J., Smith, C., and Rabiti, C. (2018). “Mining data in a dynamic PRA framework.” *Progress in Nuclear Energy*, Elsevier, 108, 99–110.

Mandelli, D., Parisi, C., Alfonsi, A., Maljovec, D., Germain, S. S., Boring, R., Ewing, S., Smith, C., and Rabiti, C. (2017). “Dynamic PRA of a Multi-Unit Plant.” *International Topical Meeting on Probabilistic Safety Assessment (PSA 2017)*.

Mandelli, D., Smith, C., Rabiti, C., Alfonsi, A., Youngblood, R., Pascucci, V.,

Wang, B., Maljovec, D., Bremer, P. T., Aldemir, T., Yilmaz, A., and Zamalieva, D. (2013a). "Dynamic PRA: An Overview of New Algorithms to Generate, Analyze and Visualize Data." *Transactions of the American Nuclear Society*.

Mandelli, D., Smith, C., Riley, T., Nielsen, J., Schroeder, J., Rabiti, C., Alfonsi, A., Cogliati, J., Kinoshita, R., Pascucci, V., Wang, B., and Maljovec, D. (2014). "Overview of New Tools to Perform Safety Analysis: BWR Station Black Out Test Case." *Probabilistic Safety Assessment & Management conference (PSAM)*.

Mandelli, D., Yilmaz, A., Aldemir, T., Metzroth, K., and Denning, R. (2013b). "Scenario clustering and dynamic probabilistic risk assessment." *Reliability Engineering and System Safety*, Elsevier, 115, 146–160.

Maskeri, G., Sarkar, S., and Heafield, K. (2008). "Mining Business Topics in Source Code using Latent Dirichlet Allocation." *In Proc of India Software Engineering Conference*, 113–120.

Matsuoka, T. (1988). "The GO-FLOW Methodology: A Reliability Analysis of the Emergency Core Cooling System of a Marine Reactor Under Accident Conditions." *Nuclear Technology*, 84.

Matsuoka, T., and Kobayashi, M. (1985). "GO-FLOW: A Reliability Analysis Methodology Applicable to Piping Systems." *International Topical Meeting on Probalistic Safety Methods and Applications*.

Matsuoka, T., and Kobayashi, M. (1987). "GO-FLOW: A New Reliability

Analysis Methodology." *Nuclear Science and Engineering*, 98, 94–78.

Mercurio, D., Podofillini, L., Zio, E., and Dang, V. N. (2009). "Identification and classification of dynamic event tree scenarios via possibilistic clustering: Application to a steam generator tube rupture event." *Accident Analysis and Prevention*, 41, 1180–1191.

Minka, T. P. (2000). *Estimating a Dirichlet distribution*. *Technical report, M.I.T*, Technical report, M.I.T.

Murata, T. (1989). "Petri Nets: Properties, Analysis and Applications." *IEEE*, 77(4), 541–580.

Nassirtoussi, A. K., Wah, T. Y., Aghabozorgi, S. R., and Ngo, D. C. L. (2014). "Text Mining for Market Prediction: A Systematic Review." *Expert Systems with Applications*, Elsevier Ltd.

Nejad-Hosseinian, S. H. (2007). "Automatic Generation of Generalized Event Sequence Diagrams for Guiding Simulation Based Dynamic Probabilistic Risk Assessment of Complex Systems." Ph.D. Thesis. University of Maryland.

Nivolianitou, Z., Amendola, A., and Reina, G. (1986). "Reliability analysis of chemical processes by the DYLAM approach." *Reliability Engineering*, 14, 163–182.

Pan, X., Maio, F. Di, and Zio, E. (2017). "A Benchmark of Dynamic Reliability Methods for Probabilistic Safety Assessment." *2nd International Conference on System Reliability and Safety*, 82–90.

Paul, M. J., and Dredze, M. (2011). "You Are What You Tweet : Analyzing Twitter for Public Health." *International AAAI Conference on Weblogs and Social Media You*, 265–272.

Qaiser, S., and Ali, R. (2018). "Text Mining : Use of TF-IDF to Examine the Relevance of Words to Documents Text Mining." *International Journal of Computer Applications*, 181(1), 25–29.

Rabiti, C., Alfonsi, A., Mandelli, D., Cogliati, J., and Martineau, R. (2012). "RAVEN as Control Logic and Probabilistic Risk Assessment Driver for RELAP-7." *ANS Winter Meeting*.

Rabiti, C., Alfonsi, A., Mandelli, D., Cogliati, J., Martineau, R., and Smith, C. L. (2013). *Deployment and Overview of RAVEN Capabilities for a Probabilistic Risk Assessment Demo for a PWR Station Blackout*. Idaho National Laboratory.

Rabiti, C., Alfonsia, A., Cogliatia, J., Mandellia, D., and Kinoshitaa, R. (2014). "RAVEN, a New Software for Dynamic Risk Analysis." *Proceedings of Probabilistic Safety Assessment and Management PSAM 12*.

Ren, Y. I., Fan, D., Wang, Z., and Yang, D. (2017). "A GO-FLOW and Dynamic Bayesian Network combination approach for reliability evaluation with uncertainty : A case study on a Nuclear." *IEEE*.

Salloum, S. A., Al-Emran, M., Monem, A. A., and Shaalan, K. (2018). "Using Text Mining Techniques for Extracting Information from Research Articles." Intelligent Natural Language Processing: Trends and Applications. Studies in

Computational Intelligence, vol 740. Springer, Cham., 373–397.

Silge, J., and Robinson, D. (2019). "Text Mining with R: Relationships between words: N-Grams and correlations." <https://www.tidytextmining.com/ngrams.html>.

Siu, N. (1994). "Risk assessment for dynamic systems: An overview." *Reliability Engineering and System Safety*, 43, 43–73.

Smidts, C. (1994). "Probabilistic dynamics: A comparison between continuous event trees and a discrete event tree model." *Reliability Engineering and System Safety*, 44, 189–206.

Swaminathan, S., and Smidts, C. (1999a). "The Event Sequence Diagram framework for dynamic Probabilistic Risk Assessment." *Reliability Engineering & System Safety*, 63, 73–90.

Swaminathan, S., and Smidts, C. (1999b). "Identification of missing scenarios in ESDs using probabilistic dynamics." *Reliability Engineering and System Safety*, 66, 275–279.

Swaminathan, S., and Smidts, C. (1999c). "The mathematical formulation for the event sequence diagram framework." *Reliability Engineering and System Safety*, 65, 103–118.

Takeshi, M. (2010). "GO-FLOW methodology-Basic concept and integrated analysis framework for its applications." *Nuclear Safety and Simulation*, 1(3).

Tang, J., Meng, Z., Nguyen, X., Mei, Q., and Zhang, M. (2014). "Understanding

the Limiting Factors of Topic Modeling via Posterior Contraction Analysis." *International Conference on Machine Learning*, 190–198.

Tavana, M. (2008). "Dynamic process modelling using Petri nets with applications to nuclear power plant emergency management." *International Journal of Simulation and Process Modelling*, 4(2), 130–138.

Tomek, L., Mainkar, V., Geist, R. M., and Trivedi, K. S. (1994). "Reliability Modeling of Life-Critical, Real-Time Systems." *IEEE*, 82(1), 108–121.

Tyrväinen, T. (2013). "Risk importance measures in the dynamic flowgraph methodology." *Reliability Engineering and System Safety*, Elsevier, 118, 35–50.

U.S. NRC. (1975). *Reactor Safety Study: An Assessment of Accident Risks in U.S. Commercial Nuclear Power Plants, WASH-1400 (NUREG-75/014)*.

U.S. NRC. (1990). *Severe Accident Risks : An Assessment for Five U.S. Nuclear Power Plants, NUREG- 1150*. U.S. Nuclear Regulatory Commission.

U.S. NRC. (1995). *RELAP5 / MOD3 Code Manual*. U.S Nuclear Regulatory Commission.

Varuttamaseni, A. (2011). "Bayesian Network Representing System Dynamics in Risk Analysis of Nuclear Systems." Ph.D. Thesis, University of Michigan.

Violos, J., Tserpes, K., Varlamis, I., and Varvarigou, T. (2018). "Text Classification Using the N-Gram Graph Representation Model Over High Frequency Data Streams." *Frontiers in Applied Mathematics and Statistics*, 4, 1–19.

Web of Science. (2020). <https://clarivate.com/webofsciencegroup/solutions/web-of-science/>.

Weber, P., and Jouffe, L. (2006). "Complex system reliability modelling with Dynamic Object Oriented Bayesian Networks (DOOBN)." *Reliability Engineering and System Safety*, 91, 149–162.

Weber, P., Simon, C., and Iung, B. (2012). "Overview on Bayesian networks applications for dependability, risk analysis and maintenance areas." *Engineering Applications of Artificial Intelligence*, Elsevier, 25, 671–682.

Williamson, R. L., Hales, J. D., Novascone, S. R., Tonks, M. R., Gaston, D. R., Permann, C. J., Andrs, D., and Martineau, R. C. (2012). "Multidimensional multiphysics simulation of nuclear fuel behavior." *Journal of Nuclear Materials*, Elsevier B.V., 423(1–3), 149–163.

World Nuclear Association. (2018). "The Harmony programme." <http://world-nuclear.org/harmony>.

Xie, H., Cai, Q., and Zhang, Y. (2010). "Iconic Representation Extension of Event Sequence Diagram Framework for Nuclear Power Plant." *The 18th International Conference on Nuclear Engineering ICONE18*.

Xinyu, D., Ming, Y., Bowen, Z., and Hongxing, L. (2017). "Hierarchical Modeling Of Go-Flow Models For Online Risk Monitoring Of Nuclear Power Plants." *the 25th International Conference on Nuclear Engineering*, 1–7.

Yin, J., Cao, J., and Wang, X. (2013). "An Implementation of DFM for Reliability

Modeling and Analyzing of AP1000 FWCS." *the 21st International Conference on Nuclear Engineering*, 1–7.

Yin, Z., Cao, L., Han, J., Zhai, C., and Huang, T. (2011). "Geographical Topic Discovery and Comparison." *International World Wide Web Conference Committee (IW3C2)*.

Yukiya Amano. (2015). *The Fukushima Daiichi Accident*. *International Atomic Energy Agency*, International Atomic Energy Agency.

Zhao, W., Chen, J. J., Perkins, R., Liu, Z., Ge, W., Ding, Y., and Zou, W. (2015). "A heuristic approach to determine an appropriate number of topics in topic modeling." *BMC Bioinformatics*, BioMed Central Ltd, 16(Suppl 13), S8.

Zio, E. (2009). "Reliability engineering : Old problems and new challenges." *Reliability Engineering and System Safety*, 94, 125–141.

Zio, E. (2014). "Integrated deterministic and probabilistic safety assessment: Concepts, challenges, research directions." *Nuclear Engineering and Design*, Elsevier B.V., 280, 413–419.

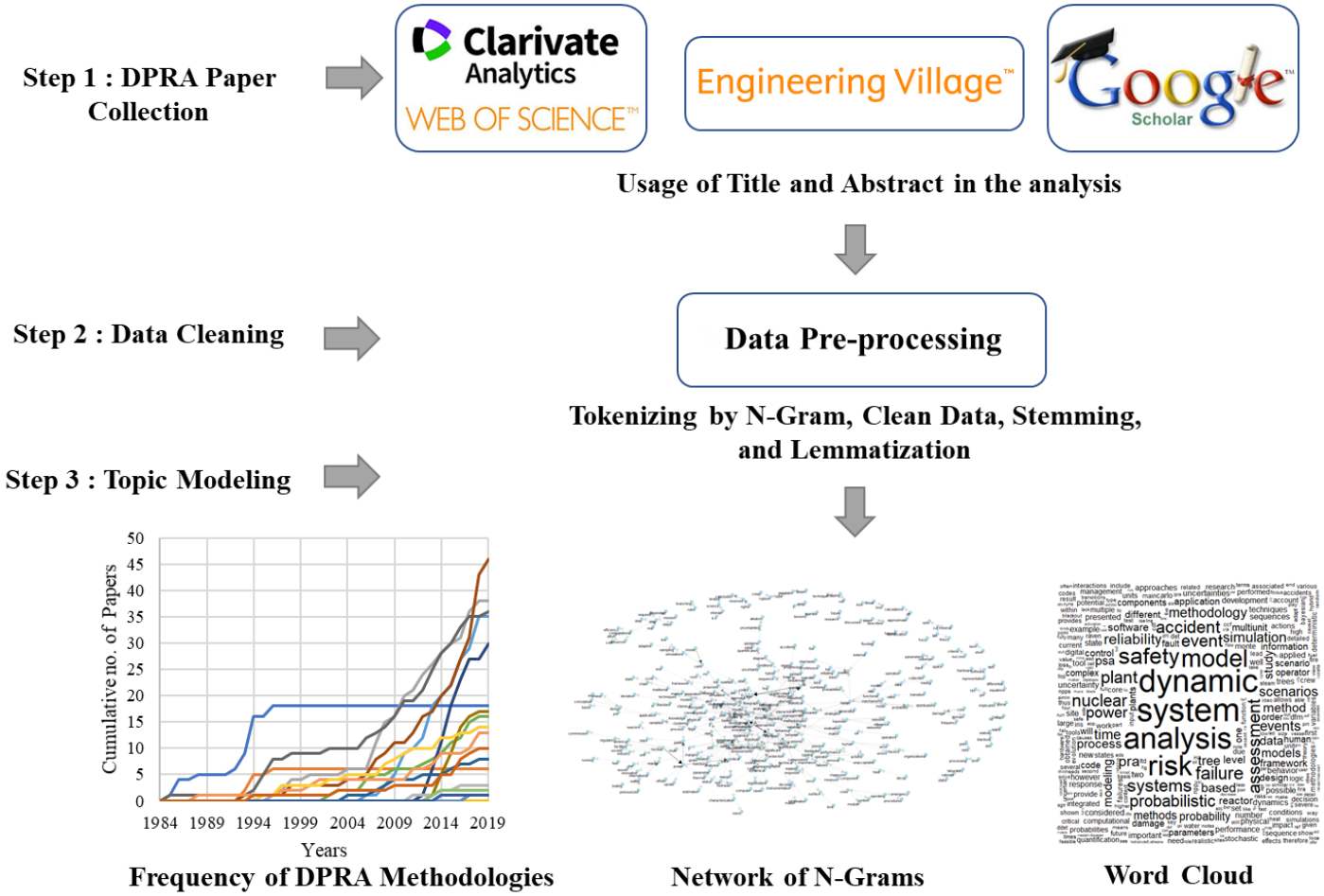

Figure 2-1: A Schematic Diagram for Text Mining Analysis Approach.

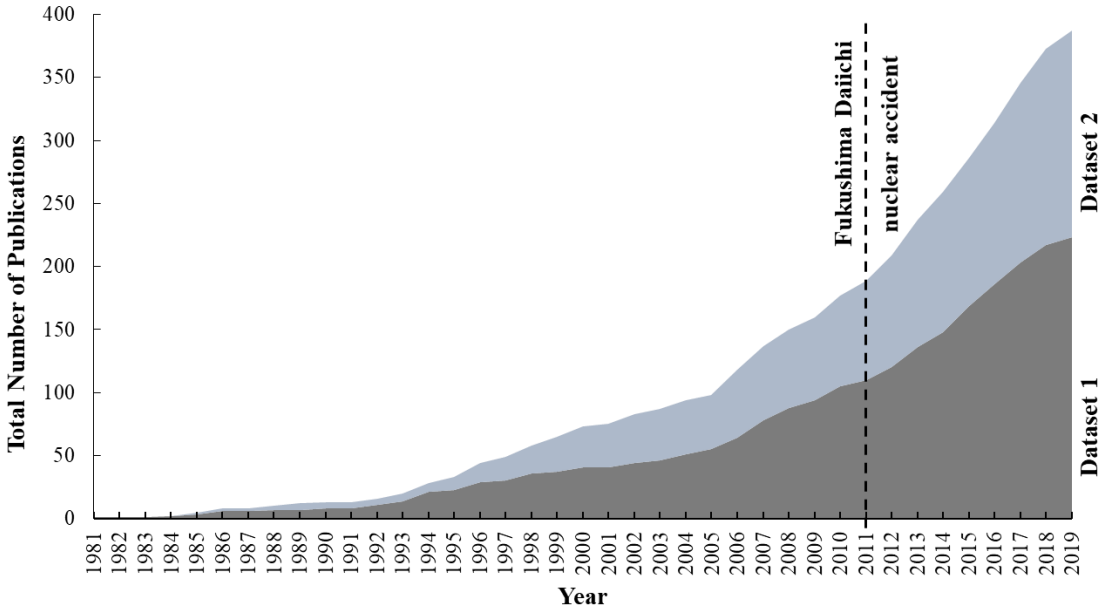

Figure 2-2: Cumulative Number of Publications for DPRA Methods from 1981 to 2019.

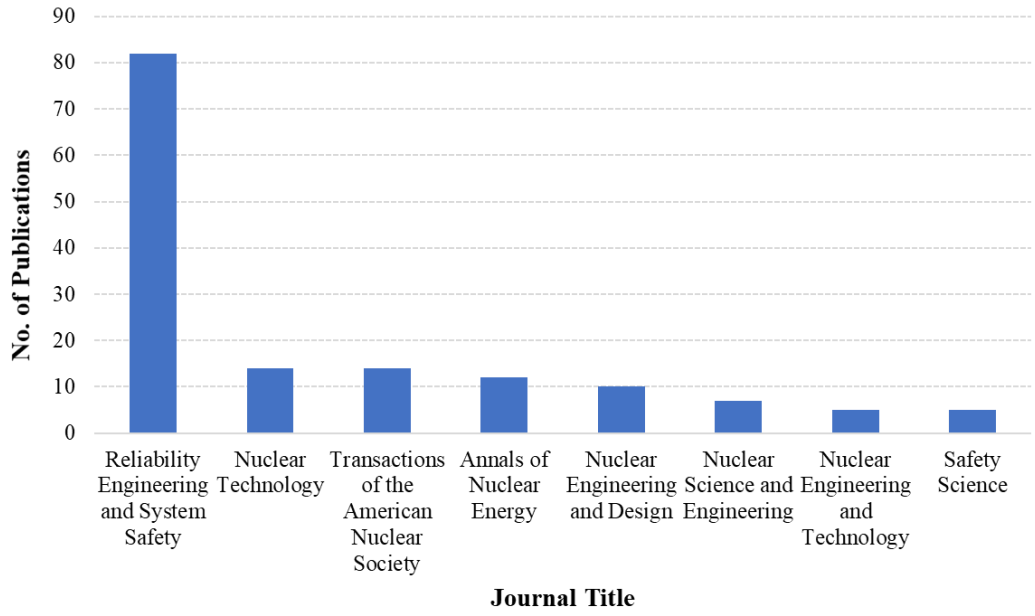

Figure 2-3: Ranking of Most Referred Journals by Number of Published Articles.

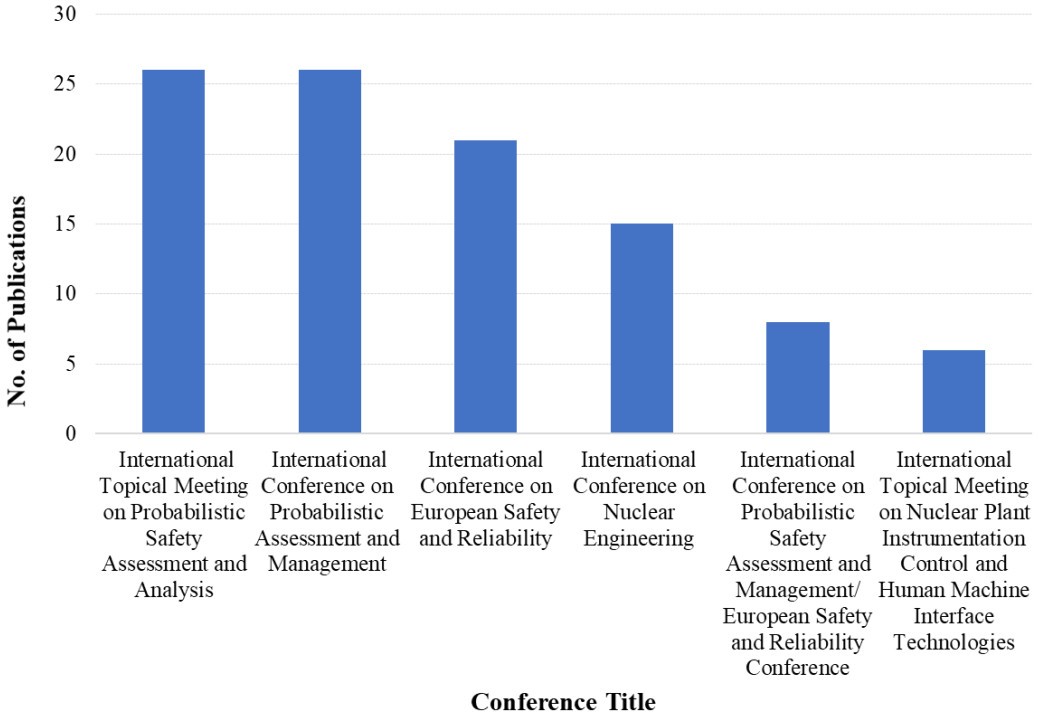

Figure 2-4: Ranking of Most Referred Conferences by Number of Published Articles.

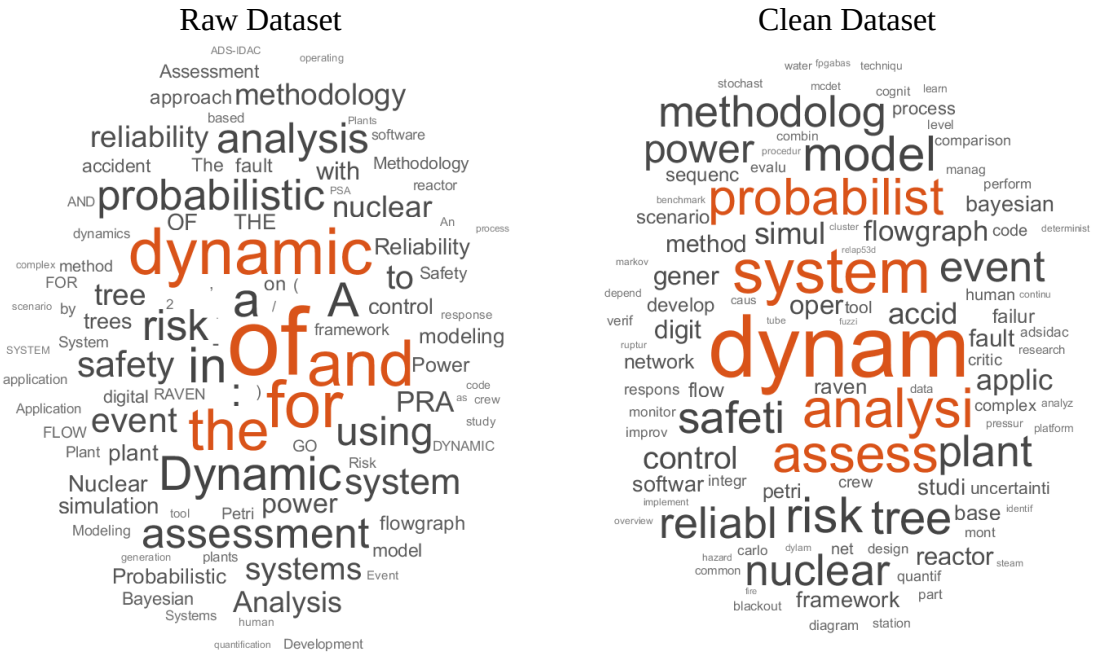

Figure 2-5: Comparison Between Raw and Clean Datasets Through Word Clouds.

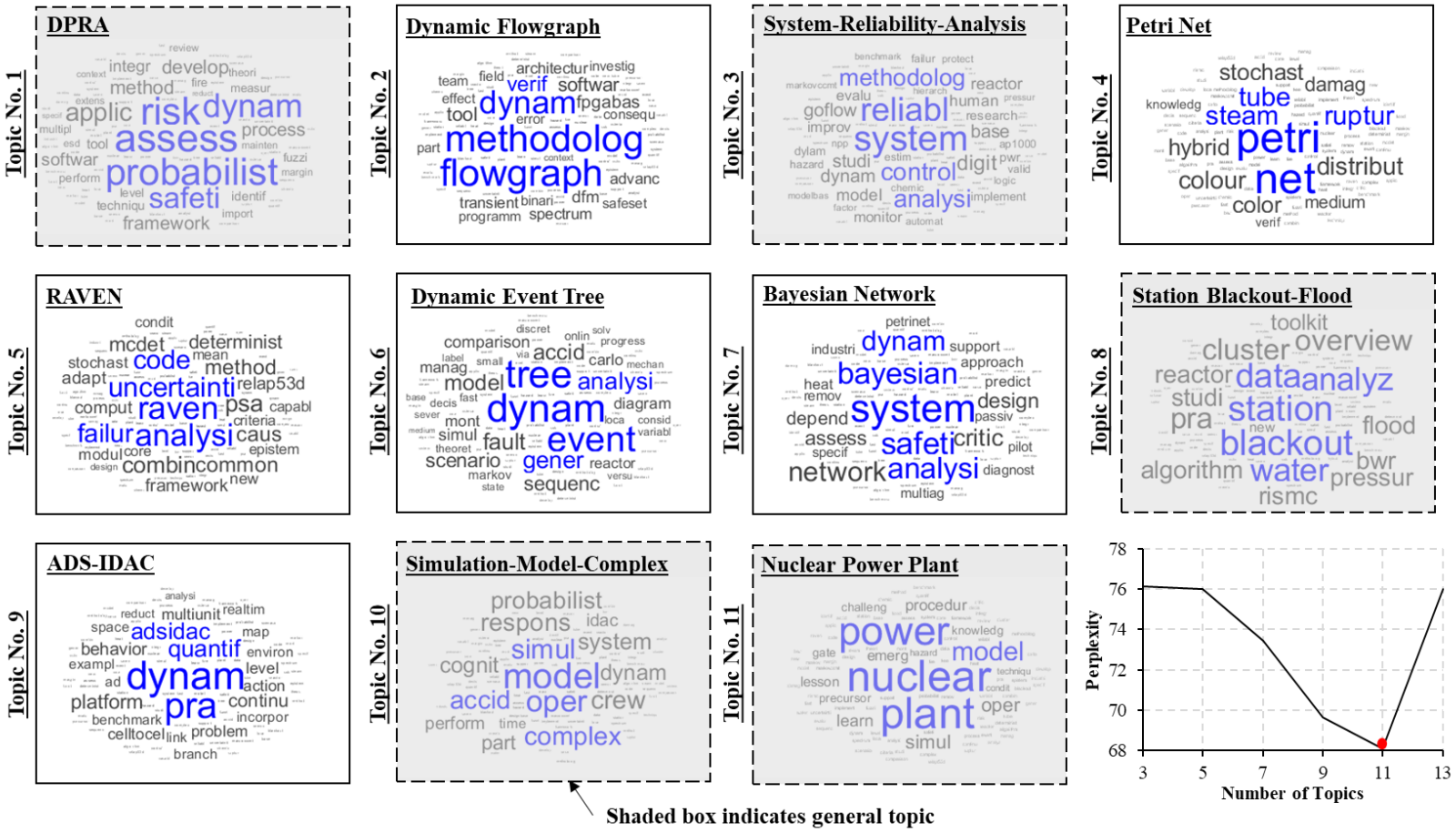

Figure 2-6: Word Cloud of Topic No.1 to Topic No.11 for DPRA Methods-Dataset A.

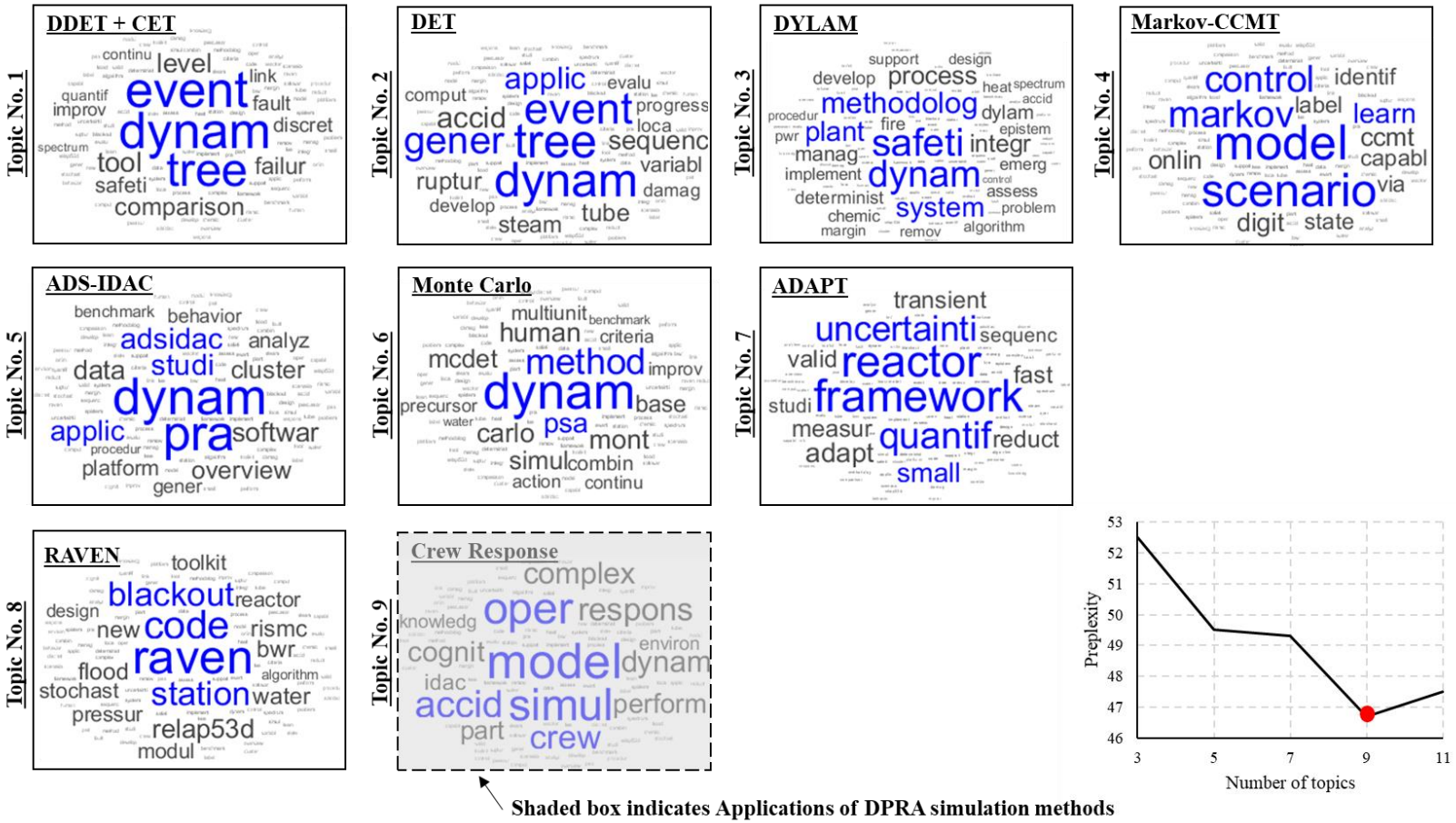

Figure 2-7: Word Cloud of Topic No.1 to Topic No.9 for DPRA Simulation Methods-Dataset 1.

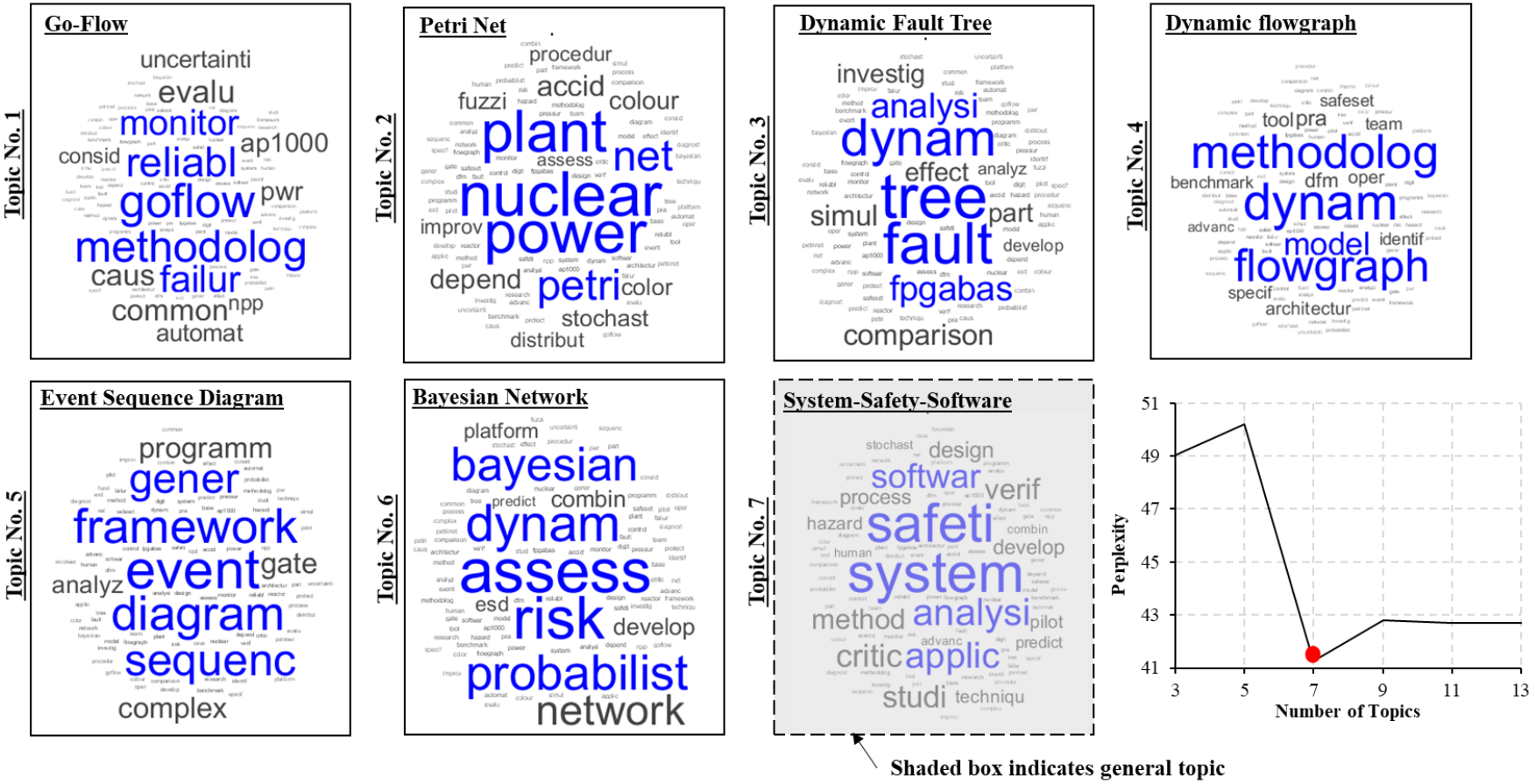

Figure 2-8: Word Cloud of Topic No.1 to Topic No.7 for DPRA Graphical Methods-Dataset 2.

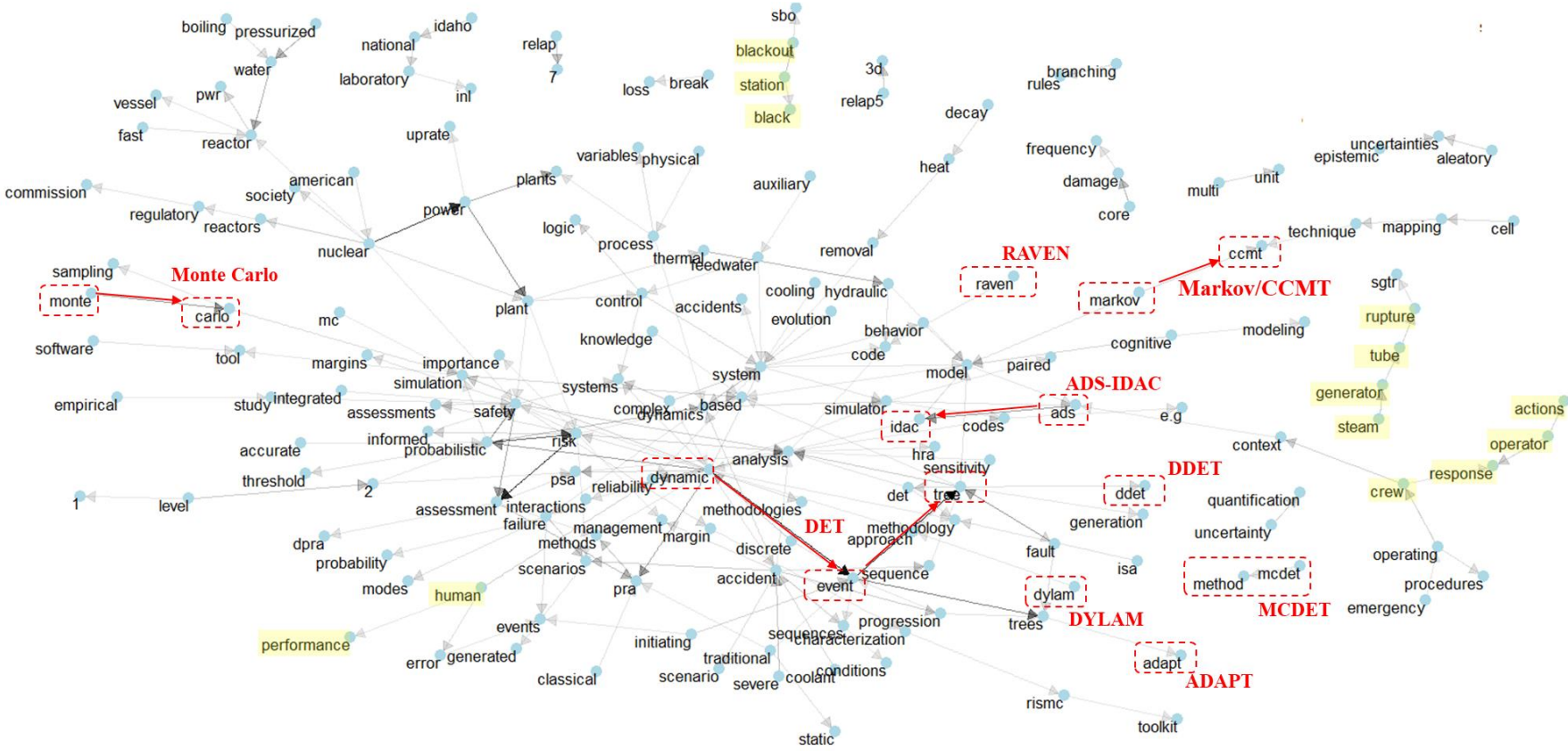

Figure 2-9: Directed graph for DPRA Simulation Methods-Dataset 1.

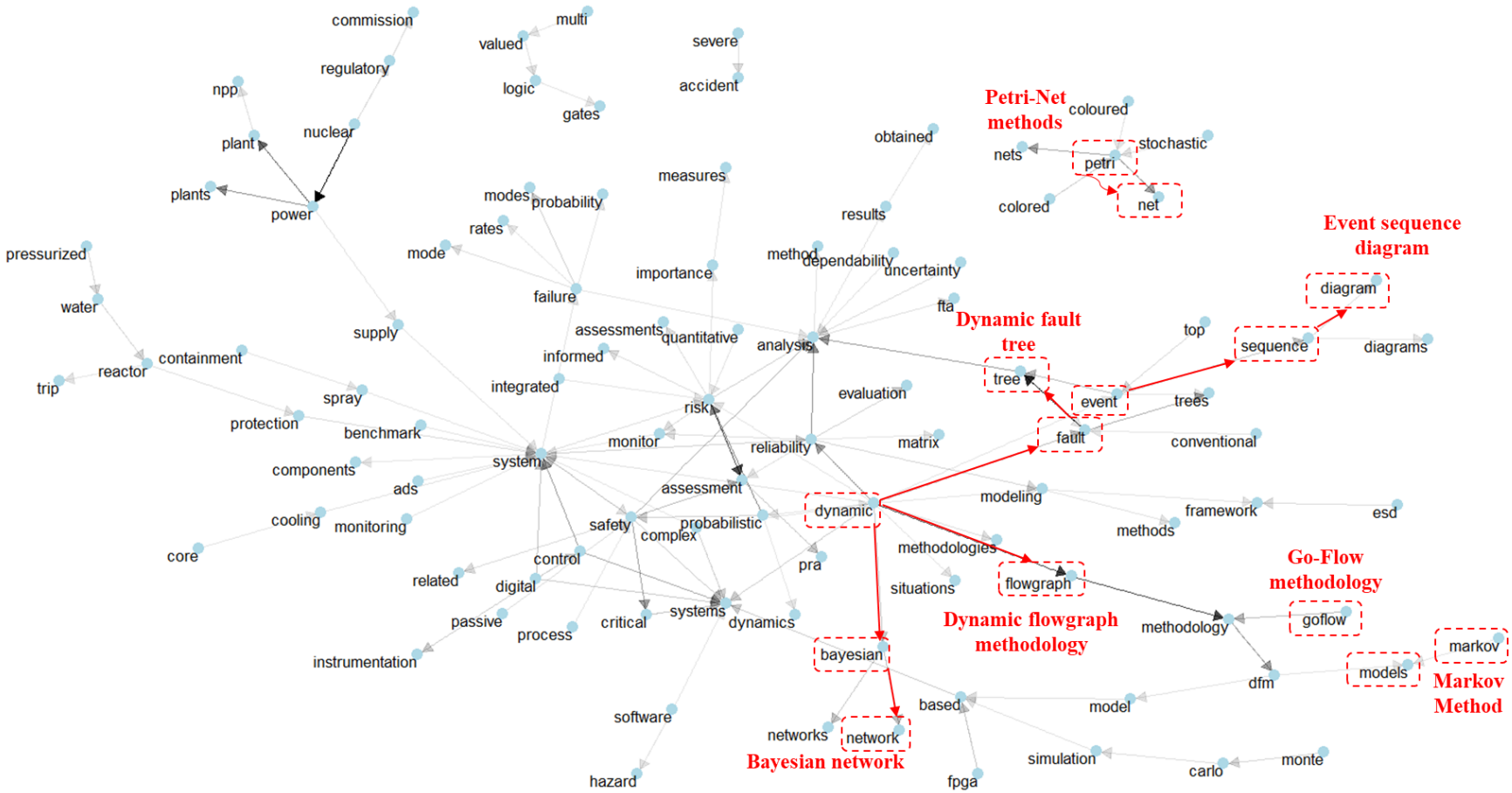

Figure 2-10: Directed Graph for DPRA Graphical Methods-Dataset 2.

a.

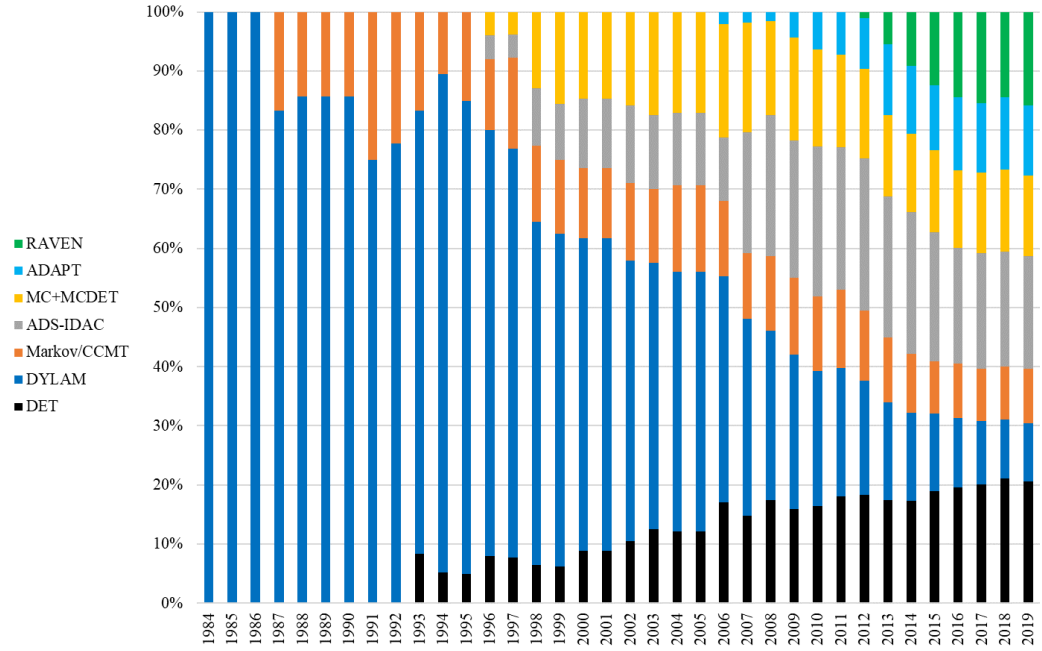

b.

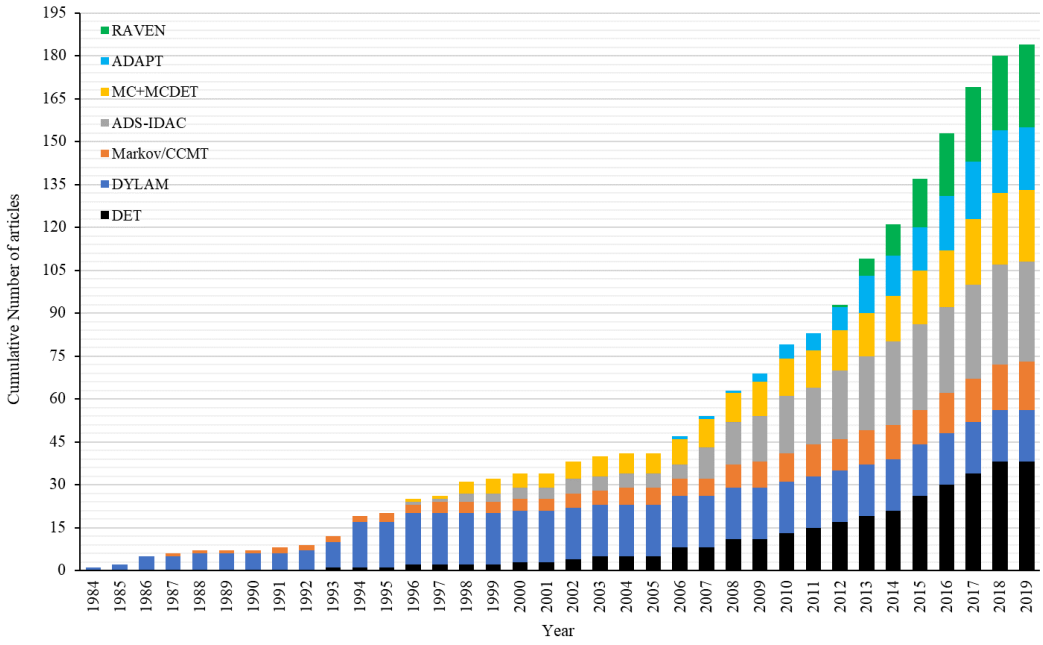

Figure 2-11: **a.** Topic distribution, and **b.** Cumulative number of publications for DPRA simulation methodologies from 1984 to 2019.

a.

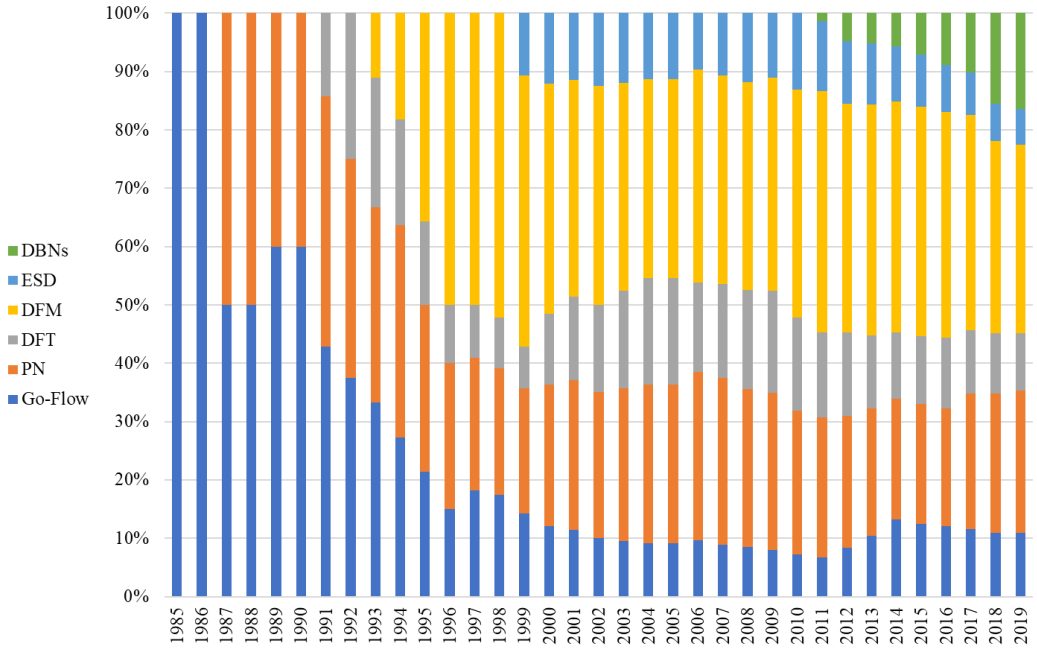

b.

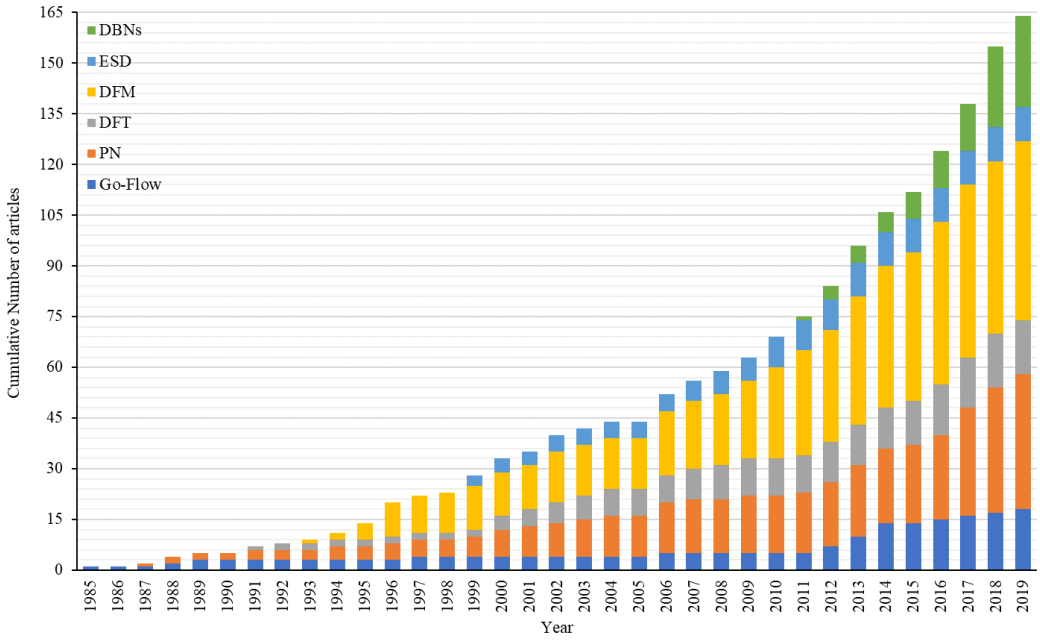

Figure 2-12: **a.** Topic distribution, and **b.** Cumulative number of publications for DPRA Graphical Topics from 1985 to 2019.

Chapter 3 : System Dynamics Simulation of the Thermal Dynamic Processes in Nuclear Power Plant

ABSTRACT

A nuclear power plant (NPP) is a highly complex system-of-systems as manifested through its internal systems interdependence. The negative impact of such interdependence was demonstrated through the 2011 Fukushima Daiichi nuclear disaster. As such, there is a critical need for new strategies to overcome the limitations of current risk assessment techniques (e.g., the use of *static* event and fault tree schemes), particularly through simulation of the nonlinear *dynamic* feedback mechanisms between the different NPP systems/components. As the first and key step towards developing an integrated NPP dynamic probabilistic risk assessment platform that can account for such feedback mechanisms, the current study adopts a system dynamics simulation approach to model the thermal dynamic processes in: the reactor core; the secondary coolant system; and the pressurized water reactor. The reactor core and secondary coolant system parameters used to develop system dynamics models are based on those of the Palo Verde Nuclear Generating Station. These three system dynamics models are subsequently validated, using results from published work, under different system perturbations including the change in reactivity, the steam valve coefficient, the primary coolant flow, and others. Moving forward, the developed system dynamics models can be

integrated with other interacting processes within a NPP to form the basis of a system-level (systemic) dynamic risk assessment tool.

Keywords: Nuclear power plant; Pressurized water reactor; Dynamic probabilistic risk assessment; System dynamics; Thermal dynamic processes.

3.1. INTRODUCTION

Nuclear power is considered a vital solution to the continuous demand for clean, secure, sustainable and reliable energy (IAEA 2016). The 448 nuclear power reactor units currently operating around the world provide 10.4% of the global electricity (World Nuclear Association 2019), while a total of 60 and 168 units are currently undergoing their construction and planning stages, respectively (Barrett 2017). As a result of their associated cost, nuclear power plants (NPP) are mega infrastructure that are expected to operate for a relatively long time span, whereas the plant design and planning decisions must account for abnormal events. Recent events (e.g., Fukushima Daiichi nuclear disaster) have highlighted that natural hazard intensity can exceed that originally used for plant design (Hassija et al. 2014). In addition to natural hazards, anthropogenic hazards (e.g., fire, internal flooding, and human-made errors) might also initiate events that lead to a component and/or system failure. In addition, both natural and anthropogenic hazards can, independently or through interaction, trigger cascade disasters (defined as disasters in which impacts progressively increase over time and cause unexpected secondary events of more significant consequences (Pescaroli and Alexander 2015)) throughout a major part of or the entire NPP, due to component/system interdependence. Such disasters have been known to cause major failures in NPP (e.g., Three Mile Island accident in 1979, Chernobyl disaster in 1986, H.B. Robinson NPP fire event in 2010, and Fukushima Daiichi disaster in 2011), as described by Little (2002), Mosleh (2014), and Perrow (2011). NPP

disasters can cause substantial economic and human losses where, for example, the Fukushima Daiichi disaster resulted in the release of a large amount of radioactive material (Chino et al. 2011), and more than 100,000 people were forced to evacuate communities within 25 miles from the NPP (Holt et al. 2012). The estimated total cost of this disaster is 500 billion U.S. dollars (ASME 2012), which includes the costs for cleanup and damaged units decommissioning and compensation to the affected people.

NPPs have typically been designed and constructed employing deterministic safety approaches, as described by IAEA safety standards (No. SSG-2) (IAEA 2009) and (Dawson 2017). These approaches assume that all the required functions can be achieved during normal and abnormal operations. Although there is a high level of confidence in NPP components when designed using such approaches (CNSC 2017), there is still a probability that a component does not perform as expected under normal operation scenarios, abnormal events, and extreme events, which necessitated adopting probabilistic risk assessment (PRA) approaches. PRA is an analytical technique that integrates the frequency of external/internal events, accident sequences, human reliability analysis, and the probability of components failure in order to evaluate NPP safety, as described in the U.S. Nuclear Regulatory Commission report NUREG/CR-2300 (1983).

The U.S. WASH-1400 was the first major PRA framework that investigated many accident sequences in NPP and provided quantitative estimates of the risk associated with these sequences (Bartel 2016). The WASH-1400 framework uses

static event and fault tree analysis schemes to simulate the accident sequences following an extreme event. Although such risk assessment techniques have experienced significant improvements, all these improvements essentially followed the WASH-1400 framework developed more than 40 years ago, as illustrated by Mosleh (2014), Dawson (2017), and Moieni and Spurgin (1994). As such, current risk assessment techniques still have significant fundamental limitations including, for example, the difficulty of developing accident scenarios for NPP risk assessment through event and fault trees, as such prescribed trees might be insufficient in terms of predicting new scenarios. The event and fault tree limitations are partly attributed to the lack of accurate physics representation when NPP systems' dynamic interdependence-induced failures are considered. The limitations are also attributed to the inability to identify the exact timing of the failure-initiating events and the corresponding value of the system variables at such a time (Mandelli et al. 2017a).

Limitations of current PRA and the occurrence of severe NPP accidents have raised the need to develop adequate methodologies that take into account the complexity of hardware/software/operator interactions inside NPP (Nejad-Hosseinian 2007). As such, developing a dynamic PRA approach has been identified as key to overcoming the limitations of current PRA. Dynamic PRA is developed in a way that considers the timing and sequencing of events during hardware/software/operator action interactions (Aldemir 2018), which is essential for NPP risk assessment (Mandelli et al. 2013a). Simulation methods of dynamic

PRA have been evolving over the past three decades including DYLAM (Amendola 1988), DETAM (Acosta and Siu 1993), ADS (Hsueh and Mosleh 1996), ADS-IDAC (Coyne and Mosleh 2014), MCDET (Hofer et al. 2002b), ADAPT (Catalyurek et al. 2010), and RAVEN (Alfonsi et al. 2013b). These platforms, however, need to be integrated with NPP simulators such as RELAP (U.S. NRC 1995) and MELCOR (Gauntt et al. 2000) that represent the dynamic behavior of NPP.

3.2. SYSTEM DYNAMICS SIMULATION APPROACH

In order to improve risk assessment techniques of NPP, there is a need for an integrated platform that simulates the NPP dynamic processes, and thus their responses under abnormal events. In this respect, the current study adopts a system dynamics (**SD**) simulation approach to assess the dynamic response of different systems in pressurized water reactor (PWR) as a first step in developing an integrated dynamic PRA platform. SD is a simulation approach has been adopted in many disciplines, and it is typically used to simulate the dynamic behavior and interdependence within large complex systems, as described by Sonnessa (2004), Sterman (2000), and Bala et al. (2017). SD was first developed in the 1950s by Jay Forrester as a way to investigate the behavior of complex economic and social systems. Recently, SD has had extensive applications in simulating numerous real-world applications (Grigoryev 2016). The concepts of SD are presented in a simplified manner through graphs and basic algebraic formulation rather than complex mathematical/numerical models. For example, Figure 3-1 shows a

schematic diagram of a PWR SD model, where the feedback loops, stocks, and flows (e.g., the rate of change in stocks) are used to represent the parameters and simulate the PWR's dynamic processes (Forrester 2009). Feedback loops are key in SD as they control the dynamic interdependence between the different system components, whereas stocks are used to quantify the system parameters at any time. SD is essentially a system of differential equations that are analyzed numerically to simulate the behavior of complex systems (Borshchev and Filippov 2004).

Similar to other disciplines, although not to the same extent, models based on SD have been recently developed for nuclear applications, such as to investigate the nuclear fuel cycle starting from the mining and enrichment processes to repository disposal (Yacout et al. 2005). In a different study, Jeong and Choi (2007) investigated the fuel cycle process in Korea using a SD model and illustrated the importance of using the spent PWR fuel in both the Canada deuterium uranium and sodium-cooled fast reactors in order to reduce the spent fuel inventory. Another recent application of SD was to investigate the effect of generating nuclear power on economic, environmental, political, and social aspects in Singapore (Chia et al. 2015). SD was also recently used to investigate the development of nuclear power in China, combining different aspects that have influences on the nuclear power development such as electricity consumption, power generation, and uranium resources (Guo and Guo 2016). While a SD simulation approach has been used in the above referenced nuclear applications, to date, no study has applied SD to simulate the thermal dynamic processes in a NPP.

The ultimate goal of the current multi-phase study is to develop a dynamic PRA platform to enhance current risk assessment techniques through considering the complex dynamic interdependence between NPP systems/components in one platform. As a first step in this endeavor, the objective of this phase of the current study is to simulate the nonlinear behavior of the thermal dynamic processes in a PWR using SD simulation approach, including the physical response of multiple parameters/systems inside a NPP that may lead to system failure. In this respect, three SD models are developed to simulate the nonlinear behavior of the thermal dynamic processes for the reactor core, secondary coolant system and complete PWR based on the PWR behavior described in Thakkar (1975), Kerlin et al. (1976), Ali (1976), Arda et al. (2013), Arda (2013), and Puchalski et al. (2017). The developed PWR models can later be further integrated with other system models to map the event consequence propagation throughout different NPP systems, thus overcoming the limitations of current static fault and tree event tree analysis schemes. A concise background on thermal dynamic processes inside the reactor core and the secondary coolant system (SCS) is provided next. Afterwards, the reactor core, SCS, and complete reactor simulation models are validated using the results from published data (Arda 2013). Finally, the responses of the developed SD models are evaluated under several different perturbations in primary coolant flow and temperature, external reactivity, and steam valve opening events.

3.3. SYSTEM DYNAMICS MODEL DEVELOPMENT OF PWR

The primary function of a PWR is to convert the heat energy produced by uranium fission to electric power. In the PWR, a reactor pressure vessel holds the enriched uranium fuel required for the fission reactions. These reactions take place inside the RPV, generating heat energy and radioactive materials. Next, a high-pressure liquid (water) is circulated in a primary coolant system to cool the reactor core. This results in hot water that leaves the reactor pressure vessel through hot legs to the metal U-tube inside a steam generator. Finally, the steam generator transfers the heat to light-water to produce steam that in turn drives the turbine to generate electricity. A schematic diagram of the PWR generating unit, including the reactor pressure vessel, steam generator, turbine, hot and cold legs, is shown in Figure 3-2.

In the current study, SD is used to simulate the thermodynamic process (i.e., the energy production, storage, transfer and conversion) in the PWR, including the reactor core, the plenums, the hot and cold legs, and the steam generator. Three models are established to predict the nonlinear behavior of a complete PWR and validated using the work of Arda (2013). The three models are intended to simulate: 1) the thermodynamic process in the reactor core; 2) the thermodynamic process in the SCS; and 3) the interdependence between the reactor core and the SCS. The reactor core and SCS parameters are based on those of the Palo Verde Nuclear Generating Station (Arda 2013). **Table 3-1** and **Table 3-2** summarize the reactor core and SCS parameters, respectively. In addition, the delayed neutron fractions β_i and the delayed neutron precursor decay constants λ_i for the six delayed-neutron

groups are based on Puchalski et al. (2017). The thermodynamic process is represented in SD models by first-order differential equations. These equations control the interdependency among the different PWR dynamic parameters (e.g., reactor thermal power, reactor fuel and primary coolant temperatures, reactivity of reactor core, metal tube and secondary coolant temperatures, and steam pressure in steam generator) in terms of static parameters such as the heat transfer coefficients, coolant flow, and fuel and coolant masses.

3.3.1. MODEL I: THERMAL PROCESS IN THE REACTOR CORE SYSTEM

The heat transfer process inside the reactor core is simulated as a function of the reactor core thermal power. This thermal power is represented by point kinetics equations since the reactor power is controlled by reactivity feedbacks due to deviations in fuel, primary coolant temperatures, and external reactivity induced by control rods. Reactivity is assumed to be zero in the reactor steady state operation phase. During the reactor power maneuvering, the reactivity feedback mechanism is controlled by equation [3-1].

$$\rho(t) = \delta\rho_{ext} + \alpha_F \delta T_F + \frac{\alpha_C}{2}\delta T_{C1} + \frac{\alpha_C}{2}\delta T_{C2} \qquad [3\text{-}1]$$

The linearized point kinetics in Eqs. [3-2] and [3-3] control the reactor core thermal power with the influence of delayed neutron precursors (Duderstadt and Hamilton 1976).

$$\frac{d\delta P}{dt} = \frac{-\beta}{\Lambda}\delta P + \sum_{i=1}^{6}\lambda_i \delta C_i(t) + \frac{P_0}{\Lambda}\delta\rho_{ext} + \frac{\alpha_F P_0}{\Lambda}\delta T_F + \frac{\alpha_C P_0}{2\Lambda}\delta T_{C1} + \frac{\alpha_C P_0}{2\Lambda}\delta T_{C2} \quad [3\text{-}2]$$

$$\frac{d\delta C_i(t)}{dt} = \frac{\beta_i}{\Lambda}\delta P - \lambda_i \delta C_i \, , i = 1,\ldots,6 \quad [3\text{-}3]$$

The current study utilizes Mann's model (Kerlin 1978) to represent the deviation in the primary coolant and fuel temperatures. As shown in Figure 3-3, this model includes one node for the uranium fuel temperature and two nodes for the primary coolant temperature. In the reactor steady state operation phase, the reactor thermal power is constant and there is no deviation in the reactor fuel and coolant temperatures. As such, fluctuation in the reactor thermal power is achieved by changing the reactor core parameters such as the inlet coolant temperature, external reactivity, and primary coolant flow. Afterwards, the feedback mechanism causes a deviation in the overall PWR response. The reactor core parameters used in the current study are provided in **Table 3-1**, as mentioned earlier. Equation [3-4] represents the deviation in the reactor fuel temperature, while Eqs. [3-5] and [3-6] control the deviation in the coolant temperature nodes from the steady state.

$$\frac{d\delta T_F}{dt} = \frac{f}{m_f c_f}\delta P - \frac{U_{FC}{}^* A_{FC}}{m_f c_f}(\delta T_F - \delta T_{C1}) \quad [3\text{-}4]$$

$$\frac{d\delta T_{c1}}{dt} = \frac{1-f}{m_c c_c}\delta P - \frac{U_{FC}{}^* A_{FC}}{m_c c_c}(\delta T_F - \delta T_{C1}) - \frac{2w_c}{m_c}(\delta T_{c1} - \delta T_{LP}) \quad [3\text{-}5]$$

$$\frac{d\delta T_{c2}}{dt} = \frac{1-f}{m_c c_c}\delta P - \frac{U_{FC}{}^* A_{FC}}{m_c c_c}(\delta T_F - \delta T_{C1}) - \frac{2w_c}{m_c}(\delta T_{c2} - \delta T_{c1}) \quad [3\text{-}6]$$

The thermal dynamic process of the reactor core is simplified in the current study using the following assumptions (Puchalski et al. 2017): 1) the fuel to coolant heat transfer coefficient is constant; 2) the coolant flow is one dimensional; and 3)

the coolant is a single phase with constant density and specific heat.

The dynamic parameters of the reactor core (e.g., fuel and coolant temperatures, reactor thermal power, and reactivity) are modeled using stocks. The rates of change of these parameters are controlled by the feedback from multiple dynamic parameters and static parameters such as the fuel and coolant masses, heat transfer coefficient, and coolant flow, as shown in Figure 3-4.

3.3.2. MODEL II: THERMAL PROCESS IN THE SECONDARY COOLANT SYSTEM

The steam generator contains number of metal U-tubes for the primary coolant flow process. These tubes are essential components that separate the secondary and primary coolants in order to prevent the transfer of radioactive material to the SCS. The primary function of the steam generator is to convert the heat energy stored in the primary coolant into electric power. This is performed by boiling the water inside the steam generator to produce steam that drives the turbine of an electric generator. Next, this steam is condensed and returned to the steam generator.

The thermodynamic process in the steam generator consists of two heat transfer processes. First, the heat stored in the primary coolant is transferred to the metal tubes. Second, the heat is transferred from the metal U-tubes to the secondary coolant. A simplified simulation for the thermodynamic process in the steam generator is performed by representing the SCS using five lumps, as shown in Figure 3-3. The primary coolant and U-tubes are each represented by two lumps to

simulate the two branches of U-tubes, while the secondary coolant is simulated by only one lump.

Several aspects of the thermodynamic process in the steam generator are considered (Ali 1976; Arda 2013): 1) the heat transfer coefficients are constant during the reactor fluctuations; 2) the thermal conductivity of the steam generator metal U-tubes is constant; 3) the coolant flow is one-dimensional; 4) the properties of the saturated water and steam are constant over the steam pressure range of 600-1000 psi; 5) the feedwater flow is controlled (i.e., the feedwater flow is equal to the steam flow); and 6) and the steam flow rate is controlled only by the steam generator pressure (i.e., critical flow assumption).

In order to simulate the heat transfer process inside the steam generator using SD, the differential equations of the SCS dynamic parameters (e.g., primary coolant, metal U-tubes, secondary coolant temperatures, and steam pressure) are adopted using the following physical phenomena (Arda 2013): 1) heat balance for primary fluid; 2) heat balance for metal tube; 3) secondary fluid (liquid and steam phase) mass balance; 4) steam generator volume balance (i.e., the change of secondary coolant volume plus the change in the steam volume is zero); and 5) secondary fluid (liquid and steam phase) energy balance. Algebraic substitutions are also performed to yield the following differential equations. After linearization, deviations in primary coolant and metal U-tube lump temperatures are expressed by Eqs. [3-7], [3-8], [3-9], and [3-10], respectively. Finally, Eqs. [3-11] and [3-12] represent the deviation in the steam pressure inside the steam generator. The steam

generator parameters used in the current study are provided in **Table 3-2**. The steam valve coefficient (C_L) in the SD model is calibrated to predict the thermal dynamic behavior of the SCS similar to that of Arda's model because this coefficient is not reported in Arda (2013).

$$\frac{d\delta T_{P1}}{dt} = \frac{1}{\tau_{P1}}\delta T_{PI} - (\frac{1}{\tau_{PM1}} + \frac{1}{\tau_{P1}})\delta T_{P1} + \frac{1}{\tau_{PM1}}\delta T_{M1} \quad [3\text{-}7]$$

$$\frac{d\delta T_{P2}}{dt} = \frac{1}{\tau_{P2}}\delta T_{P1} - (\frac{1}{\tau_{PM2}} + \frac{1}{\tau_{P2}})\delta T_{P2} + \frac{1}{\tau_{PM2}}\delta T_{M2} \quad [3\text{-}8]$$

$$\frac{d\delta T_{M1}}{dt} = \frac{1}{\tau_{MP1}}\delta T_{P1} - (\frac{1}{\tau_{MS1}} + \frac{1}{\tau_{MP1}})\delta T_{M1} + \frac{1}{\tau_{MS1}}(\frac{\partial T_{SAT}}{\partial P})\delta P_S \quad [3\text{-}9]$$

$$\frac{d\delta T_{M2}}{dt} = \frac{1}{\tau_{MP2}}\delta T_{P2} - (\frac{1}{\tau_{MS2}} + \frac{1}{\tau_{MP2}})\delta T_{M2} + \frac{1}{\tau_{MS2}}(\frac{\partial T_{SAT}}{\partial P})\delta P_S \quad [3\text{-}10]$$

$$\frac{d\delta P_S}{dt} = \frac{1}{K}\left[U_{\mathrm{ms}}S_{\mathrm{ms1}}\delta T_{M1} + U_{\mathrm{ms}}S_{\mathrm{ms2}}\delta T_{M2} - \begin{bmatrix}(U_{\mathrm{ms}}S_{\mathrm{ms1}} + U_{\mathrm{ms}}S_{\mathrm{ms2}})\left(\frac{\partial T_{SAT}}{\partial P}\right) \\ +w_{so}\frac{\partial T_{SAT}}{\partial P} + C_L(h_g - c_{pi}T_{fi})\end{bmatrix}\delta P_S \right.$$
$$\left. + w_{so}c_{pi}\delta T_{fi} - P_{S0}(h_g - c_{pi}T_{fi})\delta C_L \right] \quad [3\text{-}11]$$

$$K = \left(m_{sw}\frac{\partial h_f}{\partial P} + m_{ss}\frac{\partial h_g}{\partial P} - m_{ss}\frac{h_{fg}}{v_{fg}}\frac{\partial v_g}{\partial P}\right) \quad [3\text{-}12]$$

Stocks are used to represent the primary coolant, metal U-tube lump temperatures, and steam pressure. Equations [3-7] to [3-12] provide the rates of change of these parameters. All other parameters (e.g., coolant residence time, mass of coolant, coolant flow, and mass of metal lump) are considered as static parameters for simplicity of the model. As can be seen in Figure 3-5, the SD model of the SCS shows feedback loops between the system dynamic parameters (i.e., stocks) and the static parameters.

3.3.3. MODEL III: THERMAL PROCESS IN THE PRESSURIZED WATER REACTOR

The thermal dynamic process for the reactor core upper (outlet) and lower (inlet) plenums, steam generator outlet and inlet plenums, and the hot and cold legs are combined with the reactor core and SCS models to present a better representation for the whole PWR, as shown in Figure 3-6. The primary coolant residence time values inside the plenums, cold and hot legs are provided in **Table 3-3**. Following the thermodynamics procedure, the linearized differential equations [3-13] to [3-18] are extracted. More specifically, Eqs. [3-13] and [3-14] define the coolant temperature deviation in the upper reactor core and lower plenums, while Eqs. [3-15] and [3-16] represent the coolant temperature deviation in the inlet and outlet steam generator. Finally, Eqs. [3-17] and [3-18] provide the coolant temperature deviation in the hot and cold legs.

$$\frac{d\delta T_{UP}}{dt} = \frac{1}{\tau_{UP}}(\delta T_{c2} - \delta T_{UP}) \quad [3\text{-}13]$$

$$\frac{d\delta T_{LP}}{dt} = \frac{1}{\tau_{LP}}(\delta T_{CL} - \delta T_{LP}) \quad [3\text{-}14]$$

$$\frac{d\delta T_{IP}}{dt} = \frac{1}{\tau_{IP}}(\delta T_{HL} - \delta T_{IP}) \quad [3\text{-}15]$$

$$\frac{d\delta T_{OP}}{dt} = \frac{1}{\tau_{OP}}(\delta T_{P2} - \delta T_{OP}) \quad [3\text{-}16]$$

$$\frac{d\delta T_{HL}}{dt} = \frac{1}{\tau_{HL}}(\delta T_{UP} - \delta T_{HL}) \quad [3\text{-}17]$$

$$\frac{d\delta T_{CL}}{dt} = \frac{1}{\tau_{CL}}(\delta T_{OP} - \delta T_{CL}) \quad [3\text{-}18]$$

3.4. SYSTEM DYNAMICS MODEL VALIDATION OF PWR

3.4.1. MODEL I: THE REACTOR CORE SYSTEM

The thermal dynamic process in the reactor core is validated under an increase in the external reactivity (ρ_{ext}) by 7.3×10^{-5} at 10 s, to facilitate a direct comparison with available data (Arda 2013). This action is followed by an increase in the neutron flux that subsequently causes an immediate increase in the reactor thermal power. After reactor stability, the reactor core thermal power increases to 24.8 and 27.9 MWth in the SD model and Arda's model, respectively, as shown in Figure 3-7a. Increasing the thermal power of the reactor core is accompanied by an increase in the temperatures of the fuel and coolant nodes, as shown in Figure 3-7b. This initiates negative reactivity feedback that drives the total reactivity to decrease. As can be seen in Figure 3-7a, although the SD model shows a considerable difference in thermal power relative to Arda's model immediately after the increase in external reactivity at 10 s, the reactor power after stabilization is simulated accurately by the SD model with a deviation of only 11%. As shown in Figure 3-7b, the reactor fuel and coolant temperature values estimated by the SD model are lower than those calculated from Arda's model by 11%.

3.4.2. MODEL II: THE SECONDARY COOLANT SYSTEM

The thermal dynamic process in the SCS is validated under an increase in the inlet coolant temperature (T_{IP}) by 10^{o}F at 5 s without changing the steam valve coefficient (C_L). This is followed by an increase in the temperature of the primary

coolant lumps (T_{P1}, T_{P2}). Additional heat is transferred from the primary coolant to the metal U-tubes. As a result, the temperature of these tubes increases and additional heat energy is transferred to the secondary coolant, which in turn generates additional steam. Figure 3-8a shows similar increases in the coolant (T_{P1}) and metal U-tube (T_{m1}) temperatures after an increase in the inlet coolant temperature in both the SD model and Arda's model. Subsequently, as can be seen in Figure 3-8b, the steam pressure in the steam generator increases because the steam valve opening is maintained constant. The dynamic parameters of the SCS (i.e., primary coolant, metal tube temperatures, and steam pressure) in the SD model and Arda's model show similar nonlinear dynamic response after an increase in the inlet coolant temperature. As can be seen in Figure 3-8b, the steam pressure is increased by 51.1 and 52.4 psi in the SD model and Arda's model, respectively, a minor deviation of only 2.5%.

3.4.3. MODEL III: THE PRESSURIZED WATER REACTOR

The complete thermodynamic process in the PWR is validated under an increase in the external reactivity. This investigates the dynamic response of different parameters in the SCS to small perturbations inside the reactor core. A positive reactivity of 7.3×10^{-5} is applied at 10 s without changing the steam valve coefficient. As shown in Figure 3-9a, the reactor fuel temperature increases following the increase of the external reactivity. This causes more heat energy to be transferred from the primary coolant system to the SCS. As a result, additional steam is produced that causes an increase in the steam pressure, as shown in Figure 3-9b. It

should be noted that the reactor core inlet coolant temperature (T_{LP}) increases after a complete primary coolant cycle, as shown in Figure 3-9a, which in turn causes a high negative reactivity feedback. As such, the fuel temperature decreases after reaching the maximum value in both the SD model and Arda's model, with a maximum difference between the models of 15%. As can be seen in Figure 3-9b, the steam pressure in the SCS after a positive change in the external reactivity shows similar responses (within 5%) in the SD model and Arda's model.

3.5. PERTURBATION EVENT EFFECTS ON THERMAL DYNAMIC PROCESS IN THE PWR

Following the SD model validation, the thermal dynamic processes in the reactor core, SCS, and complete PWR are tested separately under different perturbation events to verify the interaction among feedback mechanisms. These events include either single or multiple actions at a specific time or actions that fluctuate with time.

3.5.1. MODEL I: THE REACTOR CORE SYSTEM

The response of reactor thermal power, coolant, and fuel temperatures are investigated due to a change in: 1) the external reactivity (ρ_{ext}) induced by the control rod; 2) the inlet core coolant temperature (T_{LP}); and 3) the primary coolant mass flow (w_c).

In the first event, the external reactivity is increased by 7.3×10^{-5} at 10 s. Simultaneously, three different scenarios are carried out to investigate the influence of the primary coolant mass flow on the thermal dynamic behavior of the reactor

core. More specifically, the primary coolant flow (w_c) is maintained constant in the first scenario, while this flow is increased and reduced by 20% in the second and third scenarios, respectively. As shown in Figure 3-10a, the reactor thermal power is immediately increased after adding a positive reactivity, a behavior that is observed in all scenarios. As the thermal power increases, the reactor fuel and primary coolant temperatures increase, as shown Figure 3-10b, causing negative reactivity feedback. Also, Figure 3-10b shows that the low value of the coolant mass flow in the third scenario (0.8 w_c) leads to an increase in the coolant temperature relative to first and second scenarios. In particular, the third scenario shows a higher negative reactivity feedback as expected, which leads to a reduction in the reactor thermal power by 8.6% compared to the first scenario, respectively. Increasing the primary coolant flow has the opposite effect of reducing the negative reactivity feedback, leading to a relative increase in the reactor thermal power.

The second event investigates the dynamic parameters of the reactor when the control rods are inserted (i.e., a $7.3\text{x}10^{-5}$ decrease of reactivity). Figure 3-11a shows an immediate drop in the thermal power of the reactor core, which then stabilizes to 15.7 MWth. This behavior is attributed to the control rods that capture neutrons, and simultaneously, the fuel and coolant nodes temperatures are decreased. As can be seen in Figure 3-11b, the reactor fuel and coolant nodes (T_{C2}, T_{C1}) temperatures decrease by 2.44^{o}F , 0.22^{o}F , and 0.1^{o}F, respectively.

In the third event, the temperature of the inlet coolant (T_{LP}) is increased by 5^{o}F at 10 s. This is followed by a high negative reactivity feedback that induces a

significant drop in the reactor thermal power. As can be noted from Figure 3-12a, the reactor thermal power stabilizes because of the negative reactivity feedback with a reduction in its initial value by 120 MWth. In addition, Figure 3-12b shows a reduction in the fuel temperature by 13.7^{o}F in response to the increase in the inlet coolant temperature, because of the thermal power reduction.

3.5.2. MODEL II: THE SECONDARY COOLANT SYSTEM

Fluctuations in steam pressure, primary coolant, and metal U-tube lump temperatures are investigated during several events.

In the first event, the steam valve coefficient (C_L) is decreased by 5% at 5 s. As can be seen in Figure 3-13a, this event is followed by an immediate increase in the steam pressure inside the steam generator. Then, a small amount of heat is transferred from the primary coolant system to the SCS followed by increases in the coolant and metal tube lump temperatures, as shown in Figure 3-13b.

In the second event, the temperature of the steam generator inlet coolant (T_{IP}) is increased by 10^{o}F at 5 s. Simultaneously, three different scenarios are applied to investigate the influence of steam valve opening position on the thermodynamic behavior of the SCS. In the first scenario, the steam valve coefficient is maintained constant, while the steam valve coefficient is increased and decreased by 5% in the second and third scenarios, respectively. As shown in Figure 3-14a, an immediate slight reduction in steam pressure is observed in the case of the steam valve opening (i.e., second scenario), followed quickly by a much larger increase in steam pressure as more heat is transferred from the primary to the secondary system following the

increase in the inlet coolant temperature. As can be seen also in Figure 3-14b, the primary coolant lump 1 (T_{P1}) temperature is lower for the second scenario compared to other scenarios. This is because more steam is required due to the opening of the steam valve, leading to more heat energy being transferred from the primary coolant system and therefore smaller increase in primary coolant temperature. In summary, the increase in the steam valve coefficient reduces both the steam pressure and primary coolant temperature compared to the first and third scenarios.

3.5.3. MODEL III: THE PRESSURIZED WATER REACTOR

Following the evaluation of the reactor core and the SCS to different perturbation events, a SD model of the complete thermodynamic process is essential to predict the response of the steam generator when perturbation events occur inside the reactor core and vice versa. This SD model is developed by combining the aforementioned reactor core and SCS thermal dynamic models as described earlier. In this subsection, the thermal dynamic process of a complete PWR is investigated under three different perturbation events.

First a small perturbation is applied by increasing the steam valve coefficient by 5% at 5 s. Therefore, additional steam is expected to be produced in order to balance the SCS thermal dynamic process. This event is followed by a reduction in the steam pressure (P_S) and temperature (T_{steam}) values by 29.1 psi and 3.4^{o}F, as shown in Figure 3-15a and Figure 3-15b, respectively. More heat is transferred from the primary coolant in the U-tube to the secondary system in order to accommodate the steam generation, and subsequently, the primary coolant lump temperatures

(T_{P1}, T_{P2}) are reduced. This behavior is followed by a reduction in the reactor core inlet primary coolant temperature (T_{LP}). Also, Figure 3-15b shows that the reactor core primary coolant temperatures (T_{c1}, T_{c2}) are reduced by 2.1^{o}F and 1.4^{o}F, respectively. The reduction in coolant temperature causes a positive reactivity feedback that leads to an increase in the reactor thermal power by 97 MWth, as shown in Figure 3-15a. Figure 3-15b also shows that the reactor fuel temperature is increased by 12.3^{o}F because of this increase in the reactor thermal power.

The second event investigates different steam valve opening positions after a positive reactivity of 7.3×10^{-5} is added. The first scenario is applied without changing the steam valve coefficient, while the steam valve coefficient is increased and decreased by 5% in the second and third scenarios, respectively. All scenarios show an immediate increase in the reactor thermal power (Figure 3-16b), and subsequently the fuel temperature (Figure 3-16c) increases after the external reactivity is added. However, in the third scenario, the reduction in the steam valve coefficient results in a negative reactivity feedback, primarily because of an increase in the reactor core inlet coolant temperature. As can be seen in Figure 3-16a, a reduction in the steam valve coefficient (third scenario) by 5% causes an increase in the reactor inlet coolant temperature (T_{LP}) by 4.0^{o}F. Because of the negative reactivity feedback in this scenario, the thermal power is reduced by 81.6 MWth relative to the first scenario. On the other hand, Figure 3-16b shows an increase in the reactor thermal power by 95 MWth relative to the first scenario after an increase in the steam valve coefficient. In this second scenario, the reactor core

thermal power reaches a peak value, then drops as a result of the decay of fission fragments, and finally, the reactor power starts increasing again due to the feedback of increasing the steam valve coefficient. It is clear from Figure 3-16c that the reactor fuel temperature is significantly reduced in the third scenario as a result of the negative reactivity feedback. Figure 3-16b and Figure 3-16d show that closing the steam valve by 5% reduces the thermal power of the reactor core by 81.6 MWth and increases the steam pressure by 35.3 psi relative to the first scenario, in which the deviations in the reactor thermal power and steam pressure are 12.2 MWth and 3.1 psi, respectively. On the other hand, increasing the steam valve coefficient leads to a reduction in the steam pressure by 29.6 psi and an increase in the thermal power by 95 MWth relative to the first scenario.

In the third and final events, a positive reactivity of 6.5×10^{-5} is applied for a 30 s interval through a constant steam valve coefficient, followed by a 30 s interval of zero reactivity, as shown in Figure 3-17a. This external reactivity event is mainly to investigate the nonlinear response of the reactor thermal power to the change in the position of control rods within this time frame (i.e., up to 180 s). Figure 3-17b shows an increase in the fuel, coolant nodes, and steam temperatures after the reactivity is increased. Removal of the external reactivity reduces the total reactivity immediately due to the negative fuel and coolant temperature reactivity feedback. As can be seen in Figure 3-17c, the thermal power fluctuates immediately after changing the external reactivity. The cumulative behavior of the reactor parameters shows an increase in the thermal power, as well as the fuel and coolant

temperatures. Figure 3-17d shows also an increase in the steam pressure since the increase in the coolant temperature transfers additional heat energy from the primary coolant system to the secondary system.

3.6. CONCLUSIONS

A nuclear power plant (NPP) contains multiple systems that interact through several feedback mechanisms to generate electricity. The complex dynamic interdependence among these systems, the consequence severity of interacting hazards, and the drawbacks of current risk assessment techniques have raised major concerns about NPP safety, especially after the Fukushima Daiichi disaster. To address this challange, a system dynamics (SD) approach was used to simulate the thermal dynamic processes for different systems inside a pressurized water reactor (PWR), since this process is considered as a first step to overcome the limitation of current risk assessment techniques of NPPs. Three SD models of the reactor core, secondary coolant system (SCS), and complete PWR were validated against the results of a previously published model. Subsequently, these models were evaluated under different perturbation events pertaining to the external reactivity, primary coolant flow, and the steam valve coefficient. The results obtained from the complete PWR model, combining the reactor core and SCS, were used to investigate the interconnectivity and nonlinear feedback mechanism between different systems inside the PWR.

The results of the current study demonstrate the capability of the SD approach to simulate the physical processes between major interdependent systems in NPPs

under different perturbation events. These physical processes are represented by the reactor thermal power, fuel and coolant temperatures and steam pressure. Moreover, the developed system dynamics simulation approach provides significant advantages from both the time and data storage perspectives, since the analysis of the developed SD models was very fast (e.g., the time needed for the longest perturbation event analysis is less than 60 s) with a very modest size of output data (e.g., the generated data for all perturbation events for both validation and evaluation analysis conducted in the current study was less than 500 KB). In this respect, SD is expected to facilitate the development of an integrated risk assessment technique with feedback loops that facilitates accurate simulation of several complex accident scenarios. Thus, the current study presents the first phase in a multi-phase research program aimed at developing an integrated dynamic probabilistic risk assessment platform that takes into account the interaction and interdependence of different NPP systems with an ultimate goal of enhancing the overall NPP safety.

3.7. ACKNOWLEDGMENTS

The financial support for the study was provided through the Canadian Nuclear Energy Infrastructure Resilience under Seismic Systemic Risk (CaNRisk) – Collaborative Research and Training Experience (CREATE) program of the Natural Science and Engineering Research Council (NSERC) of Canada.

3.8. NOTATION

The following symbols are used in this paper:

A_{FC}	=	Effective heat transfer surface area between the reactor fuel and primary coolant;
c_c	=	Specific heat of primary coolant;
c_f	=	Specific heat of the reactor fuel;
C_i	=	Delayed neutron precursors, i=1,……,6;
C_L	=	Steam valve coefficient;
c_m	=	Specific heat of metal U-tubes in steam generator;
c_{pi}	=	Specific heat of feedwater in steam generator;
f	=	Fraction of the total power produced in the reactor fuel;
h_f	=	Enthalpy of saturated water;
h_g	=	Enthalpy of saturated steam;
h_{fg}	=	h_f - h_g;
m_c	=	Mass of primary coolant in the core region;
$m_{c\text{-}UP}$	=	Mass of primary coolant in reactor upper plenum;
m_f	=	Mass of the reactor fuel;
m_{m1}	=	Mass of metal U-tube lump 1;
m_{m2}	=	Mass of metal U-tube lump 2;
m_{p1}	=	Mass of coolant in primary coolant lump 1;
m_{p2}	=	Mass of coolant in primary coolant lump 2;
m_{sw}	=	Mass of water in steam generator;
m_{ss}	=	Mass of steam in steam generator;
P	=	Thermal power of the reactor core;
P_o	=	Initial steady state of reactor thermal power;
P_s	=	Steam pressure;
P_{so}	=	Initial steady state of steam pressure;
S_{ms1}	=	Heat transfer area between steam generator tube metal lump 1 and secondary coolant;
S_{ms2}	=	Heat transfer area between steam generator tube metal lump 2 and secondary coolant;
S_{pm1}	=	Heat transfer area between primary coolant lump 1 and metal tube lump 1;
S_{pm2}	=	Heat transfer area between primary coolant lump 2 and metal tube lump 2;
T_{C1}	=	Primary coolant temperature at node 1;

T_{C2}	=	Primary coolant temperature at node 2;
T_{CL}	=	Primary coolant temperature in cold-leg;
T_F	=	Average fuel temperature;
T_{fi}	=	Feedwater temperature in steam generator;
T_{HL}	=	Primary coolant temperature in hot-leg;
T_{IP}	=	Primary coolant temperature in the steam generator inlet plenum;
T_{LP}	=	Primary coolant temperature in reactor lower plenum;
T_{M1}	=	Average temperature of metal tube lump 1;
T_{M2}	=	Average temperature of metal tube lump 2;
T_{OP}	=	Primary coolant temperature in the steam generator outlet plenum;
T_{P1}	=	Bulk mean temperature of primary coolant lump 1;
T_{P2}	=	Bulk mean temperature of primary coolant lump 2;
T_{UP}	=	Primary coolant temperature in reactor upper plenum;
U_{FC}	=	Heat transfer coefficient from fuel to coolant;
U_{ms}	=	Heat transfer coefficient between steam generator tube metal and secondary coolant;
U_{pm}	=	Heat transfer coefficient between primary coolant and tube metal in steam generator;
v_f	=	Specific volume of saturated water;
v_g	=	Specific volume of saturated steam;
v_{fg}	=	v_f - v_g;
w_c	=	Primary coolant mass flow rate of inside the core;
w_{so}	=	Steam flow rate;
α_c	=	Coolant temperature coefficient of reactivity;
α_F	=	Fuel temperature coefficient of reactivity;
β	=	Total delayed neutron fraction;
β_i	=	Delayed neutron fraction for the six delayed-neutron groups, i=1,……,6;
Δ	=	Deviation in the dynamic parameters from the steady state;
$\delta h_f/\delta P$	=	Change of enthalpy of saturated water versus steam pressure;
$\delta h_g/\delta P$	=	Change of enthalpy of saturated steam versus steam pressure;
$\delta T_{SAT}/\delta$	=	Slope of the change in saturation temperature with respect to steam pressure;
$\delta v_g/\delta P$	=	Change in specific volume of saturated steam versus pressure;
λ_i	=	Delayed neutron precursor decay constant for the six-delayed neutron group, i=1,……,6;

ρ = Reactivity;

ρ_{ext} = Reactivity induced by control rods;

τ_{CL} = Coolant residence time in cold-leg;

τ_{HL} = Coolant residence time in hot-leg;

τ_{IP} = Coolant residence time in steam generator inlet plenum;

τ_{LP} = Coolant residence time in reactor lower plenum;

τ_{OP} = Coolant residence time in steam generator outlet plenum;

τ_{P1} = Residence time for primary coolant lump 1;

τ_{P2} = Residence time for primary coolant lump 2;

τ_{MP1} = $m_{m1}\, c_m / U_{pm}\, S_{pm1}$= Time constant for metal tube lump 1 to primary coolant lump 1 heat transfer;

τ_{MP2} = $m_{m2}\, c_m / U_{pm}\, S_{pm2}$= Time constant for metal tube lump 2 to primary coolant lump 2 heat transfer;

τ_{MS1} = $m_{m1}\, c_m / U_{ms}\, S_{ms1}$= Time constant for metal tube lump 1 to secondary coolant heat transfer;

τ_{MS2} = $m_{m2}\, c_m / U_{ms}\, S_{ms2}$= Time constant for metal tube lump 2 to secondary coolant heat transfer;

τ_{PM1} = $m_{p1}\, c_c / U_{pm}\, S_{pm1}$= Time constant for primary coolant lump 1 to metal tube lump 1 heat transfer;

τ_{PM2} = $m_{p2}\, c_c / U_{pm}\, S_{pm2}$= Time constant for primary coolant lump 2 to metal tube lump 2 heat transfer;

τ_{UP} = $m_{c\text{-}UP} / w_c$= Coolant residence time in reactor upper plenum; and

Λ = Neutron generation time.

3.9. REFERENCES

Acosta, C., and Siu, N. (1993). "Dynamic event trees in accident sequence analysis: application to steam generator tube rupture." *Reliability Engineering and System Safety*, 41(2), 135–154.

Aldemir, T. (2018). *Advanced Concepts in Nuclear Energy Risk Assessment and Management*.

Alfonsi, A., Rabiti, C., Mandelli, D., Cogliati, J. J., Kinoshita, R. A., and Naviglio, A. (2013). "Dynamic Event Tree Analysis through RAVEN." *ANS PSA 2013 International Topical Meeting on Probabilistic Safety Assessment and Analysis*.

Ali, M. (1976). "Lumped Parameter, State Variable Dynamic Models for U-tube Recirculation Type Nuclear Steam Generators." Ph.D. Thesis, University of Tennessee.

Amendola, A. (1988). "Accident sequence dynamic simulation versus event trees." *Reliability Engineering and System Safety*, 22(1–4), 3–25.

Arda, S. (2013). "Implementing a Nuclear Power Plant Model for Evaluating Load-Following Capability on a small Grid." MASc Thesis, Arizona State University.

Arda, S., Holbert, K. E., and Undrill, J. (2013). "Development of a Linearized Model of a Pressurized Water Reactor Generating Station for Power System

Dynamic Simulations." *45th North American Power Symposium, NAPS 2013*.

ASME. (2012). *Forging a New Nuclear Safety Construct*. The ASME Presidential Task Force on Response to Japan Nuclear Power Plant Events.

Bala, B. K., Arshad, F. M., and Noh, K. M. (2017). *System Dynamics: Modelling and Simulation*. *Springer Nature*.

Barrett, J. (2017). *The Canadian Nuclear FactBook. Canadian Nuclear Association*.

Bartel, R. (2016). *WASH-1400: The Reactor Safety Study. The Introduction of Risk Assessment to the Regulation of Nuclear Reactors*. *NUREG/KM-0010*, U.S.NRC.

Borshchev, A., and Filippov, A. (2004). "From System Dynamics and Discrete Event to Practical Agent Based Modeling: Reasons, Techniques, Tools." *Simulation*, 66(11), 25–29.

Catalyurek, U., Rutt, B., Metzroth, K., Hakobyan, A., Aldemir, T., Denning, R., Dunagan, S., and Kunsman, D. (2010). "Development of a code-agnostic computational infrastructure for the dynamic generation of accident progression event trees." *Reliability Engineering and System Safety*, Elsevier, 95, 278–294.

Chia, E. S., Lim, C. K., Ng, A., and Nguyen, N. H. L. (2015). "The System

Dynamics of Nuclear Energy in Singapore." *International Journal of Green Energy*, Taylor & Francis, 12(1), 73–86.

Chino, M., Nakayama, H., Nagai, H., Terada, H., Katata, G., and Yamazawa, H. (2011). "Preliminary Estimation of Release Amounts of 131 I and 137 Cs Accidentally Discharged from the Fukushima Daiichi Nuclear Power Plant into the Atmosphere." *Journal of Nuclear Science and Technology*, 48(7), 1129–1134.

CNSC. (2017). "Probabilistic safety assessment: A tool to estimate risk and drive safety improvement at nuclear power plants." <http://nuclearsafety.gc.ca/eng/resources/educational-resources/feature-articles/probabilistic-safety-assessment.cfm>.

Coyne, K., and Mosleh, A. (2014). "Nuclear plant control room operator modeling within the ADS-IDAC, Version 2, Dynamic PRA Environment: Part 1 - General description and cognitive foundations." *International Journal of Performability Engineering*, 10(7), 691–703.

Dawson, K. M. (2017). "Advanced Thermal Hydraulic Simulations for Human Reliability Assessment of Nuclear Power Plants by." Massachusetts Institute of Technology.

Duderstadt, J., and Hamilton, L. (1976). *Nuclear Reactor Analysis*. Department of Nuclear Engineering. The University of Michigan.

Forrester, J. (2009). *Some Basic Concepts in System Dynamics*. *Sloan School of Management*, Sloan School of Management. Massachusetts Institute of Technology.

Gauntt, R.-O., Cole, R., Erickson, C. M., Gido, R. G., Gasser, R. D., Rodriguez, S. B., and Young, M. F. (2000). *MELCOR Computer Code Manuals*.

Grigoryev, I. (2016). *AnyLogic 7 in Three Days*.

Guo, X., and Guo, X. (2016). "Nuclear power development in China after the restart of new nuclear construction and approval: A system dynamics analysis." *Renewable and Sustainable Energy Reviews*, Elsevier, 57, 999–1007.

Hassija, V., Senthil Kumar, C., and Velusamy, K. (2014). "Probabilistic safety assessment of multi-unit nuclear power plant sites - An integrated approach." *Journal of Loss Prevention in the Process Industries*, Elsevier Ltd, 32, 52–62.

Hofer, E., Kloos, M., Krzykacz-Hausmann, B., Peschke, J., and Woltereck, M. (2002). "An approximate epistemic uncertainty analysis approach in the presence of epistemic and aleatory uncertainties." *Reliability Engineering and System Safety*, 77(3), 229–238.

Holt, M., Campbell, R. J., and Nikitin, M. B. (2012). *Fukushima Nuclear Disaster*. *Congressional Research Service*.

Hsueh, K. S., and Mosleh, A. (1996). "The development and application of the accident dynamic simulator for dynamic probabilistic risk assessment of nuclear power plants." *Reliability Engineering and System Safety*, 52, 297–314.

IAEA. (2009). *Deterministic Safety Analysis for Nuclear Power Plants*. *International Atomic Energy Agency*.

IAEA. (2016). *Nuclear power and sustainable development*. *Journal of International Affairs*.

Jeong, C. J., and Choi, H. (2007). "Dynamic Modeling and Analysis of Alternative Fuel Cycle Scenarios in Korea." *Nuclear Engineering and Technology*, Vol.39(1), 85–94.

Kerlin, T. (1978). "Dynamic Analysis and Control of Pressurized Water Reactors." 103–212.

Kerlin, T. W., Katz, E. M., Thakkar, J. G., and Strange, J. E. (1976). "Theoretical and experimental dynamic analysis of the HB Robinson nuclear plant." *Nuclear technology*, 30(3), 299–316.

Little, R. G. (2002). "Controlling Cascading Failure: Understanding The Vulnerabilities of Interconnected Infrastructures." *Journal of Urban Technology*, 9(1), 109–123.

Mandelli, D., Parisi, C., and Alfonsi, A. (2017). "Dynamic PRA of a multi-unit

plant." *International Topical Meeting on Probabilistic Safety Assessment (PSA 2017)*.

Manselli, D., Smith, C., Rabiti, C., Alfonsi, A., Youngblood, R., Pascucci, V., Wang, B., Maljovec, D., Bremer, P. T., Aldemir, T., Yilmaz, A., and Zamalieva, D. (2013). "Dynamic PRA: An Overview of New Algorithms to Generate, Analyze and Visualize Data." *Transactions of the American Nuclear Society*.

Moieni, P., and Spurgin, A. J. (1994). "Advances in human reliability analysis methodology. Part I : Frameworks, models and data." *Reliability Engineering and System Safety*, 44, 27–55.

Mosleh, A. (2014). "PRA: A Perspective on strengths, current limitations, and possible improvements." *Nuclear Engineering and Technology*, Korean Nuclear Society, 46(1), 1–10.

Nejad-Hosseinian, S. H. (2007). "Automatic Generation of Generalized Event Sequence Diagrams for Guiding Simulation Based Dynamic Probabilistic Risk Assessment of Complex Systems." PhD Thesis. University of Maryland.

NUREG/CR-2300. (1983). *PRA ROCEDURES GUIDE "A Guide to the Performance of Probabilistic Risk Assessments for Nuclear Power Plants."*

Perrow, C. (2011). "Fukushima and the inevitability of accidents." *Bulletin of the*

Atomic Scientists, 67(6), 44–52.

Pescaroli, G., and Alexander, D. (2015). "A definition of cascading disasters and cascading effects : Going beyond the ' toppling dominos ' metaphor." *GRF Davos Planet@Risk*, the 5th IDRC Davos 2014, 58–67.

Puchalski, B., Rutkowski, T. A., and Duzinkiewicz, K. (2017). "Nodal models of Pressurized Water Reactor core for control purposes – A comparison study." *Nuclear Engineering and Design*, Elsevier B.V., 322, 444–463.

Sonnessa, M. (2004). "Modelling and simulation of complex systems." PhD thesis. University of Turin.

Sterman, J. (2000). *Business Dynamics: Systems Thinking and Modeling for a Complex World*.

Thakkar. (1975). "Correlation of Theory and Experiment for the Dynamics of a Pressurized Water Reactor." University of Tennessee.

U.S. NRC. (1995). *RELAP5 / MOD3 Code Manual*. U.S Nuclear Regulatory Commission.

World Nuclear Association. (2019). "Nuclear Power in the World Today." <http://www.world-nuclear.org/information-library/current-and-future-generation/nuclear-power-in-the-world-today.aspx>.

Yacout, A. M., Jacobson, J. J., Matthern, G. E., Piet, S. J., and Moisseytsev, A. (2005). "Modeling The Nuclear Fuel Cycle." *The 23rd International*

Conference of the System Dynamics Society.

Table 3-1 Parameters for the reactor core system

P_o	MWth	3800	α_c	1/°F	$-1.0*10^{-4}$	U_{fc}	(Btu/hr)/(ft^2.°F)	325.588
f	—	0.975	α_f	1/°F	$-1.20*10^{-5}$	A_{fc}	ft^2	68600
β	—	0.0065	w_c	lb/hr	$164*10^{6}$	m_f	lb	$257.1*10^{3}$
β_1	—	0.000215	λ_1	1/s	0.0124	c_f	Btu/lb.°F	0.1056
β_2	—	0.001424	λ_2	1/s	0.0305	m_c	lb	30721
β_3	—	0.001274	λ_3	1/s	0.1110	c_c	Btu/lb.°F	1.448
β_4	—	0.002568	λ_4	1/s	0.3010	Λ	s	$30*10^{-6}$
β_5	—	0.000748	λ_5	1/s	1.1400			
β_6	—	0.000273	λ_6	1/s	3.0100			

Table 3-2 Parameters for the secondary coolant system

τ_{P1}	s	1.2815	$\delta T_{SAT}/\delta P$	°F/psi	0.1176	m_{sw}	lb	334000
τ_{P2}	s	1.2815	$\delta h_f/\delta P$	Btu/lb.psi	0.1508	m_{ss}	lb	36904
τ_{PM1}	s	1.2233	$\delta h_g/\delta P$	Btu/lb.psi	-0.0385	P_{so}	psi	1070
τ_{PM2}	s	0.5826	$\delta v_g/\delta P$	ft^3/lb.psi	$-4.64*10^{-4}$	c_{pi}	Btu/lb.°F	1.278
τ_{MP1}	s	0.3519	h_g	Btu/lb	1189	w_{so}	lb/hr	$17.18*10^{6}$
τ_{MP2}	s	0.1676	h_f	Btu/lb	554	c_m	Btu/lb.°F	0.10205
τ_{MS1}	s	0.3519	v_f	ft^3/lb	0.0218	T_{fi}	°F	450
τ_{MS2}	s	0.1676	v_g	ft^3/lb	0.4114	C_L	—	6

Table 3-3 Parameters for plenums, hot and cold legs

τ_{UP}	s	2.517	τ_{OP}	s	0.726
τ_{HL}	s	0.234	τ_{CL}	s	1.310
τ_{IP}	s	0.659	τ_{LP}	s	2.145

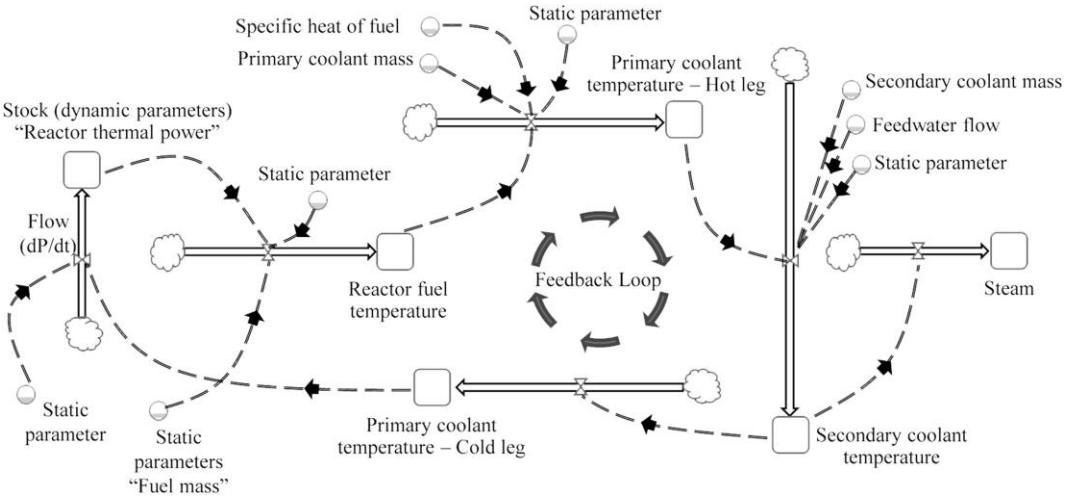

Figure 3-1: Schematic diagram of a PWR system dynamics model.

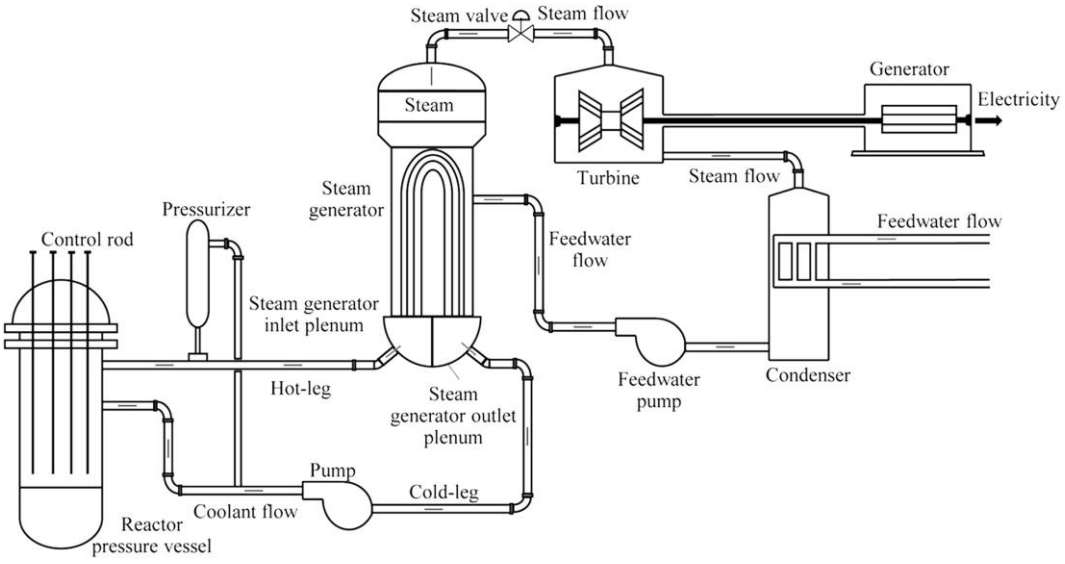

Figure 3-2: Schematic diagram of a pressurized water reactor.

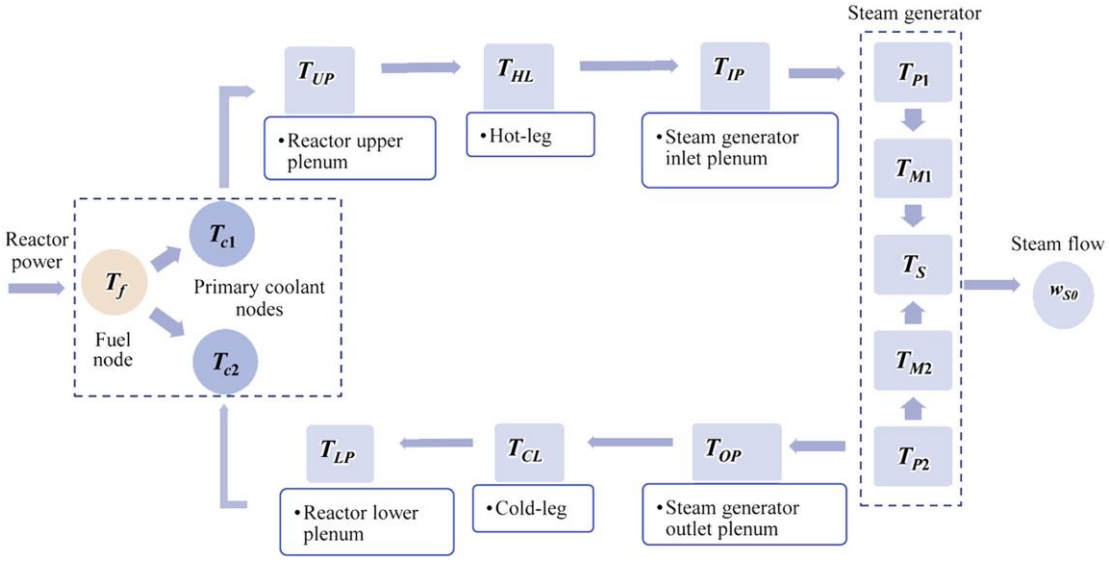

Figure 3-3: Schematic diagram of a PWR thermal dynamic process.

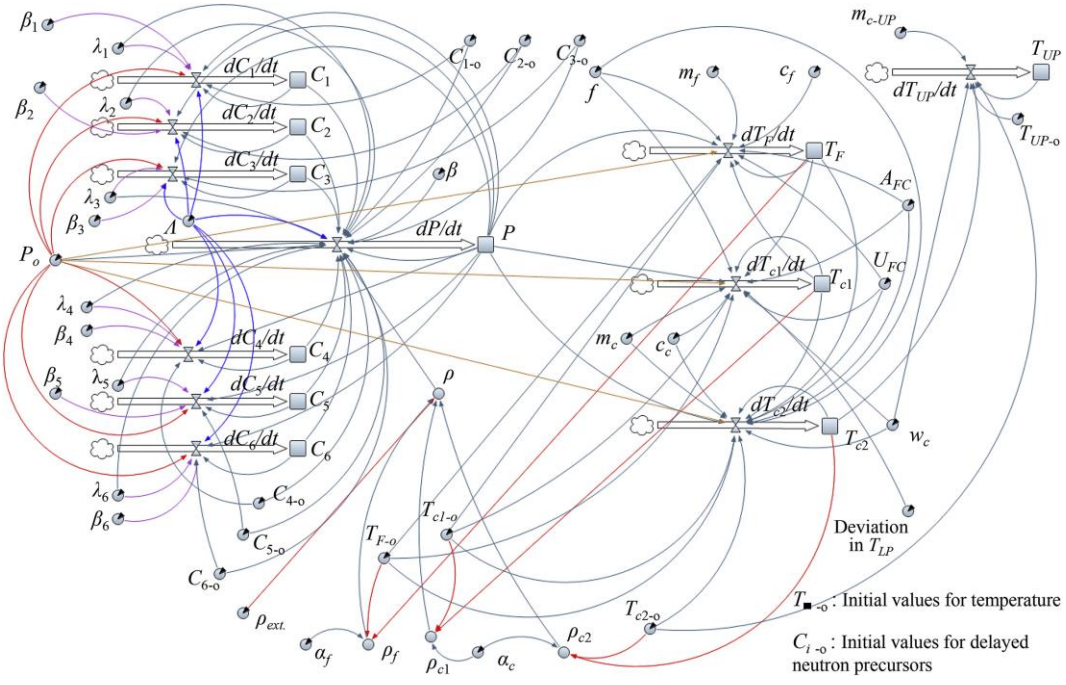

Figure 3-4: Model I: system dynamics of the thermal dynamic process in the reactor core.

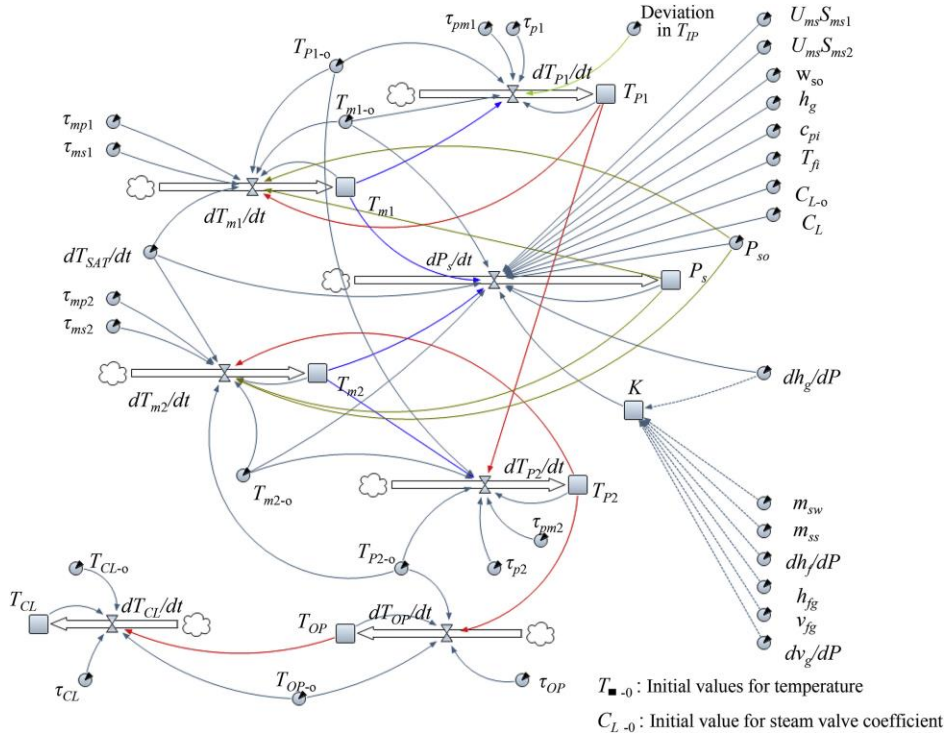

Figure 3-5: Model II: system dynamics of the thermal dynamic process in the secondary coolant system.

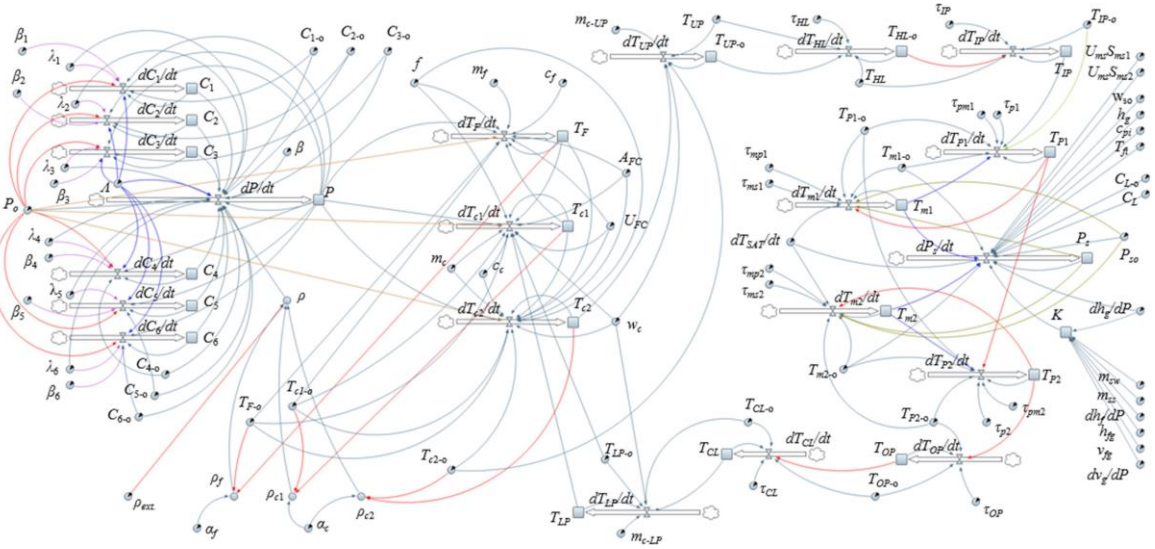

Figure 3-6: Model III: system dynamics of the complete thermal dynamic process in PWR.

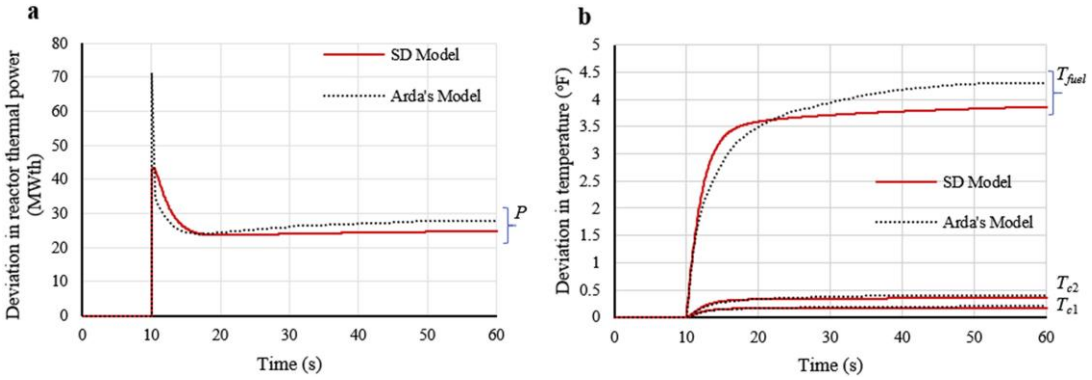

Figure 3-7: **a.** Reactor thermal power response due to adding positive reactivity (Model I). **b.** Fuel and coolant nodes temperature response due to adding positive reactivity (Model I).

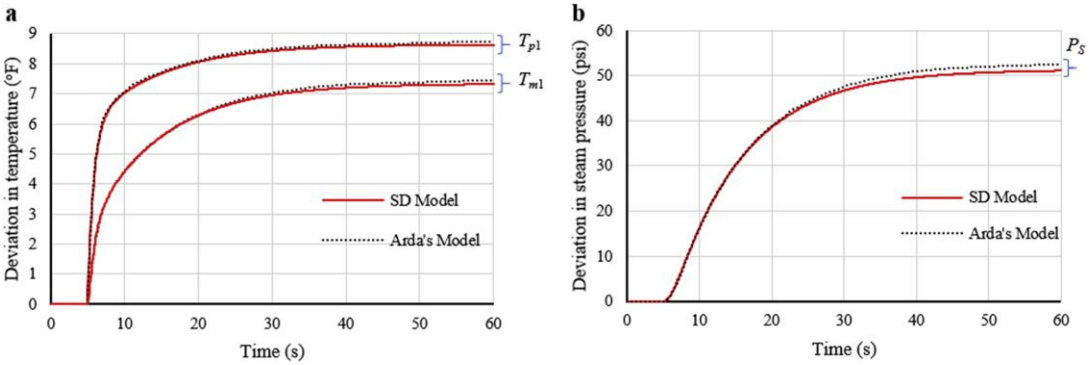

Figure 3-8: **a.** Primary coolant (T_{p1}) and metal U-tube (T_{m1}) temperature response due to an increase in inlet coolant (T_{IP}) temperature (Model II). **b.** Steam pressure response due to an increase in inlet coolant (T_{IP}) temperature (Model II).

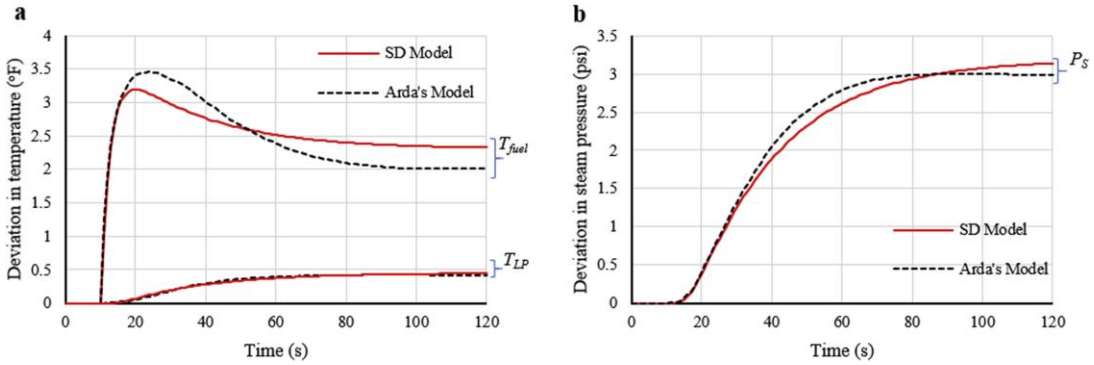

Figure 3-9: **a.** Fuel and inlet coolant (T_{LP}) temperature response due to adding positive reactivity (Model III). **b.** Steam pressure response due to adding positive reactivity (Model III).

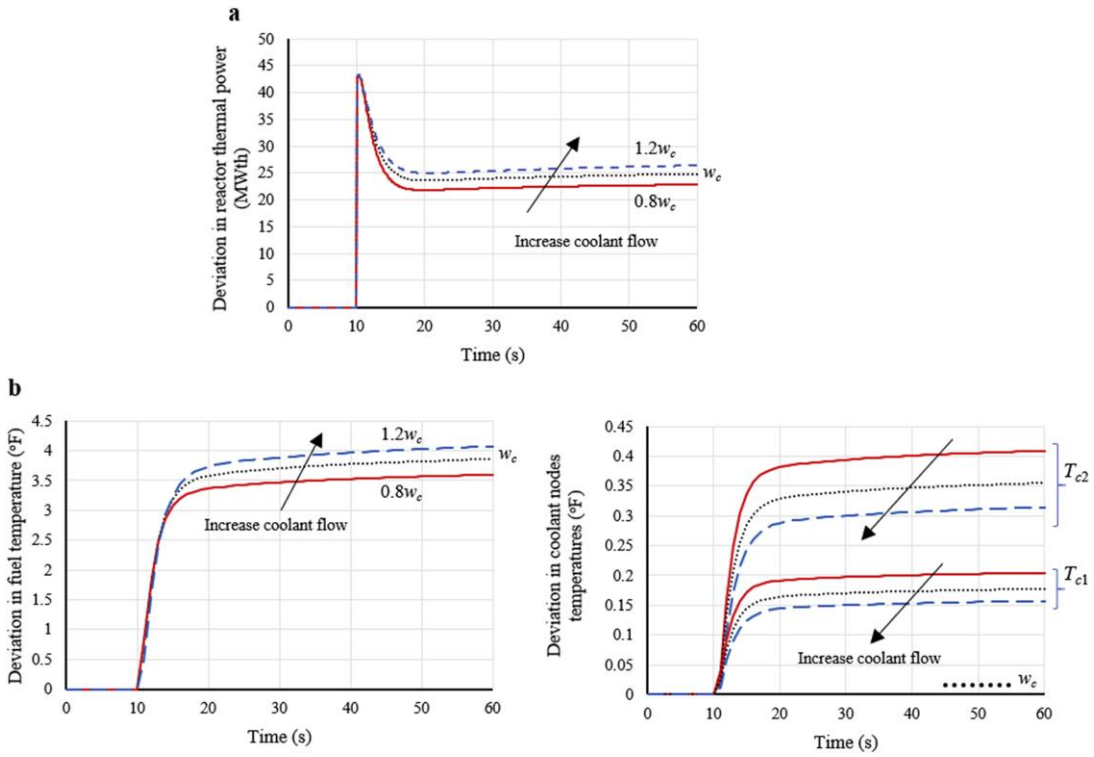

Figure 3-10: **a.** Reactor thermal power response due to adding positive reactivity for different primary coolant flow (w_c) values (Model I – 1st Event). **b.** Fuel and coolant nodes temperature response due to adding positive reactivity for different primary coolant flow (w_c) values (Model I – 1st Event).

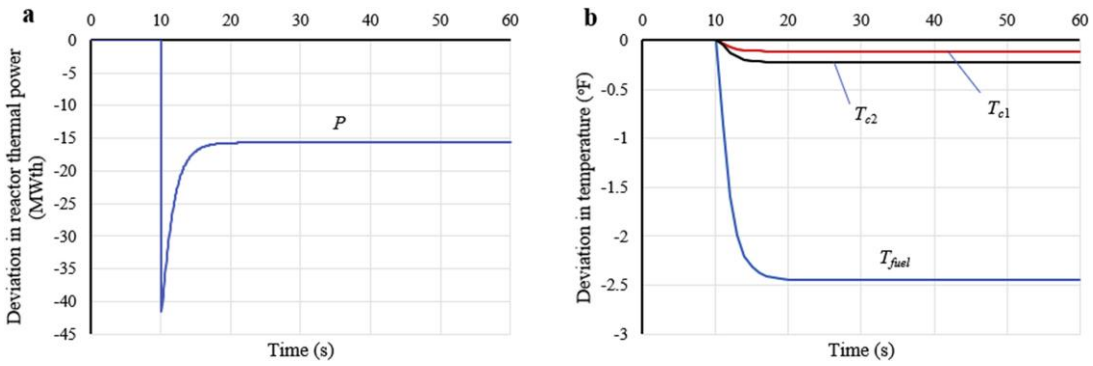

Figure 3-11: **a.** Reactor thermal power response due to adding negative reactivity (Model I – 2nd Event). **b.** Fuel and coolant nodes temperature response due to adding negative reactivity (Model I – 2nd Event).

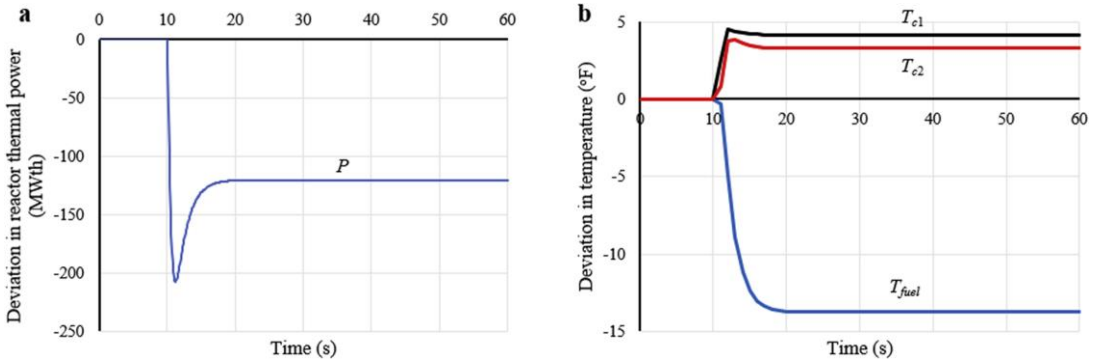

Figure 3-12: **a.** Reactor thermal power response due to an increase in the inlet coolant (T_{LP}) temperature by 5°F (Model I – 3rd Event). **b.** Fuel and coolant nodes temperature response due to an increase in the inlet coolant (T_{LP}) temperature by 5 °F (Model I – 3rd Event).

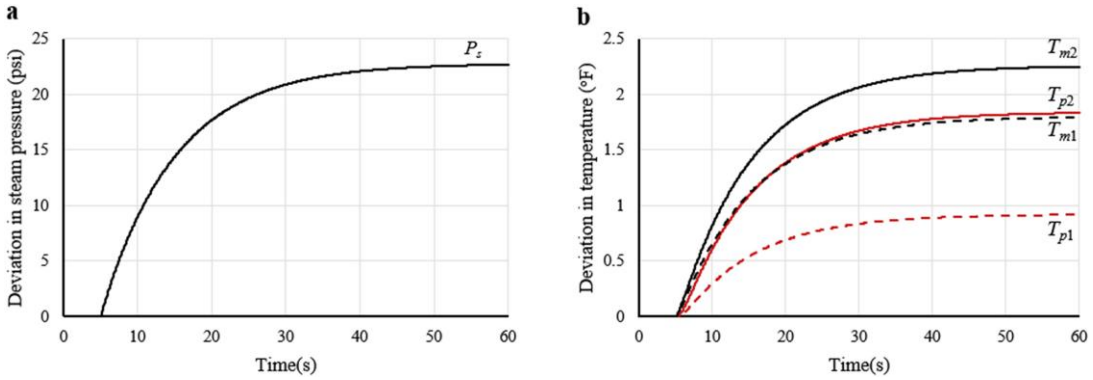

Figure 3-13: **a.** Steam pressure response due to a decrease in steam valve coefficient by 5% (Model II – 1st Event). **b.** Primary coolant and metal tube lump temperature response due to a decrease in steam valve coefficient by 5% (Model II – 1st Event).

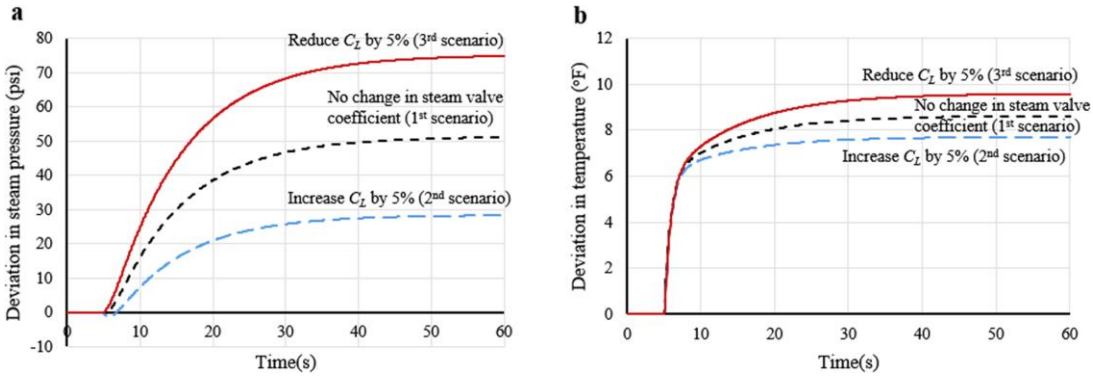

Figure 3-14: **a.** Steam pressure response due to an increase in inlet temperature (T_{IP}) by 10°F with different steam valve (C_L) coefficient (Model II – 2nd Event). **b.** Primary coolant lump (T_{p1}) temperature response due to an increase in inlet temperature (T_{IP}) by 10°F with different steam valve (C_L) coefficient (Model II – 2nd Event).

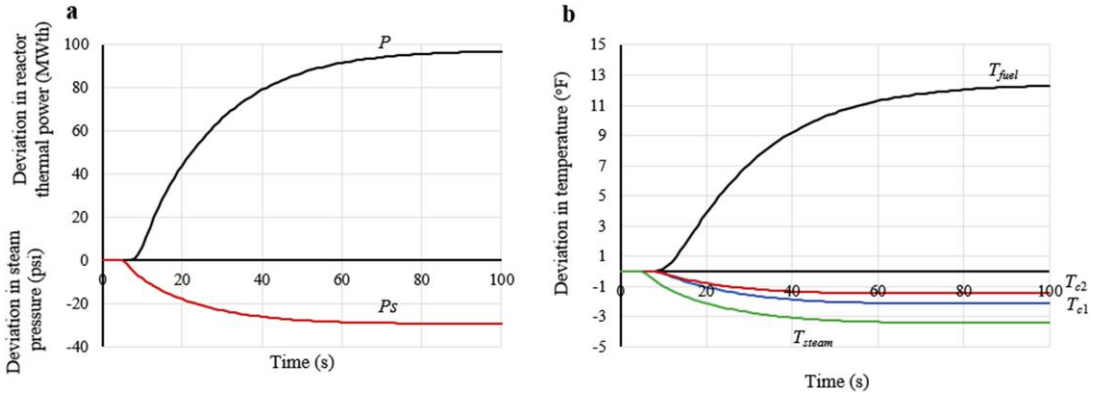

Figure 3-15: **a.** Reactor thermal power and steam pressure response due to an increase in steam valve coefficient by 5% (Model III – 1st Event). **b.** Fuel, coolant nodes, steam temperature response due to an increase in steam valve coefficient by 5% (Model III – 1st Event).

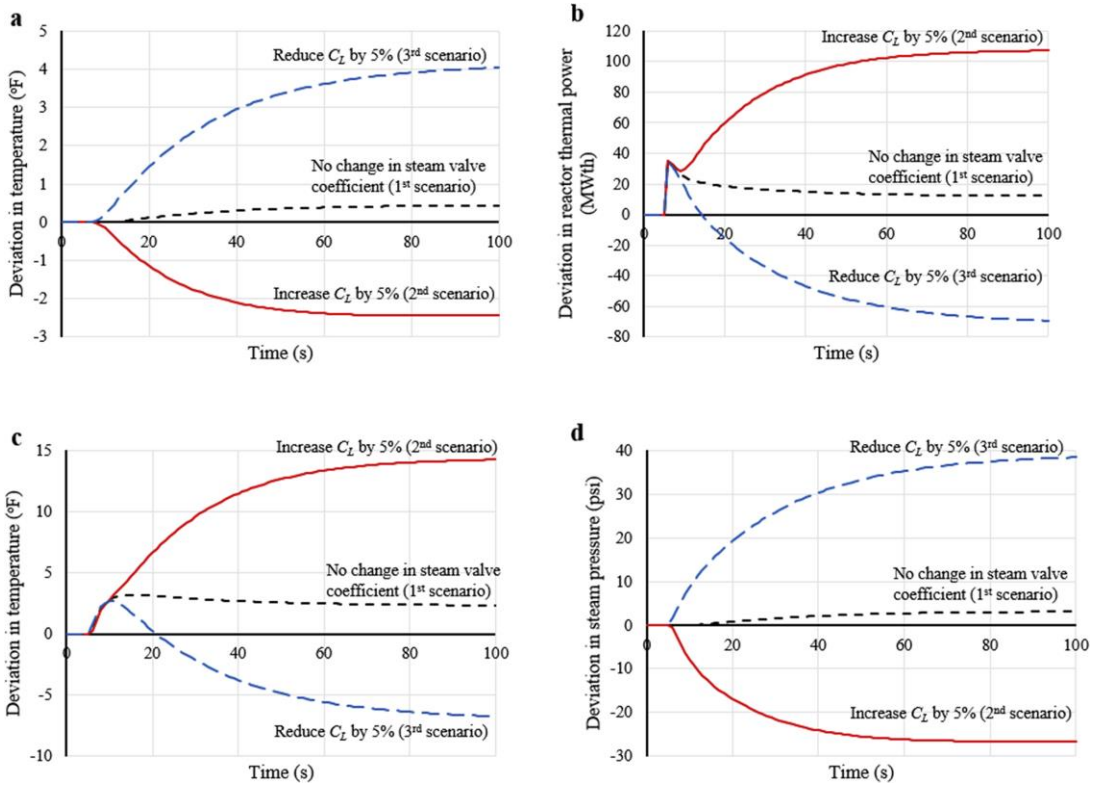

Figure 3-16: **a.** Inlet coolant (T_{LP}) temperature response due to adding positive reactivity with different steam valve coefficient (C_L) (Model III – 2nd Event).

b. Reactor thermal power response due to adding positive reactivity with different steam valve coefficient (C_L) (Model III – 2nd Event). **c.** Fuel temperature response due to an increase in reactivity with different steam valve coefficient (C_L) (Model III – 2nd Event). **d.** Steam pressure response due to an increase in reactivity with different steam valve coefficient (C_L) (Model III – 2nd Event).

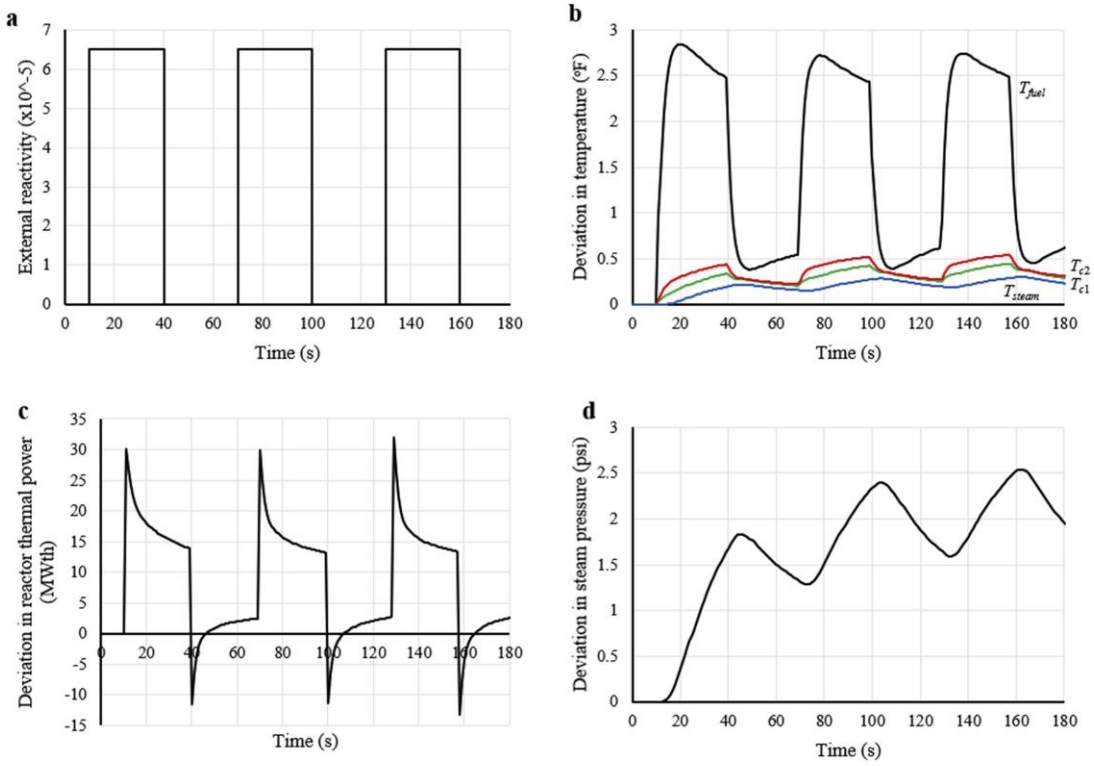

Figure 3-17: **a.** Fluctuation in external reactivity every 30 s (Model III – 3rd Event). **b.** Fuel, coolant, and steam temperature response due to adding positive reactivity every 30 s (Model III – 3rd Event). **c.** Reactor thermal power response due to adding positive reactivity every 30 s (Model III – 3rd Event). **d.** Steam pressure response due to adding positive reactivity every 30 s (Model III – 3rd Event).

Chapter 4 : Dynamic Probabilistic Risk Assessment of Core Damage under Different Transients using System Dynamics Simulation Approach

ABSTRACT

Due to the limitations of static probabilistic risk assessment (PRA) techniques, dynamic PRA (DPRA) of nuclear power plants (NPPs) has become one of the most critical research areas in the field of nuclear engineering, especially in the aftermath of the 2011 Fukushima Daiichi nuclear accident. Uncertainty in the NPP actual behavior is key when considering the safety of the plant under normal and abnormal operating conditions. Such uncertainty typically results from site operation parameters, system conditions, and modeling assumptions. The current study adopts a system dynamics (SD) simulation approach to establish a platform for DPRA of NPPs, considering different sources of uncertainty. To demonstrate the approach's applicability, the average fuel temperature is used as an indicator to estimate the probability of the reactor core damage under different transients, representing perturbations in reactivity and steam valve coefficient. A Monte Carlo simulation is subsequently employed to investigate the effect of uncertainties associated with the different model input parameters. A global sensitivity analysis demonstrates that the total delayed neutron fraction, the heat transfer coefficient from fuel to coolant, the coolant temperature coefficient of reactivity, and the fuel temperature coefficient of reactivity are the primary controllers of the plant

response variability under the transients considered. In summary, the integration of SD and Monte Carlo simulation techniques presents a useful approach to DPRA of NPPs by estimating the temporal probability of core damage, as this overcomes the limitation of static PRA techniques while minimizing the computational cost and time of DPRA analysis.

Keywords: Dynamic Probabilistic Risk Assessment; System Dynamics; Sensitivity Analysis; Uncertainty Analysis; Temporal Probability of Core Damage.

4.1. INTRODUCTION

A nuclear power plant (**NPP**) is a complex system-of-systems that requires full understanding of the behavior of each of its components, the system-level behavior, and the dynamic interaction/interdependence between these different systems and components, under both normal and abnormal operating conditions. Such understanding is now more essential than ever before because of the increased magnitude and frequency of hazard events that can exceed what was originally considered in the NPP design, causing negative impacts on the plant (Hassija et al. 2014). NPP probabilistic risk assessment (**PRA**) approaches adopt *static* event tree (**ET**) and fault tree (**FT**) analysis methods to estimate the probability of occurrence of each accident scenario and its consequences. These methods rely on the so-called *effect line* (Hofer et al. 2002a), where branching points occur based on a specific action strategy for safety systems to mitigate accident propagation. ET/FT analysis methods were previously employed to estimate the frequencies of core damage (IAEA 2010b) and containment radioactive release (IAEA 2010a) as well as the impact of the latter on the public and the economy (CNSC 2014). However, these methods have been extensively criticized (Aldemir 2013; Hsueh and Mosleh 1996; Jankovsky et al. 2018a; Mercurio et al. 2009; Siu 1994; Swaminathan and Smidts 1999a; Zio 2014) due to their inability to: *i*) account for the probabilistic time-dependent interaction among component/system behaviors and the subsequent cascading failures following extreme events; and, *ii*) consider the dynamic (time sequence) propagation of disruptive events. Lessons learned from the Fukushima

nuclear accident also highlighted the importance of enhancing existing, and developing new, PRA approaches to facilitate understanding of the complex dynamic behavior of NPPs following various independent or interrelated hazards (Mosleh 2014). In this regard, precise evaluation of NPP dynamic risks following disruptive events requires an accurate representation of the system and its components' complex interactions.

Due to the limitations of static PRA techniques (i.e., ET and FT), more advanced (*dynamic*) methods have been developed to account for the dynamic nature of NPP systems. These dynamic PRA (**DPRA**) analysis methods consider the timing and sequence of events throughout the modeled NPP systems. Examples of DPRA analysis methodologies include RAVEN (Rabiti et al. 2012, 2013), ADAPT (Hakobyan 2006; Jankovsky et al. 2018b; Kunsman et al. 2008), and dynamic Bayesian network (Jones et al. 2016; Varuttamaseni 2011; Weber et al. 2012). However, DPRA methodologies still face some challenges related to the computational cost (Maljovec et al. 2013; Mandelli et al. 2013a; b, 2017b, 2018), resulting in them being utilized to model small subsystems (Varuttamaseni 2011). More recently, system dynamics (**SD**) simulation has been shown to provide an effective technique for modeling the behavior of dynamic complex systems under different transients (El-Sefy et al. 2019). Therefore, integrating uncertainty quantification and available SD tools within a DPRA framework has the potential of providing a new DPRA platform that can overcome the limitations of static PRA approaches. Such integration can be employed in the field of nuclear engineering

to enable accurate prediction and generation of different accident scenarios including core damage.

Core damage accidents are severe events that may cause extreme damage to the reactor fuel. According to the U.S. NRC, "*thousands or even millions of accident sequences within a NPP can lead to core damage* (U.S. NRC 2016)". Natural and anthropogenic hazards (e.g., fire, internal flooding, and human errors) can also lead to concurrent or partial damage of multiple components within the NPP, which may seriously affect the reactor core integrity. Therefore, probabilistically assessing the dynamic response of NPP-systems is vital to quantify the probability of core damage and the different system contributions to the overall plant risk.

A deterministic SD model for a pressurized water reactor (**PWR**) was developed and validated in a previous study by El-Sefy et al. (2019) as a key step for developing a DPRA platform. In this respect, the present study focuses on adopting the same SD simulation approach to quantify the temporal probability of PWR core damage under different transients considering the uncertainties associated with both the plant physical parameters (e.g., the specific heat of coolant, heat transfer coefficient) and plant operating conditions (e.g., primary coolant flow rate, steam flow rate). This is particularly important as such uncertainties can have a significant influence on the dynamic response of critical parameters in the PWR system (e.g., average fuel temperature, reactor thermal power, steam pressure), and subsequently the reactor core integrity. Therefore, incorporating uncertainties into

the SD model is crucial for an accurate DPRA of the NPP. A global sensitivity analysis is also conducted to identify the most influential parameters affecting the system output (i.e., the average fuel temperature).

Following this introduction section, a brief background about the developed SD simulation approach is presented before discussing the concept and methodology applied for estimating the probability of core damage. Following that, the conducted parameter analysis is described, the details of the uncertainty and sensitivity analyses conducted are discussed, and finally, the results of the parameter analysis, temporal probability of core damage, and temporal sensitivity analysis are summarized.

4.2. SYSTEM DYNAMICS SIMULATION APPROACH

The SD simulation approach was developed by Jay Forrester (Forrester 1971) to investigate the behavior of complex economic and social systems. SD presents a comprehensive technique that can simulate the nonlinear dynamic behavior of complex systems through numerically solving the first-order differential equations describing system behavior. Feedback loops are the key elements of a SD model that describe the nonlinear interdependence between different components, and thus, enable the complete set of the system's nonlinear dynamic features to be described properly (Sterman 2000). The SD simulation approach has been extensively applied to numerous applications (e.g., ecological, agricultural, and economical systems) (Grigoryev 2016), and has been recently utilized in nuclear

applications (Chia et al. 2015; El-Sefy et al. 2019; Guo and Guo 2016; Jeong and Choi 2007)

The present study adopts a SD simulation as the backbone of the DPRA platform. A validated SD model (El-Sefy et al. 2019) was developed to simulate the deterministic physical behavior of the thermal dynamic processes within large/complex systems (i.e., reactor core, primary and secondary cooling systems, hot and cold legs of primary coolant system, and reactor core inlet and outlet plenums, steam generator inlet and outlet plenums) of a PWR. This model was described in more detail by El-Sefy et al. (2019), where the PWR system parameters were adopted from the Palo Verde NPP (Arda 2013). This SD model was validated using the results from an earlier study (Arda 2013) and was subsequently evaluted under different perturbations (El-Sefy et al. 2019). This model was found to provide significant advantages from both computational time and data storage perspectives. Nonetheless, uncertainties associated with physical parameters and plant operating conditions remained to be incorporated within such a model to adequately predict the temporal probability of core damage. Figure 4-1 shows a schematic diagram of the utilized SD model considering uncertainty in the model input parameters.

4.3. CORE DAMAGE DEFINITION

Following an initiating event, the propagation of an accident can take many different scenarios. Each of these scenarios may cause numerous undesired consequences such as reactor core damage and release of radioactivity into the environment. Core damage is one of the most extreme events that can lead to

significant adverse impacts on public health and the environment. For example, the Fukushima nuclear accident led to the meltdown of three nuclear reactors, which resulted in the emission of extensive amounts of radioactive materials to the environment (Chino et al. 2011).

The term "core damage" has multiple drastically different definitions in the literature including: uncovering of the reactor core (U.S. NRC 2010); violation of design basis limits of any of the fuel parameters (IAEA 2010b); heat increase of the reactor fuel until severe fuel damage is anticipated (Bogazici University Nuclear Engineering Department 2000); loss of core geometry or exceeding the design basis limits of any of the fuel parameters (Atomic Energy Regulatory Board 2005); and, the loss of structural integrity of multiple fuel channels (Nuclear Energy Agency 2009). Quantitatively, Knochenhauer and Holmberg (Knochenhauer and Holmberg 2011) defined core damage as the state where the local fuel temperature exceeds 2200^{o}F [1204^{o}C]; that limit is defined in section 1b of 10 CFR 50.46 (U.S. NRC 2017). Probabilistically, core damage has been defined based on a triangular probability density function (***pdf***) for the Zircaloy cladding temperature (Varuttamaseni 2011).

In the present study, the average fuel temperature (henceforth, “fuel temperature”) was utilized as the basis for evaluating the probability of core damage. The lower and upper limits of the fuel temperature were assumed to be 1600^{o}F [871^{o}C] and 2600^{o}F [1426^{o}C], respectively. The *pdf* of core damage beyond these limits was assumed to be equal to zero, whereas a triangular distribution was

used to describe that *pdf* between the upper and lower limits, as shown in Figure 4-2. A maximum accepted fuel temperature of 2200^{o}F was assumed with a corresponding core damage probability of 0.6 (Figure 4-2). This relationship follows the triangular *pdf* defined by Varuttamaseni (2011) except that both the *pdf* and the corresponding probability of core damage are evaluated based on the fuel temperature, rather than the fuel cladding temperature, as discussed by Knochenhauer and Holmberg (2011).

4.4. PARAMETER ANALYSIS

Parameter analysis is typically utilized to assess how the system response is affected by changing some, or all, of the model input parameters. Parameter analysis was applied, in the present study, to the PWR SD model developed by El-Sefy et al. (2019) in order to evaluate the influence of four different transients: *i*) reactivity (P-1); *ii*) steam valve coefficient (P-2); *iii*) reactor core inlet temperature (P-3); and *iv*) steam generator inlet temperature (P-4). For each of these, the deviations from their corresponding nominal values are given in **Table 4-1**. The PWR response (i.e., the fuel temperature, the reactor core thermal power, and the steam pressure inside the steam generator) were subsequently investigated under the considered transients to assess the influence of each transient on the PWR response, and especially to determine the transients that lead to an increase in the reactor core temperature.

4.5. UNCERTAINTY ANALYSIS

Uncertainty analysis is utilized to investigate the impact of uncertain parameters on the fuel temperature response during a transient. The response of reactor fuel temperature is predicted under uncertain physical parameters and operating conditions, leading to an estimate of the temporal probability of core damage. Uncertainty analysis first requires determining the input parameters to be included in the SD model of the PWR. PWR parameters with the expected uncertain ranges are listed in **Table 4-2**. The uncertainty associated with each of these parameters was defined in terms of a *pdf*, which was chosen based on other related studies (Brown and Zhang 2016; Demazière and Pázsit 2002; Perin and Jimenez 2017; Radaideh et al. 2018; Romojaro et al. 2019; Sánchez et al. 2018; Zimmerman et al. 1999), whereas nominal values were chosen based on those of the Palo Verde NPP (Arda 2013; El-Sefy et al. 2019). When information about any specific parameters is not available, the corresponding *pdfs* are chosen based on conservative assumptions or on similar parameters discussed in relevant literature. In this respect, the uniform distribution is chosen as a conservative assumption, when similar parameters do not exist, as minimum, maximum, and nominal values can be encountered with the same probability (Marcum and Brigantic 2015). Referring to **Table 4-2**, a total of 26 parameters follow a normal distribution and seven parameters follow a uniform distribution.

A Monte Carlo (**MC**) simulation was utilized in the present study to assess the propagation of uncertainties associated with the input parameters based on their

pdfs. This approach is preferred over other uncertainty analysis approaches as it is computationally efficient and has no restrictions on the number of uncertain parameters considered (Brown and Zhang 2016). MC simulation relies on generating multiple realizations of the input parameters (based on their corresponding *pdfs*), and subsequently estimating the statistics of the output(s). An iterative method has been utilized in the present study to estimate the number of realizations (*n*) required for applying the MC simulation, in order for the uncertainty in the output to be accurately assessed. This method was proposed by Bukaçi et al. (2016), in which *n* is determined through monitoring the convergence of the output's standard deviation.

4.6. SENSITIVITY ANALYSIS

Sensitivity analysis attempts to quantify the impact of fluctuations in different input parameters on the simulation output and/or the overall system performance. In addition, the analysis aims at investigating how the variability in the system output(s) can be allocated to different inputs (Helton et al. 2006). Therefore, sensitivity analysis provides a more precise picture of how the system inputs and outputs are interrelated. This analysis can be applied either locally or globally, where global sensitivity analysis is preferred as it considers the entire range of the input parameters as well as the interaction among multiple inputs (Ikonen 2016; Ikonen and Tulkki 2014). The Spearman's correlation, $r_{s,}$ and partial correlation coefficients, PCCs, are non-parametric statistical measures that are used to assess the interdependence between an input X and an output Y based on the ordered ranks

of the different values of each variable, and can also be used for sensitivity analysis (Hauke and Kossowski 2011). r_s is defined as the covariance of the rank variables (X and Y) divided by the product of their standard deviations. On the other hand, the PCC between X and Y represents their correlation without considering the collinearity between X and the other inputs affecting Y. Therefore, the PCC is typically used for assessing the direct influence of an input X on the output Y.

In the present study, global sensitivity analysis was applied through estimating the PCC values between the system inputs (shown in **Table 4-2**) and the fuel temperature (output). MC simulation was utilized to fluctuate the system inputs under specified transients. These transients were selected based on their impact, following the results of the parameter analysis, on increasing the fuel temperature. The selected transients include: *i*) increasing the reactivity by 0.006 (S-1); *ii*) increasing the steam valve coefficient by 20% (S-2); *iii*) decreasing the reactor core inlet temperature by 20^{o}F (S-3); and *iv*) decreasing the steam generator inlet temperature by 20^{o}F (S-4). The PCC values were subsequently calculated under each of these transients using the "*partialcorr*" function from the MATLAB statistics toolbox (MATLAB 2018a). Comparing the different PCC values indicates the relative contribution of each input to the variability in the system response (i.e., the fuel temperature) within each transient. In addition, a temporal sensitivity analysis was conducted by evaluating the PCCs at every time step under each transient in order to address time-varying sensitivities in the dynamic PWR system. It is noteworthy that the PCC-based Spearman method has also been utilized in

relevant related studies (e.g., (Brown and Zhang 2016)), and for simulating a station blackout event in the Jules Horowitz reactor (Ghione et al. 2017).

4.7. RESULTS AND DISCUSSION

4.7.1. PARAMETER ANALYSIS

Figure 4-3 shows the effect of changing the reactivity by between -0.0015 and +0.0015 (Transient P-1) on the PWR critical dynamic output parameters (i.e., fuel temperature, thermal power, and steam pressure). Increasing the reactivity levels inside the reactor core causes the neutron flux to increase, which in turn increases the fuel temperature, reactor thermal power, and steam pressure. Afterward, the steam pressure continues to increase due to the thermal energy transferred from the primary coolant system to the secondary one.

Figure 4-4 shows the dynamic responses of fuel temperature, thermal power, and steam pressure under Transient P-2 (changing the steam valve coefficient by between -10% and +10%). Increasing the steam valve coefficient leads to a decrease in the steam pressure, as well as an increase in both the fuel temperature and thermal power. This is attributed to the fact that more steam is required because of opening the steam valve, causing more heat energy to be produced inside the reactor core.

Figure 4-5 shows the effect of changing the coolant temperature by between -5^{o} F and $+5^{o}$ F (Transient P-3) on the PWR critical dynamic output parameters. Increasing the core inlet temperature yields negative reactivity feedback, and

subsequently decreases both the fuel temperature and the thermal power. On the other hand, increasing the coolant temperature leads to an increase in the steam pressure due to the heat energy transferred to the steam generator.

Figure 4-6 shows the impacts of changing the steam generator-inlet coolant temperature by between -5^{o} F and $+5^{o}$ F (Transient P-4) on the dynamic responses of fuel temperature, thermal power, and steam pressure. As expected, increasing the coolant temperature leads to an increase in the heat transferred to the steam generator, and subsequently an increasing steam pressure. However, negative reactivity feedback is developed, which decreases both the fuel temperature and thermal power.

In general, Transients P-1 and P-3 affect both the fuel temperature and thermal power relatively quickly (Figure 4-3 and Figure 4-5), whereas Transients P-2 and P-4 influence these quantities more gradually (Figure 4-4 and Figure 4-6). This is attributed to Transients P-1 and P-3 occurring inside the reactor core, leading to a rapid change in both the fuel temperature and thermal power. On the other hand, Transients P-1 and P-3 affect the steam pressure inside the steam generator at later times (Figure 4-3 and Figure 4-5) because these transients occurred inside the reactor core and an approximately half coolant cycle is required to impact the secondary coolant system (**SCS**). In summary, based on the considered transients, the following lead to an increase in the reactor fuel temperature: increasing the reactivity, increasing the steam valve coefficient, decreasing the reactor core inlet temperature, and decreasing the steam generator-inlet coolant temperature. Thus,

these are considered the basis for both the subsequent uncertainty and sensitivity analysis.

4.7.2. UNCERTAINTY ANALYSIS AND TEMPORAL PROBABILITY OF CORE DAMAGE

As discussed before, an iterative method was utilized to assess the number of realizations (i.e., *n*) required for the MC-based uncertainty analysis. In this method, different values for *n* were assumed and the corresponding estimates of fuel temperature were analyzed under steady-state conditions (i.e., at 100 s) to determine a value of *n* at which the standard deviation has converged. The results showed that both the mean and minimum fuel temperature do not change over the different number of realizations assumed, whereas the maximum fuel temperature showed a variation as the number of realizations increased. This was partially attributed to approximately 1% of the fuel temperature outputs (Figure 4-7a) being statistical outliers. Outliers arise because of the variety of parameters that influence the system outputs, particularly the uniform distribution that was conservatively assumed for system parameters that do not have more well-defined statistical distributions. As these statistical outliers arise because of the confluence of these conservative assumptions and do not reflect the likely real statistical distribution of system outputs, they are eliminated in order to provide a more robust analysis of the results (Ghosh and Vogt 2012) by avoiding over-conservative estimates of the average values, maximum fuel temperature, and the probability of reactor core

damage. In this regard, a point is considered a statistical outlier if its value lies more than three times the scaled median absolute deviations away from the median, which is identified using the "*isoutlier*" function from the MATLAB statistics toolbox (MATLAB 2018a). The standard deviation of maximum fuel temperature data was subsequently evaluated without considering the outliers to evaluate the convergence of the standard deviation as *n* increased, as shown in Figure 4-7b. In this respect, a total of 5,000 realizations was consided in the uncertainty analysis because the standard deviation results were stable by that number of realizations.

According to the results from the parameter analysis described previously, the PWR considered was tested under two transients that could increase the fuel temperature. These transients were: *i*) increasing the reactivity sequentially from 0.001 to 0.016 (U-1); and, *ii*) increasing both the reactivity and steam valve coefficient from 0.002 to 0.016 and from 5% to 30% (U-2), respectively. The temporal probability of core damage was subsequently evaluated, based on the fuel temperature, under each of these transients.

In Transient U-1, the input parameters together with their corresponding statistical distributions (**Table 4-2**) were employed, and the corresponding dynamic responses of fuel temperature were monitored under different levels of reactivity. A MC simulation with 5,000 realizations was adopted at each reactivity level, and the ensemble average of the fuel temperature realizations at different reactivity levels is shown in Figure 4-8. For example, Figure 4-9a and Figure 4-9b show the average, the upper bound, the lower bound, the 25^{th} percentile, and the 75^{th}

percentile of the fuel temperature and the probability of core damage at a reactivity level of +0.015. When the reactivity increased to 0.015, the following responses occur: *i*) the propagation of uncertainties in the PWR system led to an increase in the fuel temperature at 100 s by up to 12.9% relative to the average value of fuel temperature, 1672^{o}F; *ii*) both the fuel temperature and the probability of core damage follow an approximately 3-parameter lognormal distribution, where the majority of their responses are around the mean with relatively few responses that are extremely high or low; and *iii*) the mean and maximum probability of core damage at 100 s are 0.01 and 0.045, respectively. Similar measures can be obtained at other reactivity levels through dissecting the surface plot shown in Figure 4-8.

In Transient U-2, the impact of uncertainty within the input parameters on the PWR was evaluated under a concurrent change in the reactivity levels and the steam valve coefficient. Both the fuel temperature and the probability of core damage were estimated similarly to Transient U-1. Figure 4-10a shows a contour plot for the ensemble average of the fuel temperature realizations at 100 s under different levels of reactivity and steam valve coefficient. As shown in Figure 4-10a, the mean fuel temperature increased with the increase in either the reactivity or the steam valve coefficient. For example, when the reactivity and the steam valve coefficient increased by 0.014 and 30%, respectively, the following was observed: *i*) both the fuel temperature and the probability of core damage follow an approximately 3-parameter lognormal distribution (Figure 4-11a and Figure 4-11b); *ii*) the mean and maximum probability of core damage at 100 s are 0.018 and 0.068, respectively;

and, *iii*) the uncertainties in the input parameters have a significant impact on the fuel temperature, especially under high levels of reactivity (Figure 4-10b), since the fuel temperature is increased by 13.45% and 2.4% at reactivity levels of 0.016 and 0.002, respectively.

The results obtained from Transients U-1 and U-2 demonstrate the importance of considering system uncertainties in evaluating the PWR system's critical parameters since the maximum fuel temperature increased significantly compared to the mean value. Moreover, this study demonstrated a DPRA measurement method that can quantify operational NPP risk and calculate of a core damage probability for the two different initiating events.

4.7.3. SENSITIVITY ANALYSIS

The sensitivity measures for fuel temperature (i.e., PCC) were dynamically evaluated to obtain the different inputs governing the transient history, as shown in Figure 4-12. The same number of realizations (5,000) employed in the uncertainty analysis was also adopted here. The transient ensemble average PCCs for all inputs were replaced by their corresponding squared values to remove the effect of correlation direction (i.e., direct or inverse correlation). The analysis results show that the coolant temperature coefficient of reactivity (α_c) had a significant influence on the fuel temperature in the different transients considered in the sensitivity analysis. However, α_c had a lower impact during the first 25 seconds of the reactivity transient S-1 compared to other transients. This is attributed to the relatively long time required for the coolant to complete a full cycle. The fuel

temperature coefficient of reactivity (α_F) was also found to have a significant impact on the fuel temperature, especially in the cases including positive reactivity transients. These confirm the influence of both α_c and α_F on controlling the stability within the PWR core. In addition, the heat transfer coefficient from the fuel to coolant (U_{FC}) had a significant influence on the fuel temperature within all transients. This is expected as U_{FC} controls the transfer of the thermal energy from the fuel to the primary coolant system. The results from the sensitivity analysis show that α_c, α_F, and U_{FC} are the primary governing parameters of the fuel temperature variability. In addition, the total delayed neutron fraction (β) can also considerably impact the fuel temperature, especially at earlier times, due to the high rate of change in the reactor thermal power at the beginning of the transients. Furthermore, the coolant mass flow was found to have a considerable impact on the fuel temperature in the transients related to a change in the coolant temperature within either the core or the steam generator (Figure 4-12 and Figure 4-13).

Figure 4-13 shows the PCC values between the different inputs and the fuel temperature at 100 s under the selected ranges of the considered transients. Among these inputs, α_F was found to be negatively correlated with the fuel temperature (i.e., can reduce the fuel temperature). This is expected as the selected transients typically lead to an increasing fuel temperature. Therefore, increasing α_F can bring the core back to a stable condition. In addition, α_c was found to be negatively correlated with the fuel temperature within the reactivity transient S-1 only, whereas they were positively correlated in other transients. These interrelations are

attributed to the impact of the different transients on the primary coolant temperature. For example, adding a positive reactivity to the system yields an increasing coolant temperature. Subsequently, α_c induces a negative reactivity feedback which, in turn, decreases the fuel temperature. U_{FC} was found to be inversely related to the fuel temperature as the increase in the heat energy transferred to the coolant can decrease the fuel temperature. Furthermore, uncertainty of the parameters pertaining to the steam generator system (e.g., τ_{PM1}, τ_{PM2}, τ_{MP1}, τ_{MP2}, τ_{MS1}, τ_{MS2},) was also found to have a significant impact on the fuel temperature when Transients S-2 and S-4 occur within the SCS (e.g., changing the steam valve coefficient and fluctuating the steam generator inlet temperature). Finally, the remaining parameters had minor impacts on the fuel temperature compared to those discussed above.

4.8. CONCLUSIONS

This study utilized a SD simulation approach for DPRA of nuclear power plants to estimate the risk associated with various plant transients. The transients that are expected to occur during plant operation cause challenges to NPP systems and operators, potentially leading to core damage. As such, identifying and addressing the potential risk associated with NPP transients is vital to ensure the safety of NPPs. In this regard, parameter analysis was performed to investigate the behavior of fuel temperature, reactor thermal power, and steam pressure under different transients. These transients included changing the reactivity, the steam valve coefficient, the reactor core inlet temperature, and the steam generator inlet

temperature. Afterward, the developed DPRA platform was used to predict the nonlinear dynamic response of fuel temperature within a PWR when uncertainty in the reactor physical parameters and operating conditions were considered under different transients. The fuel temperature was subsequently used to estimate the temporal probability of core damage based on a triangular probability density function of core damage. Monte Carlo simulation was adopted to predict how the propagation of uncertainty associated with each of the input parameters would affect the temporal probability of core damage. This probability was estimated under: *i*) increasing reactivity levels; and, *ii*) a simultaneous increase in the steam valve coefficient and reactivity. Finally, a global sensitivity analysis was performed to identify the uncertain parameters that significantly impact the average fuel temperature.

The results of the current study demonstrate that the newly developed DPRA platform is able to consider the dynamic interaction among several complex systems inside the NPP, including the reactor core, primary and secondary cooling systems, hot and cold legs, reactor core inlet and outlet plenums, and steam generator inlet and outlet plenums, and therefore, overcome the challenges facing existing DPRA approaches in simulating large complex systems. Moreover, the results from the Monte Carlo simulation revealed that both the fuel temperature and the probability of core damage follow a 3-parameter lognormal distribution under the considered transients. Furthermore, the impact of uncertain input parameters was found to amplify with increasing transient severity. A global sensitivity

analysis also demonstrated that the coolant temperature coefficient of reactivity, the fuel coefficient of reactivity, the heat transfer coefficient from fuel to coolant, and the total delayed neutron fraction are the primary controllers of the fuel temperature variability under the different transients considered. In addition, the primary coolant mass flow rate had a considerable impact on the fuel temperature variability during the transients related to the core and steam generator inlet temperatures.

The results from the present study demonstrate the influence of integrating the uncertainty analysis and SD simulation approach to estimate the temporal probability of core damage, thus overcoming the limitations of static PRA methods. In this respect, the developed platform is a crucial step toward minimizing the computational cost of DPRA methods (e.g., the analysis time needed to estimate the temporal probability of core damage for transients U-1 or U-2 is only about 10-15 min) and integrating many systems in order to establish a DPRA approach for simulating large, complex NPP systems.

4.9. ACKNOWLEDGMENTS

The financial support for the study was provided through the Canadian Nuclear Energy Infrastructure Resilience under Seismic Systemic Risk (CaNRisk) – Collaborative Research and Training Experience (CREATE) program of the Natural Science and Engineering Research Council (NSERC) of Canada. The support from the INTERFACE Institute and the INViSiONLab, both of McMaster University, is also acknowledged.

4.10. REFERENCES

Aldemir, T. (2013). "A survey of dynamic methodologies for probabilistic safety assessment of nuclear power plants." *Annals of Nuclear Energy*, Elsevier Ltd, 52, 113–124.

Arda, S. (2013). "Implementing a Nuclear Power Plant Model for Evaluating Load-Following Capability on a small Grid." MASc Thesis, Arizona State University.

Atomic Energy Regulatory Board. (2005). *Glossary of terms for nuclear and radiation safety. Technical report.*

Bogazici University Nuclear Engineering Department. (2000). "PSA Glossary."

Brown, C. S., and Zhang, H. (2016). "Uncertainty quantification and sensitivity analysis with CASL Core Simulator VERA-CS." *Annals of Nuclear Energy journal*, 95, 188–201.

Bukaçi, E., Korini, T., Periku, E., Allkja, S., and Sheperi, P. (2016). "Number of iterations needed in Monte Carlo Simulation using reliability analysis for tunnel supports." *Journal of Engineering Research and Applications*, 6(6), 60–64.

Chia, E. S., Lim, C. K., Ng, A., and Nguyen, N. H. L. (2015). "The System Dynamics of Nuclear Energy in Singapore." *International Journal of Green Energy*, Taylor & Francis, 12(1), 73–86.

Chino, M., Nakayama, H., Nagai, H., Terada, H., Katata, G., and Yamazawa, H. (2011). "Preliminary Estimation of Release Amounts of 131 I and 137 Cs

Accidentally Discharged from the Fukushima Daiichi Nuclear Power Plant into the Atmosphere." *Journal of Nuclear Science and Technology*, 48(7), 1129–1134.

CNSC. (2014). *Safety Analysis: Probabilistic Safety Assessment (PSA) for Nuclear Power Plants*. *REGDOC-2.4.2*, Canadian Nuclear Safety Commission.

Demazière, C., and Pázsit, I. (2002). "Evaluation of the Boron Dilution Method for Moderator Temperature Coefficient Measurements." *Nuclear Technology*, 140, 147–163.

El-Sefy, M., Ezzeldin, M., El-Dakhakhni, W., Wiebe, L., and Nagasaki, S. (2019). "System Dynamics Simulation of the Thermal Dynamic Processes in Nuclear Power Plants." *Nuclear Engineering and Technology*, Elsevier Ltd, 51(6), 1540–1553.

Forrester, J. (1971). "Counterintuitive Behavior of Social Systems." *MIT Technology Review*, 73 (3), 52–68.

Ghione, A., Noel, B., Vinai, P., and Demazière, C. (2017). "Uncertainty and sensitivity analysis for the simulation of a station blackout scenario in the Jules Horowitz Reactor." *Annals of Nuclear Energy*, Elsevier Ltd, 104, 28–41.

Ghosh, D., and Vogt, A. (2012). "Outliers: An Evaluation of Methodologies. Joint Statistical Meetings. San Diego, CA: American Statistical Association.

Grigoryev, I. (2016). *AnyLogic 7 in Three Days*.

Guo, X., and Guo, X. (2016). "Nuclear power development in China after the restart of new nuclear construction and approval: A system dynamics analysis." *Renewable and Sustainable Energy Reviews*, Elsevier, 57, 999–1007.

Hakobyan, A. P. (2006). "Severe accident analysis using dynamic accident progression event trees." Ph.D. Thesis, The Ohio State University.

Hassija, V., Senthil Kumar, C., and Velusamy, K. (2014). "Probabilistic safety assessment of multi-unit nuclear power plant sites - An integrated approach." *Journal of Loss Prevention in the Process Industries*, Elsevier Ltd, 32, 52–62.

Hauke, J., and Kossowski, T. (2011). "Comparison of Values of Pearson's and Spearman's Correlation Coefficients on the Same Sets of Data." *Quaestiones Geographicae*, 30(2).

Helton, J. C., Johnson, J. D., Sallaberry, C. J., and Storlie, C. B. (2006). "Survey of sampling-based methods for uncertainty and sensitivity analysis." 91, 1175–1209.

Hofer, E., Kloos, M., Krzykacz-Hausmann, B., Peschke, J., and Sonnenkalb, M. (2002). "Dynamic event trees for probabilistic safety analysis." *EUROSAFE Forum 2002: convergence of nuclear safety practices in Europe Papers, Germany*.

Hsueh, K. S., and Mosleh, A. (1996). "The development and application of the accident dynamic simulator for dynamic probabilistic risk assessment of

nuclear power plants." *Reliability Engineering and System Safety*, 52, 297–314.

IAEA. (2010a). *Development and Application of Level 1 Probabilistic Safety Assessment for Nuclear Power Plants*. *IAEA Safety Standards Series No. SSG-3, IAEA, Vienna (2010).*

IAEA. (2010b). *Development and Application of Level 2 Probabilistic Safety Assessment for Nuclear Power Plants*.

Ikonen, T. (2016). "Comparison of global sensitivity analysis methods – Application to fuel behavior modeling." *Nuclear Engineering and Design*, Elsevier B.V., 297, 72–80.

Ikonen, T., and Tulkki, V. (2014). "The importance of input interactions in the uncertainty and sensitivity analysis of nuclear fuel behavior." *Nuclear Engineering and Design*, Elsevier B.V., 275, 229–241.

Jankovsky, Z. K., Denman, M. R., and Aldemir, T. (2018a). "Dynamic event tree analysis with the SAS4A/SASSYS-1 safety analysis code." *Annals of Nuclear Energy*, Elsevier Ltd, 115, 55–72.

Jankovsky, Z. K., Haskin, T., and Denman, M. (2018b). *How to ADAPT*. Sandia National Laboratories.

Jeong, C. J., and Choi, H. (2007). "Dynamic Modeling and Analysis of Alternative Fuel Cycle Scenarios in Korea." *Nuclear Engineering and Technology*, Vol.39(1), 85–94.

Jones, T. B., Darling, M. C., Groth, K. M., Denman, M. R., and Luger, G. F.

(2016). “A Dynamic Bayesian Network for Diagnosing Nuclear Power Plant Accidents.” *The 29th International Florida Artificial Intelligence Research Society Conference*, 179–184.

Knochenhauer, M., and Holmberg, J. E. (2011). *Guidance for the Definition and Application of Probabilistic Safety Criteria*. Swedish Radiation Safety Authority.

Kunsman, D. M., Dunagan, S., Aldemir, T., Denning, R., Hakobyan, A., Metzroth, K., Catalyurek, U., and Rutt, B. (2008). *Development and Application of the Dynamic System Doctor to Nuclear Reactor Probabilistic Risk Assessments*. Sandia National Laboratories.

Maljovec, D., Wang, B., Pascucci, V., and Mandelli, D. (2013). “Analyzing Dynamic Probabilistic Risk Assessment Data through Topology-Based Clustering.” *ANS PSA 2013 International Topical Meeting on Probabilistic Safety Assessment and Analysis*, 1–16.

Mandelli, D., Maljovec, D., Alfonsi, A., Parisi, C., Talbot, P., Cogliati, J., Smith, C., and Rabiti, C. (2018). “Mining data in a dynamic PRA framework.” *Progress in Nuclear Energy*, Elsevier, 108, 99–110.

Mandelli, D., Parisi, C., Alfonsi, A., Maljovec, D., Germain, S. S., Boring, R., Ewing, S., Smith, C., and Rabiti, C. (2017). “Dynamic PRA of a Multi-Unit Plant.” *International Topical Meeting on Probabilistic Safety Assessment (PSA 2017)*.

Mandelli, D., Smith, C., Rabiti, C., Alfonsi, A., Youngblood, R., Pascucci, V.,

Wang, B., Maljovec, D., Bremer, P. T., Aldemir, T., Yilmaz, A., and Zamalieva, D. (2013a). "Dynamic PRA: An Overview of New Algorithms to Generate, Analyze and Visualize Data." *Transactions of the American Nuclear Society*.

Mandelli, D., Yilmaz, A., Aldemir, T., Metzroth, K., and Denning, R. (2013b). "Scenario clustering and dynamic probabilistic risk assessment." *Reliability Engineering and System Safety*, Elsevier, 115, 146–160.

Marcum, W. R., and Brigantic, A. J. (2015). "Applying uncertainty and sensitivity on thermal hydraulic subchannel analysis for the multi-application small light water reactor." *Nuclear Engineering and Design*, Elsevier B.V., 293, 272–291.

MATLAB Statistics Toolbox Release 2018a, The MathWorks, Inc., Natick, Massachusetts, United States." (2018). .

Mercurio, D., Podofillini, L., Zio, E., and Dang, V. N. (2009). "Identification and classification of dynamic event tree scenarios via possibilistic clustering: Application to a steam generator tube rupture event." *Accident Analysis and Prevention*, 41, 1180–1191.

Mosleh, A. (2014). "PRA: A Perspective on strengths, current limitations, and possible improvements." *Nuclear Engineering and Technology*, Korean Nuclear Society, 46(1), 1–10.

Nuclear Energy Agency. (2009). *Probabilistic Risk Criteria and Safety Goals*.

Perin, Y., and Jimenez, J. (2017). "Application of the best-estimate plus

uncertainty approach on a BWR ATWS transient using the NURESIM European code platform." *Nuclear Engineering and Design*, Elsevier B.V., 321, 48–56.

Rabiti, C., Alfonsi, A., Mandelli, D., Cogliati, J., and Martineau, R. (2012). "RAVEN as Control Logic and Probabilistic Risk Assessment Driver for RELAP-7." *ANS Winter Meeting*.

Rabiti, C., Alfonsi, A., Mandelli, D., Cogliati, J., Martineau, R., and Smith, C. L. (2013). *Deployment and Overview of RAVEN Capabilities for a Probabilistic Risk Assessment Demo for a PWR Station Blackout*. Idaho National Laboratory.

Radaideh, M. I., Wieselquist, W. A., Ridge, O., and Kozlowski, T. (2018). "A new framework for sampling-based uncertainty quantification of the six-group reactor kinetic parameters." *Annals of Nuclear Energy*.

Romojaro, P., Álvarez-Velarde, F., and García-Herranz, N. (2019). "Sensitivity methods for effective delayed neutron fraction and neutron generation time with summon." *Annals of Nuclear Energy*, Elsevier Ltd, 126, 410–418.

Sánchez, A. I., Villanueva, J. F., Carlos, S., and Martorell, S. (2018). "Uncertainty analysis of a large break loss of coolant accident in a pressurized water reactor using non-parametric methods." *Reliability Engineering and System Safety*, Elsevier Ltd, 174, 19–28.

Siu, N. (1994). "Risk assessment for dynamic systems: An overview." *Reliability Engineering and System Safety*, 43, 43–73.

Sterman, J. (2000). *Business Dynamics: Systems Thinking and Modeling for a Complex World*. Boston: Irwin/McGraw-Hill.

Swaminathan, S., and Smidts, C. (1999). "The Event Sequence Diagram framework for dynamic Probabilistic Risk Assessment." *Reliability Engineering & System Safety*, 63, 73–90.

U.S. NRC. (2016). *Probabilistic Risk Assessment and Regulatory Decisionmaking: Some Frequently Asked Questions*.

U.S. NRC. (2017). *Acceptance criteria for emergency core cooling systems for light-water nuclear power reactors*.

U.S. NRC. (2010). *Risk Assessment of Operational Events- Volume 3: SPAR Model Reviews*.

Varuttamaseni, A. (2011). "Bayesian Network Representing System Dynamics in Risk Analysis of Nuclear Systems." Ph.D. Thesis, University of Michigan.

Weber, P., Simon, C., and Iung, B. (2012). "Overview on Bayesian networks applications for dependability, risk analysis and maintenance areas." *Engineering Applications of Artificial Intelligence*, Elsevier, 25, 671–682.

Zimmerman, S. G., Brittingham, J. C., Reed, M. L., Bandera, R. P., and Crawley, P. F. (1999). *PWR Reactor Physics Methodology Using CASMO-4/SIMULATE-3*. Arizona Public Service Company.

Zio, E. (2014). "Integrated deterministic and probabilistic safety assessment: Concepts, challenges, research directions." *Nuclear Engineering and Design*, Elsevier B.V., 280, 413–419.

Table 4-1 The different ranges of the transients employed in the present study

Transient description	Transient level	Nominal values (Arda 2013; El-Sefy et al. 2019)
Transient P-1: Changing the reactivity (ρ)	Max= 0.0015 Min= -0.0015	0.0 [Steady State]
Transient P-2: Changing the steam generator-steam valve coefficient (C_L)	Max= 10% Min= -10%	6.0
Transient P-3: Changing the reactor core inlet temperature (T_{LP})	Max= 5^{o}F Min= -5^{o}F	296.3^{o}F
Transient P-4: Changing the steam generator inlet temperature (T_{IP})	Max= 5^{o}F Min= -5^{o}F	625.0^{o}F

Table 4-2 Selected SD model input uncertanties: standard deviation and distributions

Parameter	Symbol	Nominal (Mean)	Standard Deviation	Reference*
Normal Distributed Inputs				
Specific heat of primary coolant [Btu/lb.^{o}F]	c_c	1.448	0.01448	------
Specific heat of the reactor fuel [Btu/lb.^{o}F]	c_f	0.1056	0.001056	(Sánchez et al. 2018)
Specific heat of feedwater in steam generator [Btu/lb.^{o}F]	c_{pi}	1.278	0.01278	------
Enthalpy of saturated water [Btu/lb]	h_f	554	1.108	(Perin and Jimenez 2017)
Enthalpy of saturated steam [Btu/lb]	h_g	1189	2.378	------
Heat transfer coefficient from fuel to coolant [Btu/sec.ft^2.^{o}F]	U_{FC}	0.090441111	9.0441×10^{-3}	(Sánchez et al. 2018)
Delayed neutron precursor decay constant for the six-delayed neutron group, i=1,……,6 [1/s]	λ_1	0.0124	2.48×10^{-4}	(Radaideh et al. 2018)
	λ_2	0.0305	8.235×10^{-4}	
	λ_3	0.111	3.33×10^{-3}	
	λ_4	0.301	9.632×10^{-3}	
	λ_5	1.14	0.09918	
	λ_6	3.01	0.23779	
Total delayed neutron fraction	β	0.0065	4.615×10^{-4}	(Radaideh et al. 2018)
Delayed neutron fraction for the six delayed-neutron groups, i=1,……,6;	β_1	0.000215	1.8275×10^{-5}	
	β_2	0.001424	8.9712×10^{-5}	
	β_3	0.001274	1.223×10^{-4}	
	β_4	0.002568	1.926×10^{-4}	
	β_5	0.000748	9.5744×10^{-5}	
	β_6	0.000273	4.6137×10^{-5}	
Fuel temperature coefficient of reactivity	α_F	-1.2×10^{-5}	-1.968×10^{-6}	(Zimmerman et al. 1999)

Time constant for primary coolant lump 1 to metal tube lump 1 heat transfer [s]	τ_{PM1}	1.2233	0.1233	------
Time constant for primary coolant lump 2 to metal tube lump 2 heat transfer [s]	τ_{PM2}	0.5826	0.05826	------
Time constant for metal tube lump 1 to primary coolant lump 1 heat transfer [s]	τ_{MP1}	0.3519	0.03519	------
Time constant for metal tube lump 2 to primary coolant lump heat transfer [s]	τ_{MP2}	0.1676	0.01676	------
Time constant for metal tube lump 1 to secondary coolant heat transfer [s]	τ_{MS1}	0.3519	0.03519	------
Time constant for metal tube lump 2 to secondary coolant heat transfer [s]	τ_{MS2}	0.1676	0.01676	------
Uniform Distributed Inputs			Values	
Primary coolant mass flow rate of inside the core [lb/s]	w_c	45555.56	Min= 44189 Max= 46922	(Brown and Zhang 2016)
Primary coolant mass flow rate in the hot leg [lb/s]	$w_{c\text{-}hl}$	22777.78	Min= 22094 Max= 23461	------
Primary coolant mass flow rate in the cold leg [lb/s]	$w_{c\text{-}cl}$	11388.88	Min= 11047 Max= 11730	------
Primary coolant mass flow rate in steam generator [lb/s]	$w_{c\text{-}sg}$	22777.78	Min= 22094 Max= 23461	------

Steam flow rate [lb/s]	w_{so}	4772.22	Min= 4629 Max= 4915	------
Coolant temperature coefficient of reactivity	α_c	$-1.0\text{x}10^{-4}$	Min= $-7.504\text{x}10^{-5}$ Max= $-1.2496\text{x}10^{-4}$	(Demazière and Pázsit 2002)
Neutron generation time [s]	Λ	0.00003	Min= $2.965\text{x}10^{-5}$ Max= $3.035\text{x}10^{-5}$	(Romojaro et al. 2019)

* Uncertainties associated with the model input parameters are determined based on references in **Table 4-2**.

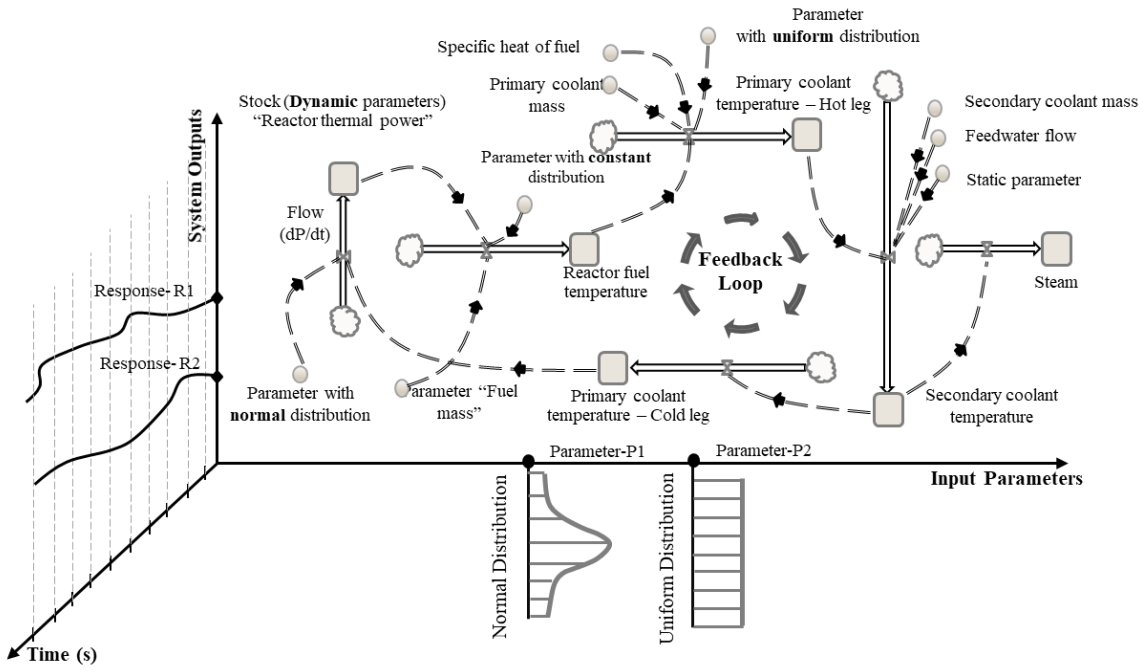

Figure 4-1: Schematic diagram of SD model of a PWR considering uncertainties associated with the input parameters.

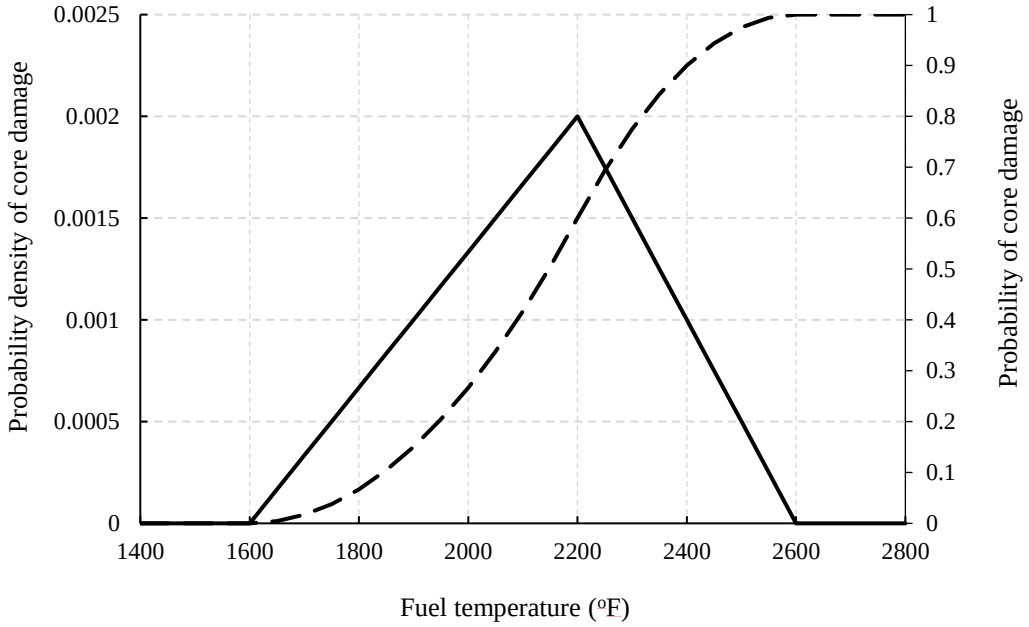

Figure 4-2: Probability density and probability distribution of core damage at different fuel temperatures.

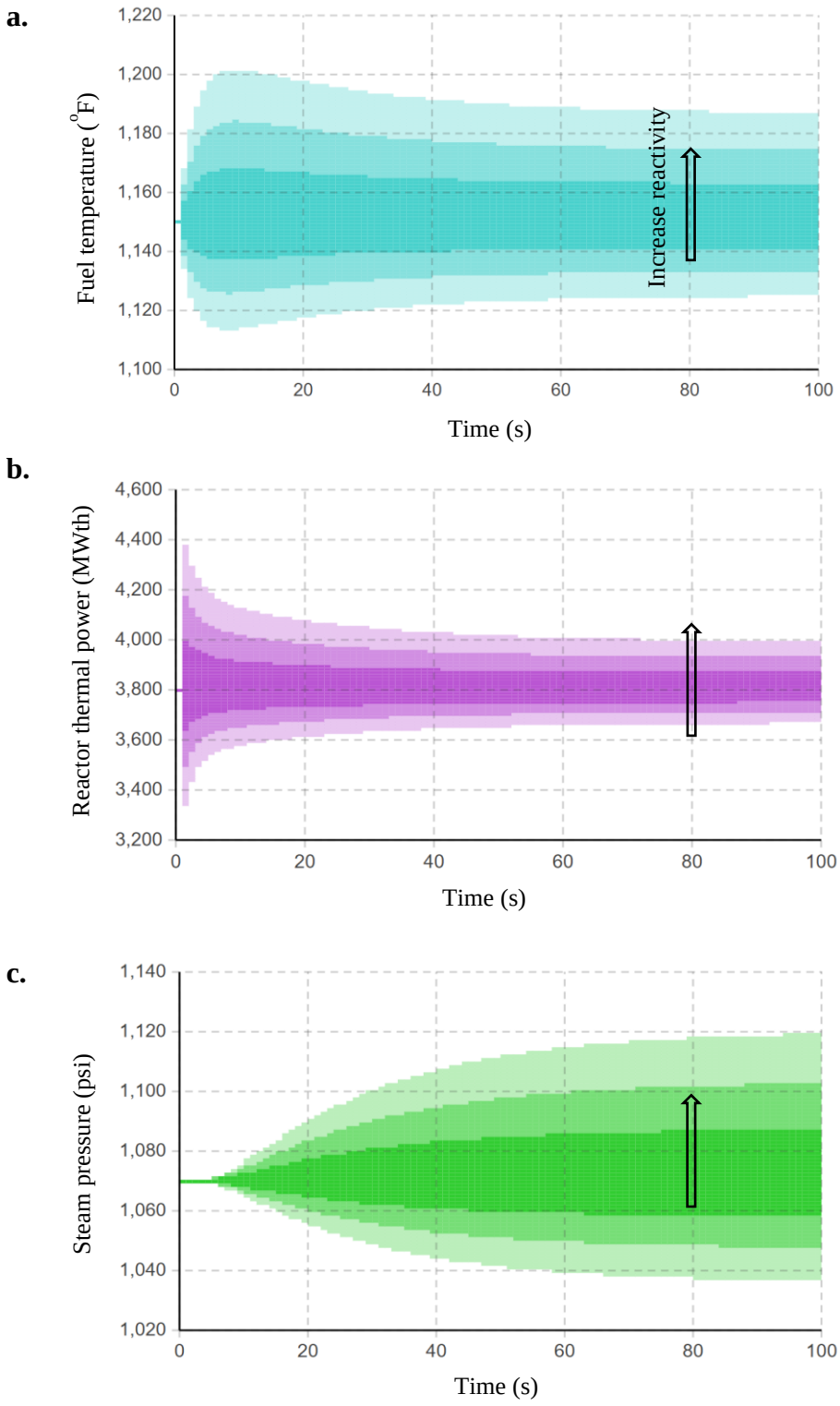

Figure 4-3: **a.** Fuel temperature, **b.** Reactor thermal power, and **c.** Steam pressure responses due to changing the reactivity levels (Transient P-1).

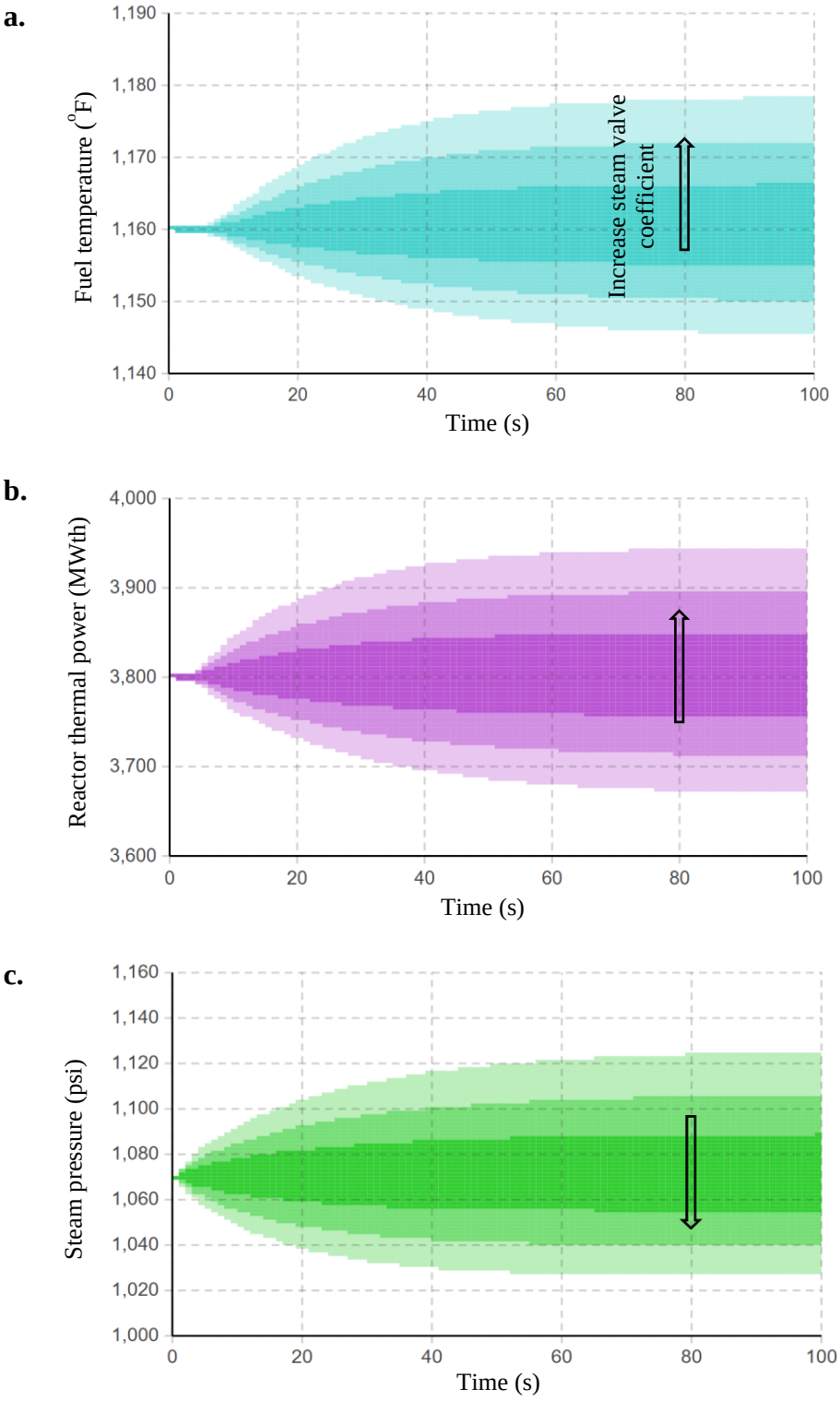

Figure 4-4: **a.** Fuel temperature, **b.** Reactor thermal power, and **c.** Steam pressure responses due to changing the steam valve coefficient (Transient P-2).

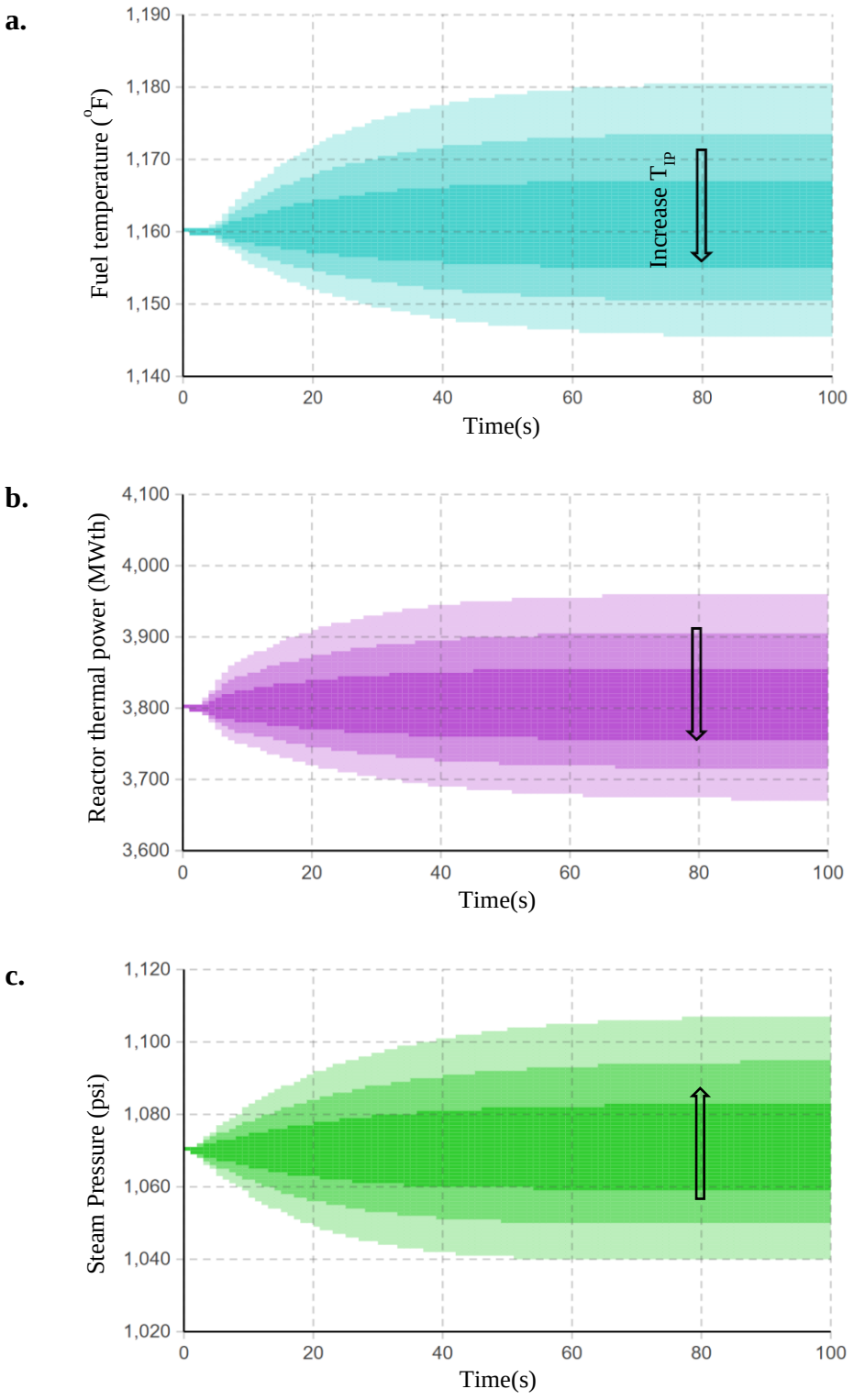

Figure 4-5: **a.** Fuel temperature, **b.** Reactor thermal power, and **c.** Steam pressure responses due to changing the reactor core inlet temperature (Transient P-3).

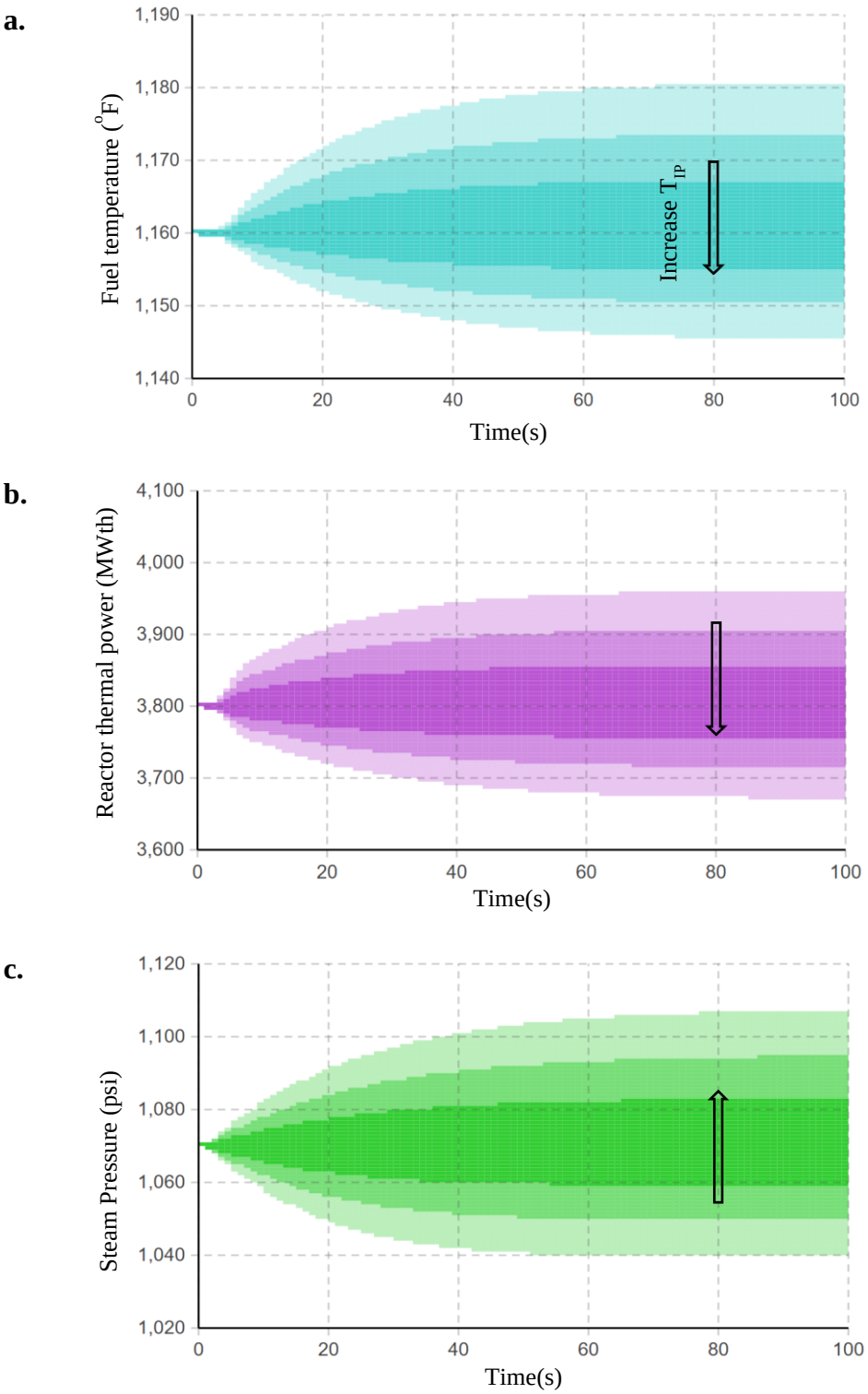

Figure 4-6: **a.** Fuel temperature, **b.** Reactor thermal power, and **c.** Steam pressure responses due to changing the steam generator inlet temperature (Transient P-4).

a.

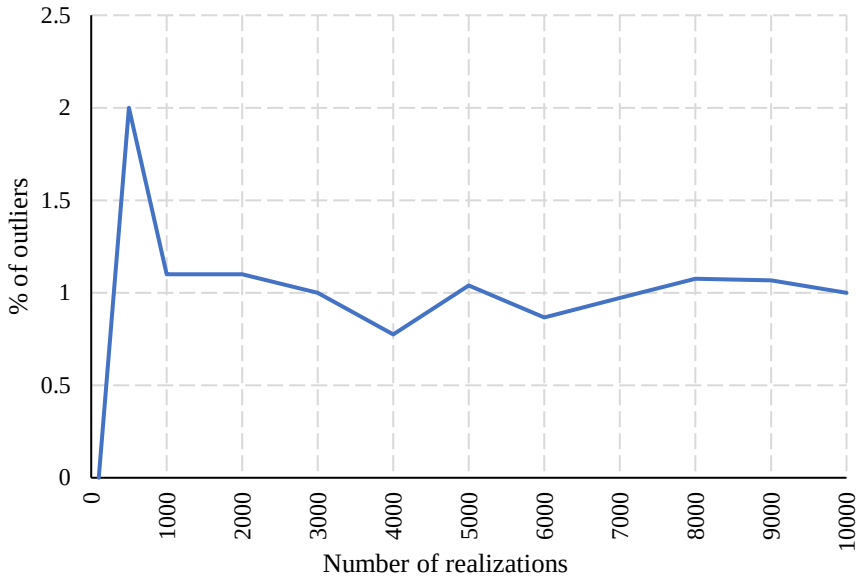

b.

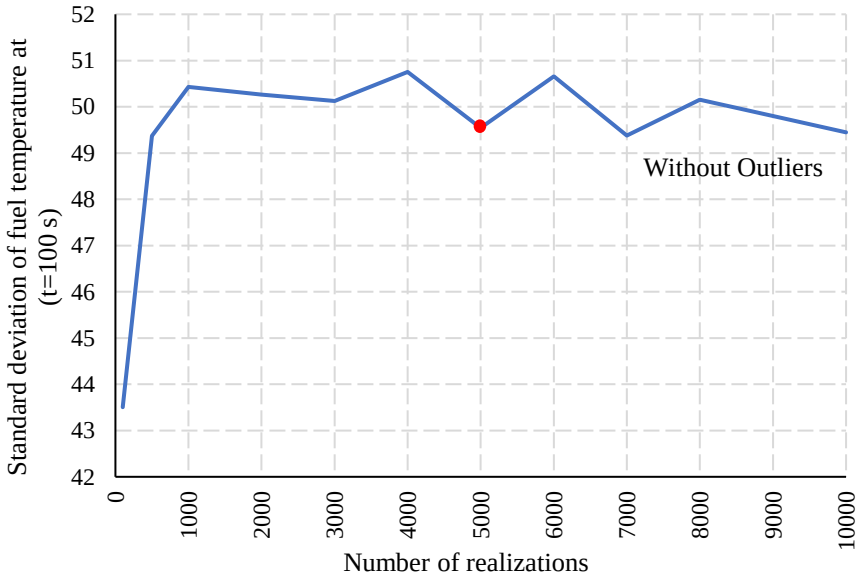

Figure 4-7: **a.** Percentage of outliers in the data with number of realizations. **b.** Convergence analysis of standard deviation of the fuel temperature.

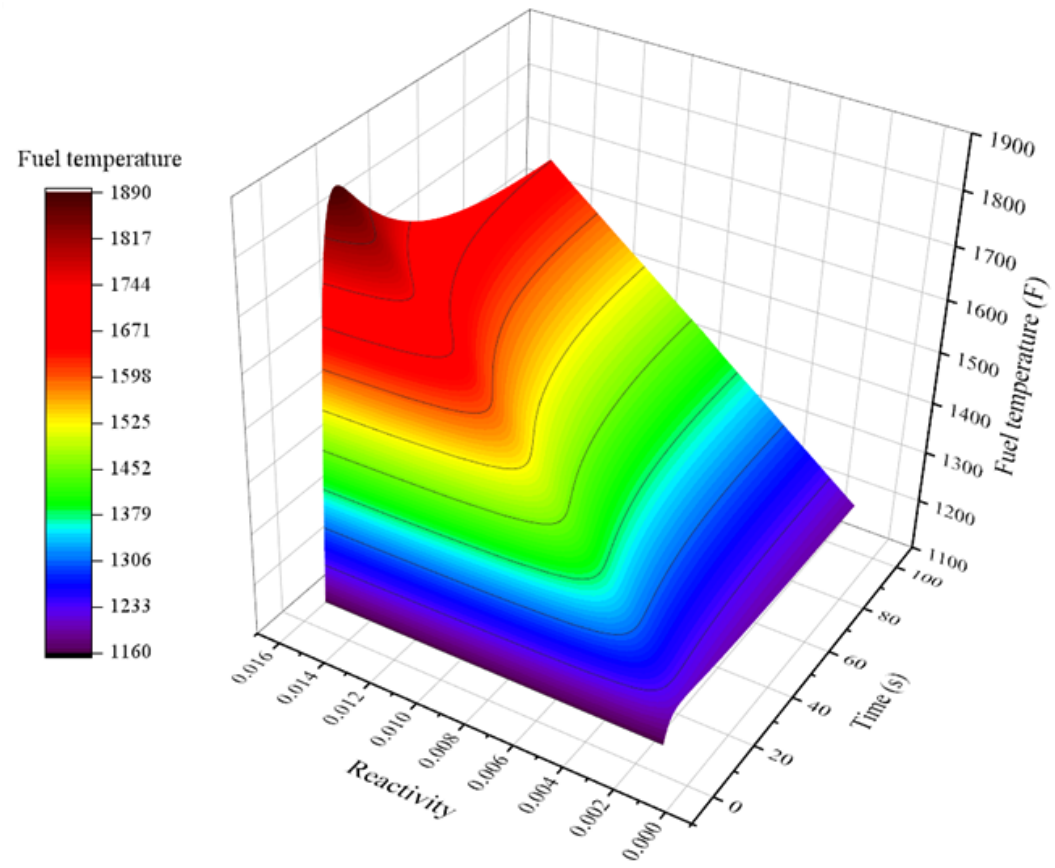

Figure 4-8: Ensemble average of the fuel temperature realizations under increasing reactivity levels.

a.

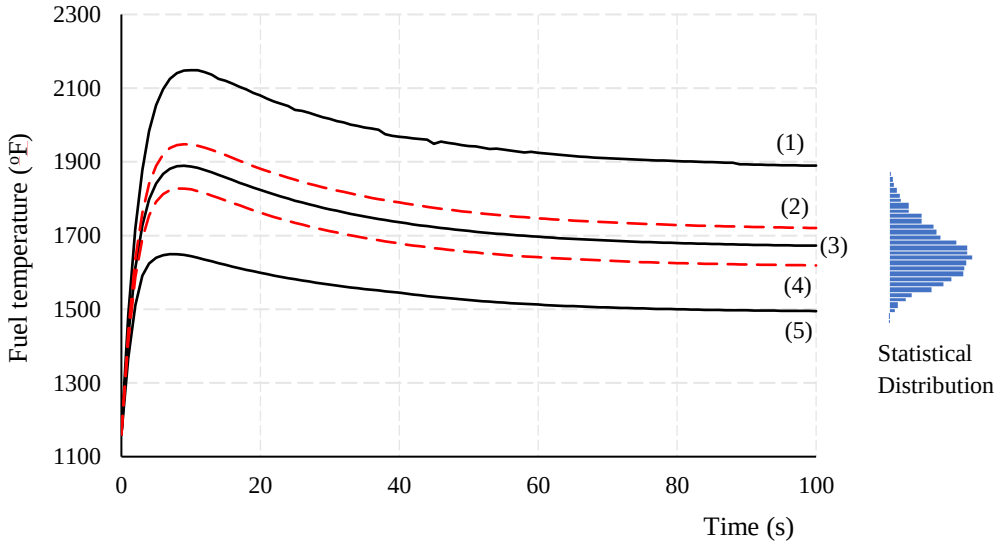

(1) $P_{f\text{-}max}$, (2) 75th percentile, (3) $P_{f\text{-}mean}$, (4) 25th percentile, and (5) $P_{f\text{-}min}$

b.

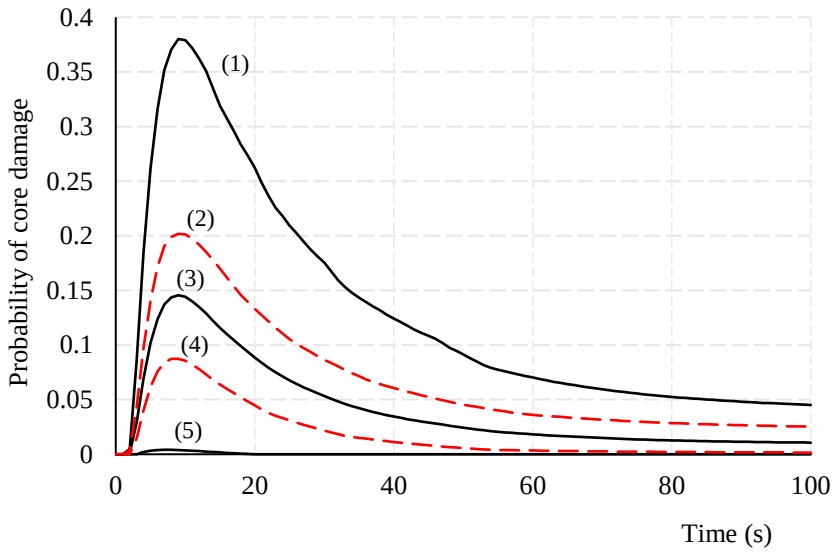

(1) $P_{f\text{-}max}$, (2) 75th percentile, (3) $P_{f\text{-}mean}$, (4) 25th percentile, and (5) $P_{f\text{-}min}$

Figure 4-9: **a.** Dynamic response of fuel temperature at a +0.015 increase in the reactivity level. **b.** Temporal probability of core damage at the same transient.

a.

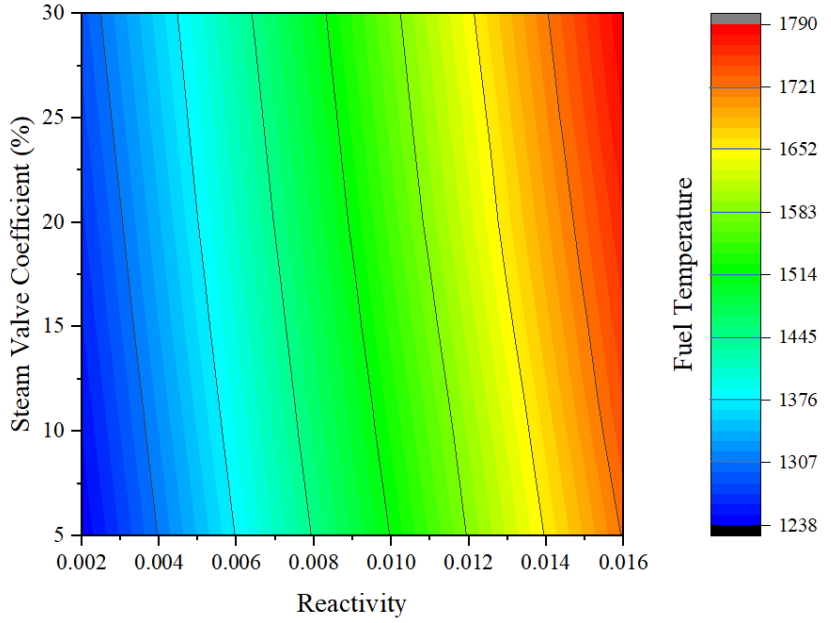

b.

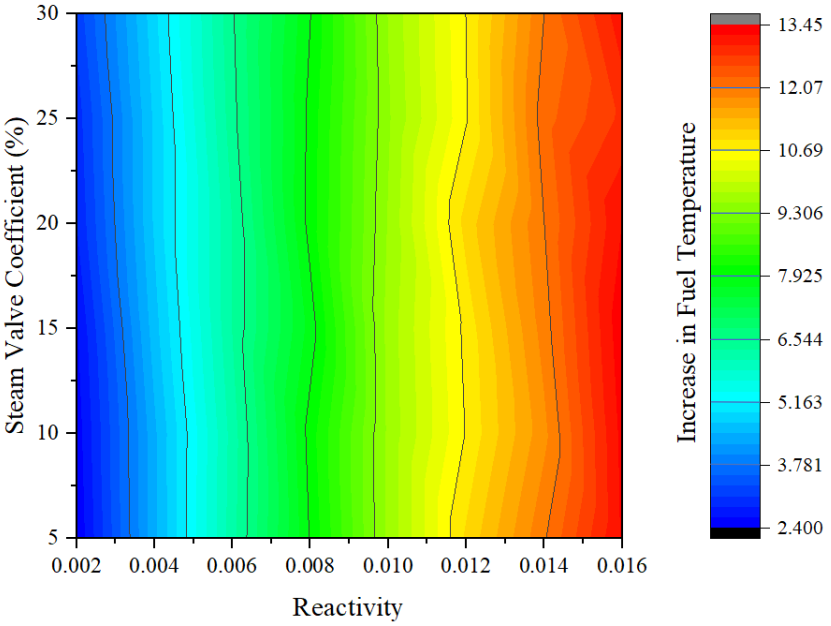

Figure 4-10: **a.** Ensemble average of the fuel temperature realizations under an increasing reactivity and steam valve coefficient. **b.** Percentage increase in the maximum fuel temperature relative to the mean values.

a.

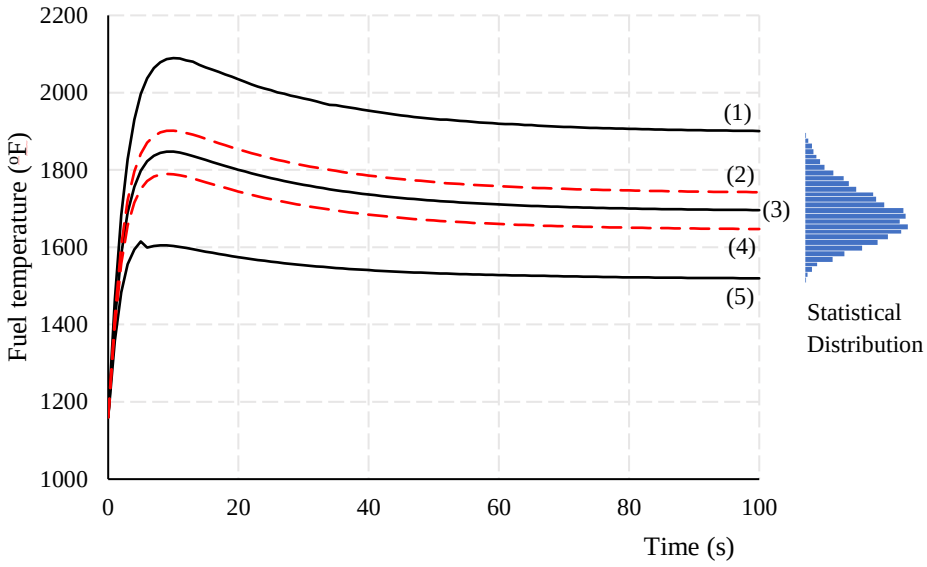

(1) $T_{f\text{-}max}$, (2) 75th percentile, (3) $T_{f\text{-}mean}$, (4) 25th percentile, and (5) $T_{f\text{-}min}$

b.

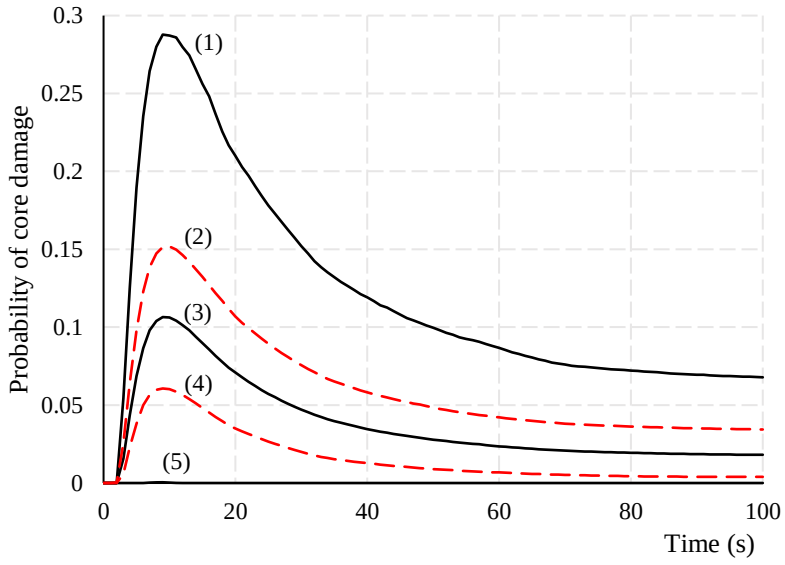

(1) $T_{f\text{-}max}$, (2) 75th percentile, (3) $T_{f\text{-}mean}$, (4) 25th percentile, and (5) $T_{f\text{-}min}$

Figure 4-11: **a.** Dynamic response of fuel temperature at an increase in the reactivity and steam valve coefficient by +0.014 and 30%, respectively. **b.** Temporal probability of core damage at the same transient.

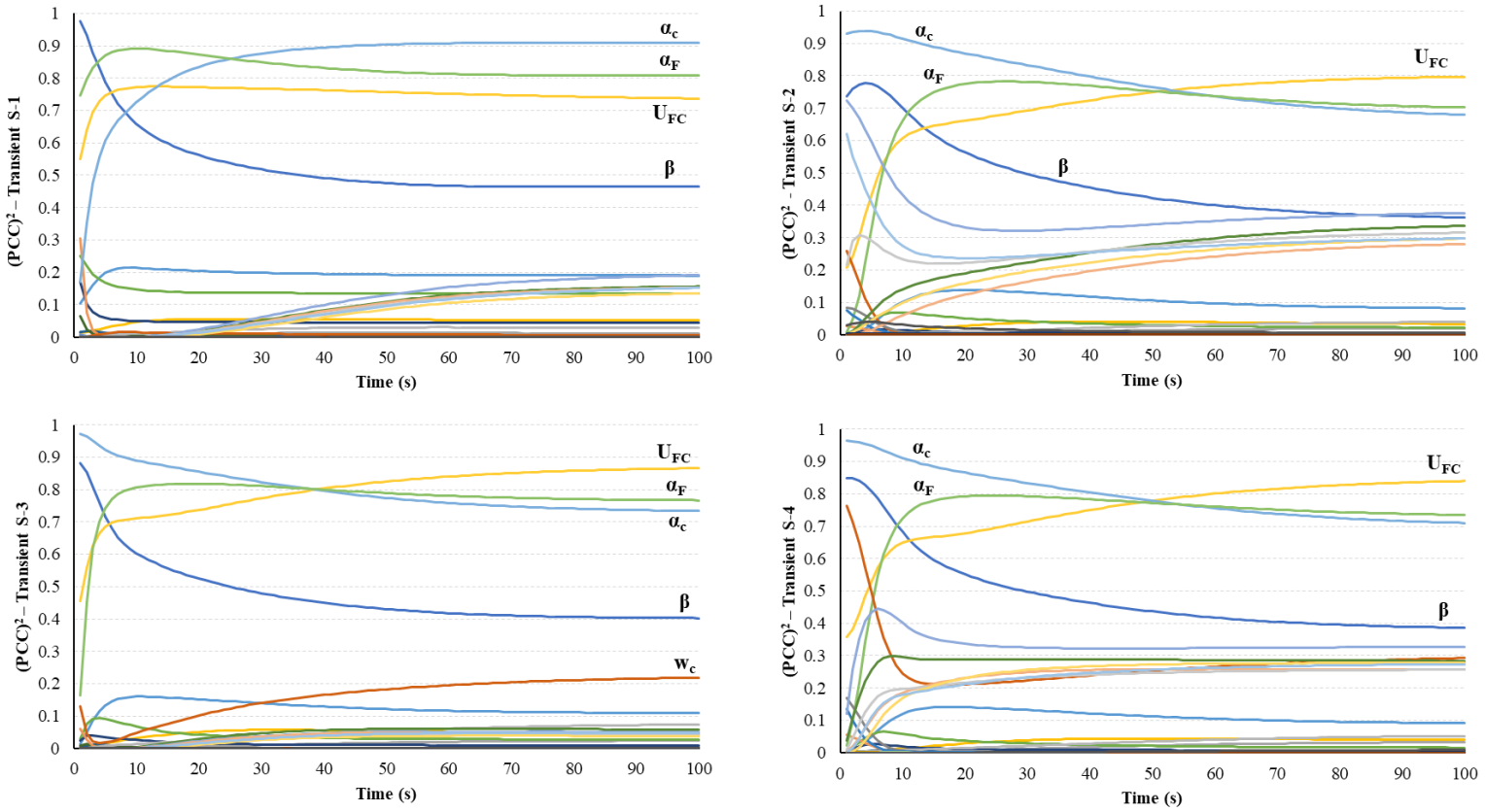

Figure 4-12: PCCs between the fuel temperature and the input parameters under four transients including: S-1. reactivity increases by 0.006; S-2. steam valve coefficient increases by 25%; S-3. core inlet temperature decreases by 20°F; and S-4. steam generator inlet temperature decreases by 20°F.

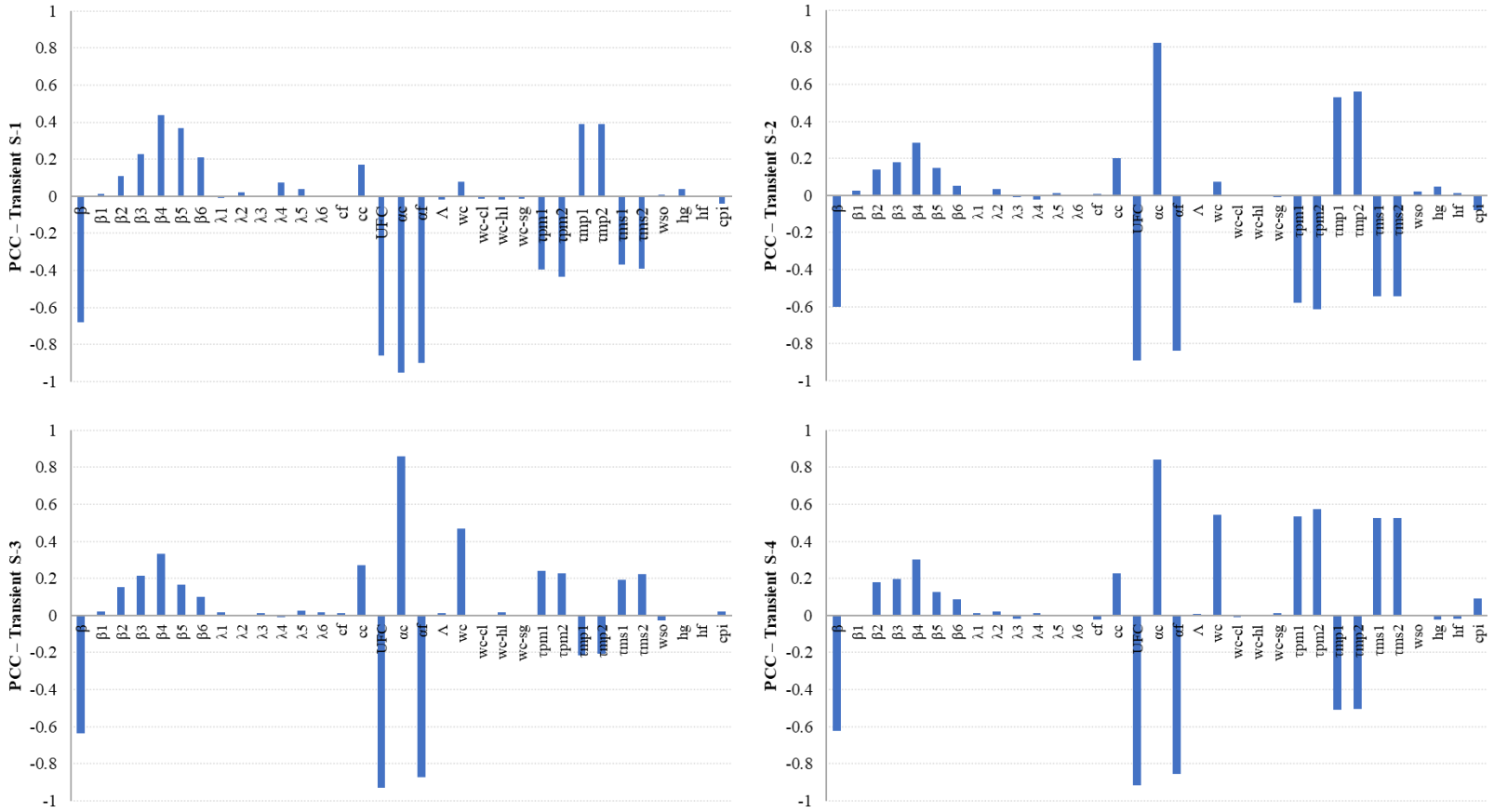

Figure 4-13: PCC between the fuel temperature and the different input parameters at 100 s under transients S-1 to S-4.

Chapter 5 : Artificial Neural Network for Predicting Nuclear Power Plant Dynamic Behavior

ABSTRACT

A Nuclear Power Plant (NPP) is a complex system-of-systems with dynamic behavior during its operations. In order to control the plant operation under both normal and abnormal conditions, different systems in NPPs (e.g., the reactor core components, primary and secondary coolant systems) are usually monitored continuously, leading to very large amounts of data. This opens the possibility of integrating relevant qualitative and quantitative knowledge with artificial intelligence techniques to provide faster and more accurate predictions, leading to more rapid decisions, based on the NPP operation data. Data-driven models (DDM) rely on artificial intelligence to learn automatically based on patterns in data, and they represent alternatives to physics-based models that typically require significant computational burden and might not fully represent the actual operation conditions of an NPP. In this study, a feed-forward backpropagation artificial neural network (ANN) model was trained to simulate the interaction between the reactor core and the primary and secondary coolant systems in a pressurized water reactor. The transients used for model training included perturbations in reactivity, steam valve coefficient, reactor core inlet temperature, and steam generator inlet temperature. Uncertainties of the plant physical parameters and operating conditions were also incorporated in these transients. Eight training functions were adopted during the

training stage to develop the most efficient network. The developed ANN was subsequently tested under new different transients. The developed ANN model was able to accurately predict the considered plant behavior under the new transients. Overall, through rapid prediction of NPP behavior under different transients, the study aims at demonstrating the potential of artificial intelligence to empower rapid emergency response planning and risk mitigation strategies.

Keywords: Data-driven models; Machine learning; Artificial Neural Network; Nuclear Power Plant; Back-Propagation Algorithm.

5.1. INTRODUCTION

A nuclear power plant (**NPP**) is a complex system-of-systems that contains highly dynamic, interconnected, and interdependent subsystems such as the reactor core and primary and secondary coolant systems. Each of these subsystems consists of multiple critical components where the malfunction of any has the potential to initiate an accident that can propagate through the whole plant causing serious negative consequences. NPP safety and performance are key concerns during the plant's service life that require a sufficient understanding of the plant's nonlinear dynamic behavior to control the reactor power, cool the reactor fuel, and contain the radioactivity. Lessons learnt from the Fukushima Daiichi nuclear accident showed that the monitoring systems used were ineffective, leading to poor pre-accident operation and management (IAEA 2015). Early warning systems are therefore essential as, in addition to monitoring, they also include analysis abilities to accurately predict the nonlinear dynamic behavior of the components, subsystems, as well as the whole system under normal and transient conditions (Min et al. 2019). A quick early warning system can contribute to effective risk mitigation strategies, based on complex considerations, to serve as a rapid decision support system (**DSS**) (Korovin and Kalyaev 2015; Tamimi et al. 2019) for plant operators.

Decision-making for a complex dynamic system can be challenging, especially for highly interdependent and interconnected systems such as NPPs. As such, aside from physics-based models, each NPP must adopt an intelligent and

adaptive plant-specific DSS to ensure the safety of the plant, environment, and public. An intelligent DSS aims to collect, organize, and analyze large amounts of data such that decision-makers can take informed actions during emergency situations (Ahmad and Simonovic 2006). Intuitive interpretation of such data is typically challenging, and more sophisticated tools are thus necessary to predict the system response under different operating conditions. Artificial intelligence (**AI**) provides faster and effective tools that can learn automatically based on patterns in data, and therefore have the potential to predict the behavior of complex systems and create intelligent DSSs (Filip 2008; Phillips-Wren 2013).

Several data-driven models (**DDMs**) have been developed based on AI, and have been rapidly progressing over the past few years due to the complex nature of real-world systems, the flourishing of database management (Rätz et al. 2019), and the continuous development of powerful machine learning algorithms (Bao et al. 2019). DDMs utilize the available data for a specific system operation to obtain mathematical relationships between the system state variables (i.e., inputs and outputs), albeit with limited knowledge about the physical/mathematical interdependence of such variables (Solomatine and Ostfeld 2008). *Learning from data* is the main feature of DDMs, where the mathematical interdependence between the system inputs and outputs is discovered iteratively through minimizing the deviation between observed and estimated values (Mitchell 1997). Additionally, DDMs can be applied to gain valuable insights from the system state variables in an unsupervised fashion (i.e., cluster analysis). DDMs provide a different concept

to analyze challenging problems in science and engineering (Montáns et al. 2019), and have been widely applied to simulate the dynamic behavior of different complex systems (e.g., transportation, finance, management, climate, medicine, and environment) (Burchard-levine et al. 2014; Holdaway 2014; Oxtoby et al. 2018; Solomatine and Ostfeld 2008; Zhang et al. 2011). However, the application of AI-based DDMs in the field of nuclear engineering is still limited and has been identified only recently as a critically important research area (Gomez et al. 2017).

Several DDMs have been developed over the past decades, including regression models, artificial neural networks, and cluster analysis (Fahrmeir et al. 2013; Foshch et al. 2016; Maljovec et al. 2016; Patra et al. 2010), of which the artificial neural network (**ANN**) shows superior efficiency in uncovering complex relationships between system inputs and outputs (Abiodun et al. 2018; Kang et al. 2019). Several types of ANNs have been developed to date (e.g., feed-forward back propagation neural network, recurrent neural network, convolutional neural network) (Li. et al. 2012; Mikolov et al. 2010; O'Shea and Nash 2015), each of which is appropriate for certain applications. Training is the first stage in developing an ANN, and several training algorithms have been developed, such as gradient descent algorithms (**GD**), conjugate gradient algorithms (**CG**), and quasi-newton algorithms (**QN**) (Battiti 1992; Hagan and Menhaj 1994; Moller 1997, 1993; Nawi et al. 2008). Training an ANN is a challenging step because: *i*) a proper combination of learning, transfer, and training functions is usually needed (Sharma and Venugopalan 2014); *ii*) different training algorithms result in different accuracy

levels (Mustafidah et al. 2014); *iii*) training performance depends on the range and amount of data employed (Sug 2010); and, *iv*) overfitting may be encountered (Lawrence et al. 1997). Once trained with enough and representative data, an ANN can be used subsequently to predict the system response under new input values. ANNs have been previously employed within the field of nuclear engineering to predict NPP response under multiple core power inputs and loss of flow accidents (Gomez et al. 2017), to simulate the intermediate heat exchanger of a nuclear reactor (Patra et al. 2010), to develop a plant-wide management plan (i.e., transient identification, plant-wide monitoring, analysis of vibrations, monitoring of performance and efficiency) (Uhrig 1993), and to model the thermal dynamic behavior of an NPP (Guo and Uhrig 2017).

Several previous studies (Knochenhauer and Holmberg 2011; U.S. NRC 2017; Varuttamaseni 2011) have utilized the fuel temperature to estimate the probability of core damage. In addition, fuel temperature and steam pressure are the primary controllers of the reactor core and secondary coolant systems' integrity. Thus, developing a model to estimate the temporal fuel temperature and steam pressure is key for effective early warning. In this respect, the present study aims at developing an intelligent DSS based on a DDM to predict the critical state variables in a pressurized water reactor (**PWR**); this includes predicting the reactor fuel temperature and steam pressure in the PWR under four different transients (a change of reactivity, a change of steam valve coefficient, a deviation in the core inlet temperature, and a change of steam generator inlet temperature) considering

uncertainty in physical parameters and system operating conditions. Each of the considered transients is represented through eight different severity levels. A feed-forward backpropagation ANN is developed based on data obtained from a previously developed system dynamics (**SD**) model of a PWR, including uncertainties in the physical parameters and plant operating conditions. Three algorithms (GD, CG, QN), represented by eight training functions, are tested during the training stage, and the best function is identified based on the network performance. The developed ANN serves as a rapid early warning system and intelligent DSS that can enable the development of quick and proper risk mitigation strategies under changing and dynamically challenging operating conditions.

5.2. DATASET

An SD model has been previously developed by El-Sefy et al. (2019) to simulate the nonlinear dynamic behavior of a PWR. The developed SD model represents a single loop reactor in which the feedback mechanisms between the reactor core, the secondary coolant system, the primary coolant system, and the plenums are simulated based on the mathematical descriptions employed in previous studies (Ali 1976; Arda 2013; Arda et al. 2013; Kerlin et al. 1976; Puchalski et al. 2017; Thakkar 1975). The nominal values of PWR system parameters are adopted from those of the Palo Verde NPP. Uncertainties associated with the system physical parameters (e.g., the specific heat of primary coolant, heat transfer coefficient from fuel to coolant, coolant temperature coefficient of reactivity) and operating conditions (e.g., primary coolant mass flow rate of inside the core, steam flow rate)

were also considered in that SD model. Such uncertainties were represented in terms of probability distributions similar to those employed in previous studies (Brown and Zhang 2016; Demazière and Pázsit 2002; Perin and Jimenez 2017; Radaideh et al. 2018; Romojaro et al. 2019; Sánchez et al. 2018; Zimmerman et al. 1999). A normal distribution was assumed for 26 parameters, while the other seven parameters were assumed to follow uniform distributions. A schematic diagram of the PWR generating unit, including the feedback loops between the SD representations of the reactor core and secondary coolant system, is shown in Figure 5-1. The reader is referred to El-Sefy et al. (2019, 2020) for detailed descriptions of the SD model employed in the present study.

The SD model developed by El-Sefy et al. (2019, 2020) was utilized in the current study to obtain synthetic, real-time data corresponding to different transients. Four transients were considered, each of which was represented by eight different levels of severity, as summarized in **Table 5-1**. A total of 32 different transients were simulated, and the corresponding SD model outputs (i.e., reactor core reactivity (ρ), reactor core thermal power (P_{th}), reactor core inlet temperature (T_{IP}), steam generator inlet temperature (T_{LP}), steam valve coefficient (c_l), fuel temperature (T_f), and steam pressure(P_s)) were monitored and recorded continuously. The SD model was embedded within a Monte-Carlo framework, where a total of 5,000 realizations was employed for each transient in order to consider the impact of uncertain physical parameters and operating conditions. The number of realizations was determined based on the study by El-Sefy et al. (2020),

who investigated the probabilistic dynamic behavior of the same PWR using a SD modelling approach. The outputs of the SD model were subsequently employed for the development of a corresponding ANN to investigate if the latter can reproduce the same results, albeit faster and without overburdening the model with handling the complex physics-based interactions within the system.

The reactor core reactivity, reactor core thermal power, reactor core inlet temperature, steam generator inlet temperature, and steam valve coefficient were selected as the ANN inputs, while the fuel temperature T_f and the steam pressure P_s were selected as the outputs because T_f provides an indication for the probability of core damage and P_s controls the secondary coolant system integrity. Each of the ANN inputs/outputs was represented by a time series over a time frame of 80 seconds. Eleven realizations corresponding to the minimum and maximum values of T_f and P_s together with those corresponding to each decile (i.e., 10^{th} to 90^{th} percentile range) were used to represent each transient, and were subsequently employed for the development of the ANN. Figure 5-2 shows a portion of SD dataset utilized for the development of the ANN. A total of 57,024 (32 Transients x 11 realizations x 2 outputs x 81 time-steps) samples were thus adopted for the development of the ANN using the *NN* toolbox in MATLAB statistics toolbox (MATLAB 2018a). The total number of samples was divided into 70% training (representing 39,916 samples), 15% validation (representing 8,554 samples), and 15% testing (representing 8,554 samples) subsets. The training subset was used to build the ANN through adjusting the network parameters. The validation subset

was used within the training process to prevent overfitting, while the testing subset was utilized to test the trained network to obtain the performance under data not employed for training (Perez 2019).

5.3. ARTIFICIAL NEURAL NETWORK

5.3.1. NETWORK ARCHITECTURE

ANN is one of the most popular DDM tools that depends on the concept of learning to replicate the behavior of complex dynamic systems (Arce-Medina and Paz-Paredes 2009). ANN was inspired by biological neural systems (e.g., the human brain) that can learn to perform tasks through exposure to different examples without being constrained to task-specific rules. Therefore, ANNs present an alternative to complex mathematical/physics models without prior knowledge of the underlying processes. In addition, ANNs typically show excellent prediction capabilities when appropriately trained. Due to their capability to simulate nonlinear behaviors, approximate input-output relationships, and recognize patterns within a reasonable amount of time, ANNs are seeing an explosion of application to different research areas (Rallo et al. 2002).

The feed-forward ANN (hereafter referred to simply as ANN) was employed in the present study, and a detailed description of it is provided herein. An ANN typically consists of three main components: the input layer, the hidden layer, and the output layer (Figure 5-3). The input and output layers consist of a group of nodes, each of which corresponds to an input or output. The hidden layer contains

a collection of artificial neurons that are highly interconnected to the input nodes. The links between input nodes and hidden layer neurons represent the flow of data between the two layers, where weights are assigned to represent the amount of information shared. A hidden layer is followed by an activation function (e.g., step function, ramp function, or sigmoid function) that is used to limit the amplitude of a neuron output (Haykin and H 1999). Bias is also introduced when the activation function is applied such that the hidden layer output matches the actual output. In general, in an ANN, biased weighted inputs are passed to an activation function to capture the behavior of complex systems (Arce-Medina and Paz-Paredes 2009). The ANN output(s) can be represented mathematically as:

$$\boldsymbol{O} = f(\boldsymbol{XW} + \boldsymbol{b}) \quad [5\text{-}1]$$

where $\boldsymbol{O}$, $\boldsymbol{X}$, $\boldsymbol{W}$, and $\boldsymbol{b}$ represent the outputs, inputs, weights, and bias in matrix notation, respectively. The function f in Equation [5-2] represents the activation function, where the sigmoid function was utilized in the present study as follows:

$$f(z) = \frac{1}{1+e^{-z}} \quad [5\text{-}2]$$

where z is an arbitrary input variable. The weights and bias (i.e., $\boldsymbol{W}$ and $\boldsymbol{b}$) are adjusted iteratively through a backpropagation algorithm such that the network output $\boldsymbol{O}$ matches the actual output ($\boldsymbol{P}$). This is referred to as the training process, as the ANN parameters (i.e., $\boldsymbol{W}$ and $\boldsymbol{b}$) are adjusted to fit the relationships inherited within the data. In this study, a backpropagation algorithm was applied using different functions (referred to as training functions), and the mean squared error ($\boldsymbol{MSE}$) was utilized to evaluate the performance of corresponding networks. It is

noteworthy that a more complex ANN with multiple hidden layers may be used when highly nonlinear behavior cannot be captured through simple network architecture (i.e., an ANN with a single hidden layer). A mathematical formula, similar to Equation [5-1], can then be applied to estimate the network output (i.e., $\boldsymbol{O}$). However, the use of one hidden layer has been proven to be efficient in approximating continuous nonlinear functions according to the universal approximation theorem (Cybenkot 1989; Gandomi and Roke 2015).

The present study employed an ANN with a single hidden layer containing n_h neurons (Figure 5-4) to predict the nonlinear response of a PWR. Identifying the number of hidden layer neurons is crucial as small n_h values disable the neural network from capturing the relationship between the inputs and outputs (i.e., the model can neither fit the training data nor be generalized) whereas large n_h values may lead to the problem of overfitting (Xu and Chen 2008). Overfitting occurs when the results from an ANN cannot be generalized (i.e., the ANN is constrained to the training data only) (Lawrence et al. 1997). In the present study, n_h is determined based on the number of inputs, n_i, according to Kalmogorov's theorem (Hecht-Nielsen 1987):

$$n_h \leq 2n_i + 1 \qquad [5\text{-}3]$$

5.3.2. TRAINING ALGORITHMS

As mentioned before, different functions may be used for training an ANN. In general, the most appropriate function is that enables the network to simulate the underlying system behavior (i.e., T_f and P_s of a PWR in the context of the present

study) for the training subset of the available data within a reasonable amount of time and minimum *MSE*. Three backpropagation algorithms with eight training functions were assessed in this study. These algorithms, together with the corresponding training functions, are given in **Table 5-2** as: *i*) the GD algorithm (*traingd*, *traingdm*, and *trainrp*); *ii*) the CG algorithm (*trainscg*, *traincgp*, and *traincgf*); and *iii*) the QN algorithm (*trainbfg*, and *trainlm*). GD is the most widely applied training algorithm that adjusts $\boldsymbol{W}$ and $\boldsymbol{b}$ based on the descending gradient direction of the function (Sharma and Venugopalan 2014). The GD algorithm typically shows a fast-initial convergence rate but a slow zigzagging behavior when approaching the final solution (Krylatov and Hirokolobova 2017). Although the convergence of the GD algorithm is in the steepest descent direction, this may not necessarily produce the fastest convergence. The CG algorithm is, in contrast, performed along the conjugate direction, which generally provides a faster convergence rate than the steepest descent direction (Johansson et al. 1992). The QN algorithm relies on defining a better search direction based on the Hessian matrix (i.e., a matrix of the second derivatives of the error function at the current values of the weights and biases) (Moller 1997). An approximated version of the Hessian matrix is adopted within the QN algorithm to overcome the complexity and the large memory size that typically results from computing the exact one (Setiono and Hui 1995). Although the convergence of the QN algorithm is typically faster than that of the CG algorithm, the latter is simpler and easy to apply (Sug 2010). In this study, all of the training functions were applied for different values of n_h in

order to obtain the best ANN architecture that resulted in the highest correlation coefficient (*R*) and lowest *MSE* between ***O*** and ***P*** during the training stage.

5.4. RESULTS AND DISCUSSION

5.4.1. NETWORK TRAINING, TESTING AND VALIDATION

The dataset obtained from the SD model of the PWR system was divided into three portions (training, validation, testing), as discussed above. The training and validation portions were used together for training purposes (i.e., obtaining the optimum values for ***W*** and ***b*** in Equation [5-1]). For training, the following parameters were fixed for all training functions within the MATLAB-*NN* toolbox: *i*) the performance function = *MSE*; *ii*) performance goal = 0; *iii*) the adaptation learning function = LEARNGDM; *iv*) learning rate parameter = 0.1; *v*) the activation function = TANSIG; and *vi*) number of training iterations (max_epochs) = 1,000. In addition, numerical measures haven been defined to assess the performance of each training function. Such measures include *MSE*, the Central Processing Unit (**CPU**) time elapsed by the end of the training, the number of epochs at the end of the training, and the average regression value (***R***) over the training, validation, and testing subsets. The ANN was trained with each training function until the *MSE* did not change for six consecutive epochs, except with the training function *trainbfg*, which reached the maximum of 1,000 epochs first. As retraining the network typically results in different values of ***W*** and ***b***, the training stage was repeated 100 times using the same dataset. **Table 5-2** shows the average

training measures for each of the different ANNs that result from combining the different training functions with the different n_h values.

The training functions *traingd* and *traingdm* could not converge and therefore the corresponding ANNs were eliminated in this study. On the other hand, the ANNs corresponding to the rest of the training functions (i.e., *trainrp*, *trainscg*, *traincgp*, *traincgf*, *trainbfg*, and *trainlm*) were all adequately trained, but with differences in the CPU time used for training and the *MSE* values. The training function *trainlm* (a QN training algorithm) with eleven neurons showed the best performance in terms of the lowest *MSE* (**Table 5-2**), and the corresponding ANN is referred to as the developed ANN.

Figure 5-5 shows the *MSE* between the estimated and actual outputs under the *trainlm* training function. Large average *MSE* values were encountered during the first few iterations (<20) and subsequently decreased to smaller values. The results of the training stage demonstrate the ability of the developed ANN to successfully learn from the SD model-based dataset despite the complex dynamic behavior of the underlying PWR system, and highlight the potential to use the developed ANN to predict the system response under new transients (i.e., new input values). Subsequently, Figure 5-6 shows the relationship between the NN estimated values (vertical axis) and SD actual outputs (horizontal axis) for the training, validation, and testing subsets when the *trainlm* training function was adopted with n_h equal to eleven. The line of best fit through the data for all three subsets (i.e., training, validation, and testing) has nearly a unit slope and zero intercept, reflecting

the ability of the developed ANN to replicate the SD model outputs.

5.4.2. ADDITIONAL NETWORK TESTING

After training, it is crucial to test the developed ANN to ensure its efficacy to predict the response of the PWR system under new transients. Therefore, the SD model was used to simulate the PWR behavior under new transients, and the corresponding outputs were used for additionally testing the developed ANN. These new transients were: 1) a perturbation in reactivity by +0.001; 2) a perturbation in reactivity by +0.001 including uncertainties in the system physical parameters and operating conditions; 3) a perturbation in steam valve coefficient by +7.5%; 4) a deviation in steam valve coefficient by +7.5% including uncertainties in the system physical parameters and operating conditions; and, 5) a perturbation in core inlet temperature by +7.5^{o}F.

Transient 1: Increase in Reactivity

In Transient 1, the performance of the developed ANN was evaluated under an increase of reactivity by +0.001. Increasing the reactivity level leads to a higher fuel temperature, which subsequently causes more heat energy to transfer to the primary cooling system. Such heat then transfers to the secondary coolant system through the metal U tubes and converts the secondary coolant into steam. As a result, additional steam is produced in the steam generators, leading to a higher steam pressure as long as there is no change in the steam valve opening. The developed ANN sufficiently reproduced the SD model estimates of fuel

temperature and steam pressure under transient 1, as shown in Figure 5-7a and Figure 5-7b, respectively. The developed ANN underestimated the fuel temperature at the beginning of the transient (t = 0 s) by only 1.6%, and the deviations between the ANN and SD model estimates of fuel temperature decreased significantly as the reactor approached steady-state conditions. On the other hand, the developed ANN efficiently replicated the temporally changing steam pressure values estimated by the SD model with negligible deviations.

Transient 2: Increase in Reactivity with Uncertain Other Parameters

Several sources of uncertainty are typically present in complex systems (e.g., uncertainty in input parameters, uncertainty in model structure). Integrating the uncertainty of the input parameters in the developed ANN is therefore essential to reflect the real behavior inside the underlying PWR. The effect of the uncertain physical parameters and operating condition on the system response were considered during the additional testing of the developed ANN. A total of 5,000 realizations of the SD model parameters were generated, and the corresponding outputs were estimated under a reactivity change of +0.001. The ANN inputs (i.e., ρ, P_{th}, T_{IP}, T_{LP}, c_l) were extracted from the SD model outputs, and were used to predict the uncertain temporal fuel temperature and steam pressure. The temporal minimum, median, and maximum fuel temperature and steam pressure were predicted, as shown in Figure 5-8a and Figure 5-8b, respectively. The considered uncertainty led to an increase in the fuel temperature and steam pressure by 1.2% and 1.6% compared to the median value, respectively, at the reactor steady state.

The developed ANN produced similar results to those of the SD model with negligible differences. In addition, the statistical distributions of fuel temperature and steam pressure predicted using the developed ANN do not follow a uniform distribution but rather an approximately 3-parameter lognormal distribution, where the maximum and minimum responses have a lower probability of occurring compared to the mean response. These statistical distributions are similar to those estimated using the SD model.

Transient 3: Increase in Steam Valve Coefficient

The developed ANN was also tested under an increase of the steam valve coefficient by +7.5%, which represents an increase in the steam valve opening. The steam pressure inside the steam generator decreases immediately after increasing the steam valve opening. This is followed by a reduction in the reactor core inlet temperature, which causes a positive reactivity and a subsequent increase in the fuel temperature, as shown in Figure 5-9a. As a result, more heat energy is generated inside the reactor core to accommodate the reduction in steam pressure. The developed ANN sufficiently simulated this physical behavior and reproduced the SD model outputs under this transient, with maximum differences of 0.14% and 1.16% in the fuel temperature (t = 80 s) and the steam pressure (t = 0 s), respectively (Figure 5-9a and Figure 5-9b).

Transient 4: Increase in Steam Valve Coefficient with Uncertain Other Parameters

In Transient 4, the developed ANN was tested under an increase in the steam valve coefficient by +7.5% considering uncertain physical parameters and operating conditions. Similar to the transient 2, a total of 5000 realizations were utilized as the inputs for the developed ANN and the corresponding uncertain temporal fuel temperature and steam pressure were predicted. The SD model estimates were efficiently reproduced using the developed ANN, with maximum differences of 0.162% and 0.137% in the minimum and maximum fuel temperature at t = 80 s, respectively, and 1.145% in the steam pressure at t = 0 s (Figure 5-10). In addition, the statistical distribution of the ANN predictions can be approximated by a 3-parameter lognormal distribution (Figure 5-10a and Figure 5-10b).

Transient 5: Increase in Reactor Inlet Temperature

Finally, the performance of the developed ANN was evaluated under an increase in the reactor core inlet temperature of 7.5^{o}F. Increasing the coolant temperature results in a negative reactivity feedback that reduces the fuel temperature, as shown in Figure 5-11a. On the other hand, more heat energy is transferred to the secondary coolant system due to the increasing coolant temperature in the primary coolant system. In addition, the secondary coolant is converted into steam, leading to a higher steam pressure. The SD model outputs were adequately predicted using the developed ANN under this transient, with

maximum difference of 1.0 % in the fuel temperature at t = 1 s and negligible deviations in the steam pressure as shown in Figure 5-11a and Figure 5-11b, respectively.

Overall Evaluation of Additional Network Testing

Overall, the developed ANN is adequately trained under 32 different transients to simulate the dynamic interaction between complex systems inside the PWR. The ANN performance under Transients 1 through 5 supports its ability to predict the PWR physical behavior similar to a SD modeling approach, but with lower computational cost and time. Therefore, the developed ANN can be used to provide the plant operators with early warnings under the considered transients. This can reduce the likelihood of having severe accident consequences and ultimately enhance the overall safety conditions.

5.5. CONCLUSIONS

The present study aimed at exploring the potential of applying AI tools within the nuclear engineering field, and specifically for the prediction of NPP response. A previously published validated SD (physics-based) model was employed to generate data pertaining to PWR dynamic behavior under different transients. The data was subsequently utilized to develop a corresponding ANN (data-driven) model. The uncertainty associated with the PWR system's physical parameters and operating conditions were also incorporated in these transient analyses. A feed-forward backpropagation ANN was trained based on 32 transients to model the

interaction between complex systems inside the PWR, including the reactor core, primary and secondary cooling systems, hot and cold legs, reactor core inlet and outlet plenums, and steam generator inlet and outlet plenums. The ANN was developed with an input layer with five nodes, a single hidden layer with different numbers of neurons, and an output layer with two nodes. Three backpropagation algorithms with eight training functions were utilized during the model training stage. The ANN corresponding to the *trainlm* function, with eleven neurons in the hidden layer, showed the best performance compared to other training functions.

The developed ANN was subsequently tested under new transients representing perturbations in reactivity, steam valve coefficient, and core inlet temperature. In all cases, the developed ANN reproduced the SD model estimates of the temporal fuel temperature and steam pressure with negligible differences (no more than 1.6%). In addition, the predicted statistical distributions of fuel temperature and steam pressure using ANN are compatible with the corresponding distributions from the SD simulation model when the input uncertainties are considered. In an actual NPP, the developed ANN would provide a computationally efficient alternative compared to physics-based models, especially for considering the uncertain system physical parameters and operating conditions. In addition, the developed ANN can be utilized as an early warning tool that enables the development of effective risk mitigation strategies under unexpected operating conditions, and can therefore serve as a rapid decision support systems for NPP operators and managers. Moving forward, the developed ANN can be trained using

real plant operation data and different transients in different systems in order to cover all possible scenarios that can occur during normal or abnormal operating conditions. Finally, the adoption and development of AI tools within the nuclear engineering field will enable major breakthroughs in mitigating the risk of accidents and human errors when dealing with systems as complex, dynamic and critical such as NPPs.

5.6. ACKNOWLEDGMENTS

The financial support for the study was provided through the Canadian Nuclear Energy Infrastructure Resilience under Seismic Systemic Risk (CaNRisk) – Collaborative Research and Training Experience (CREATE) program of the Natural Science and Engineering Research Council (NSERC) of Canada. Additional support from the INTERFACE Institute and the INViSiONLab is also acknwledged.

5.7. REFERENCES

Abiodun, O. I., Jantan, A., Omolara, A. E., Dada, K. V., Mohamed, N. A., and Arshad, H. (2018). "State-of-the-art in artificial neural network applications: A survey." *Heliyon*.

Ahmad, S., and Simonovic, S. P. (2006). "An Intelligent Decision Support System for Management of Floods." *Water Resources Management*, 391–410.

Ali, M. (1976). "Lumped Parameter, State Variable Dynamic Models for U-tube Recirculation Type Nuclear Steam Generators." Ph.D. Thesis, University of Tennessee.

Arce-Medina, E., and Paz-Paredes, J. I. (2009). "Artificial neural network modeling techniques applied to the hydrodesulfurization process." *Mathematical and Computer Modelling*, Elsevier Ltd, 49(1–2), 207–214.

Arda, S. (2013). "Implementing a Nuclear Power Plant Model for Evaluating Load-Following Capability on a small Grid." MASc Thesis, Arizona State University.

Arda, S., Holbert, K. E., and Undrill, J. (2013). "Development of a Linearized Model of a Pressurized Water Reactor Generating Station for Power System Dynamic Simulations." *45th North American Power Symposium, NAPS 2013*.

Bao, H., Dinh, N. T., Lane, J. W., and Youngblood, R. W. (2019). "A data-driven

framework for error estimation and mesh-model optimization in system-level thermal-hydraulic simulation." *Nuclear Engineering and Design*, Elsevier, 349, 27–45.

Battiti, R. (1992). "First- and Second-Order Methods for Learning: Between Steepest Descent and Newton's Method." *Neural Computation*, 4, 141–166.

Brown, C. S., and Zhang, H. (2016). "Uncertainty quantification and sensitivity analysis with CASL Core Simulator VERA-CS." *Annals of Nuclear Energy journal*, 95, 188–201.

Burchard-levine, A., Liu, S., Vince, F., Li, M., and Ostfeld, A. (2014). "A hybrid evolutionary data driven model for river water quality early warning." *Journal of Environmental Management*, Elsevier Ltd, 143, 8–16.

Cybenkot, G. (1989). "Approximation by Superpositions of a Sigmoidal Function." *Mathematics of Control, Signals, and Systems*, 2, 303–314.

Demazière, C., and Pázsit, I. (2002). "Evaluation of the Boron Dilution Method for Moderator Temperature Coefficient Measurements." *Nuclear Technology*, 140, 147–163.

El-Sefy, M., Ezzeldin, M., El-Dakhakhni, W., Nagasaki, S., and Wiebe, L. (2020). "Dynamic Probabilistic Risk Assessment of Core Damage under Different Transients using System Dynamics Simulation Approach, In Progress."

El-Sefy, M., Ezzeldin, M., El-Dakhakhni, W., Wiebe, L., and Nagasaki, S. (2019).

"System Dynamics Simulation of the Thermal Dynamic Processes in Nuclear Power Plants." *Nuclear Engineering and Technology*, Elsevier Ltd, 51(6), 1540–1553.

Fahrmeir, L., Kneib, T., Lang, S., and Marx, B. (2013). *Regression Models*. Springer, Berlin, Heidelberg.

Filip, F. G. (2008). "Decision support and control for large-scale complex systems." 32, 61–70.

Foshch, T., Portela, F., Machado, J., and Maksimov, M. (2016). "Regression models of the nuclear power unit VVER-1000 using data mining techniques." *Procedia Computer Science*, 100, 253–262.

Gandomi, A. H., and Roke, D. A. (2015). "Advances in Engineering Software Assessment of artificial neural network and genetic programming as predictive tools." *Advances in Engineering Software*, Elsevier Ltd, 88, 63–72.

Gomez, M., Tokuhiro, A., Welter, K., and Wu, Q. (2017). "Nuclear energy system's behavior and decision making using machine learning." *Nuclear Engineering and Design*, Elsevier, 324, 27–34.

Guo, Z., and Uhrig, R. E. (2017). "Use of Artificial Neural Networks to Analyze Nuclear Power Plant Performance." *Nuclear Technology*, 5450(May).

Hagan, M. T., and Menhaj, M. B. (1994). "Training Feedforward Networks with

the Marquardt Algorithm." *IEEE Transactions on Neural Networks*, 5(6), 2–6.

Haykin, S., and H, S. (1999). *Neural Networks: A Comprehensive Foundation*. 2nd edition, Prentice Hall PTR, Upper Saddle River, NJ, United States.

Hecht-Nielsen, R. (1987). "Kolmogorov's mapping neural network existence theorem." *the IEEE First International Conference on Neural Networks*, San Diego, CA.

Holdaway, K. R. (2014). *Harness oil and gas big data with analytics: Optimize exploration and production with data-driven models*. John Wiley and Sons, Hoboken, New Jersey.

IAEA. (2015). *Accident Monitoring Systems for Nuclear Power Plants, NP-T-3.16. International Atomic Energy Agency*.

Johansson, E. M., Dowla, F. U., and Goodman, D. M. (1992). "Backpropagation Learning for Multilayer Feed-Forward Neural Networks Using the Conjugate Gradient Method." *International Journal of Neural Systems*, 2, 291–301.

Kang, H. H., Kaya, M., and Hajimirza, S. (2019). "A data driven artificial neural network model for predicting radiative properties of metallic packed beds." *Quantitative Spectroscopy & Radiative Transfer*, 66–72.

Kerlin, T. W., Katz, E. M., Thakkar, J. G., and Strange, J. E. (1976). "Theoretical and experimental dynamic analysis of the HB Robinson nuclear plant."

Nuclear technology, 30(3), 299–316.

Knochenhauer, M., and Holmberg, J. E. (2011). *Guidance for the Definition and Application of Probabilistic Safety Criteria*. Swedish Radiation Safety Authority.

Korovin, I. S., and Kalyaev, I. A. (2015). "Modern Decision Support Systems in Oil Industry: Types, Approaches and Applications." *International Conference on Test, Measurement and Computational Method*, 141–144.

Krylatov, A. Y., and Hirokolobova, A. P. (2017). "Projection Approach Versus Gradient Descent for Network' s Flows Assignment Problem." *Learning and Intelligent Optimization*.

Lawrence, S., Giles, C. L., and Tsoi, A. C. (1997). "Lessons in Neural Network Training: Overfitting May be Harder than Expected." *Proceedings of the Fourteenth National Conference on Artificial Intelligence, AAAI-97*, AAAI Press, Menlo Park, California, 540–545.

Li., J., Cheng, J., Shi, J., and Huang, F. (2012). "Brief Introduction of Back Propagation (BP) Neural Network Algorithm and its Improvement." *Advances in Computer Science and Information Engineering*, Springer, Berlin, Heidelberg, 169.

Maljovec, D., Liu, S., Wang, B., Mandelli, D., Bremer, P., Pascucci, V., and Smith, C. (2016). "Analyzing simulation-based PRA data through traditional

and topological clustering : A BWR station blackout case study." *Reliability Engineering and System Safety*, Elsevier, 145, 262–276.

MATLAB Statistics Toolbox Release 2018a, The MathWorks, Inc., Natick, Massachusetts, United States." (2018). .

Mikolov, T., Karafiat, M., Burget, L., Cernock, J., and Khudanpur, S. (2010). "Recurrent neural network based language model." *Interspeech*.

Min, J. H., Kim, D., and Park, C. (2019). "Demonstration of the validity of the early warning in online monitoring system for nuclear power plants." *Nuclear Engineering and Design*, Elsevier, 349, 56–62.

Mitchell, T. M. (1997). *Machine Learning*. McGraw-Hill, New York.

Moller, M. (1997). "Efficient Training of Feed-Forward Neural Networks." Aarhus University, Computer Science Department, Ph.D. Thesis.

Moller, M. F. (1993). "A Scaled Conjugate Gradient Algorithm for Fast Supervised Learning." *Neural Networks*, 6, 525–533.

Montáns, F. J., Chinesta, F., Gómez-Bombarelli, R., and Kutz, J. N. (2019). "Data-driven modeling and learning in science and engineering." *Comptes Rendus Mecanique*, Elsevier Masson SAS, 347(11), 845–855.

Mustafidah, H., Hartati, S., Wardoyo, R., and Harjoko, A. (2014). "Selection of Most Appropriate Backpropagation Training Algorithm in Data Pattern Recognition." *International Journal of Computer Trends and Technology*,

14(2), 92–95.

Nawi, N. M., Ransing, R. S., and Ransing, M. R. (2008). "An Improved Conjugate Gradient Based Learning Algorithm for Back Propagation Neural Networks." *International Journal of Computational Intelligence*, 46–55.

O'Shea, K., and Nash, R. (2015). "An Introduction to Convolutional Neural Networks."

Oxtoby, N. P., Young, A. L., Cash, D. M., Benzinger, T. L. S., Fagan, A. M., Morris, J. C., Bateman, R. J., Fox, N. C., Schott, J. M., and Alexander, D. C. (2018). "Data-driven models of dominantly-inherited Alzheimer's disease progression." *Braina Journal of Neurology*, 1–16.

Patra, S. R., Jehadeesan, R., Rajeswari, S., and Satyamurthy, S. A. . (2010). "Artificial Neural Network Model for Intermediate Heat Exchanger of Nuclear Reactor." *International Journal of Computer Applications*, 1(26).

Perez, C. (2019). *Neural Networks Using Matlab. Cluster Analysis And Classification*. Lulu Press, Inc.

Perin, Y., and Jimenez, J. (2017). "Application of the best-estimate plus uncertainty approach on a BWR ATWS transient using the NURESIM European code platform." *Nuclear Engineering and Design*, Elsevier B.V., 321, 48–56.

Phillips-wren, G. (2018). *Intelligent Decision Support Systems*.

Puchalski, B., Rutkowski, T. A., and Duzinkiewicz, K. (2017). "Nodal models of Pressurized Water Reactor core for control purposes – A comparison study." *Nuclear Engineering and Design*, Elsevier B.V., 322, 444–463.

Radaideh, M. I., Wieselquist, W. A., Ridge, O., and Kozlowski, T. (2018). "A new framework for sampling-based uncertainty quantification of the six-group reactor kinetic parameters." *Annals of Nuclear Energy*.

Rallo, R., Arenas, A., and Giralt, F. (2002). "Neural virtual sensor for the inferential prediction of product quality from process variables." *Computers and Chemical Engineering*, 26, 1735/ 1754.

Rätz, M., Javadi, A. P., Baranski, M., Finkbeiner, K., and Müller, D. (2019). "Automated data-driven modeling of building energy systems via machine learning algorithms." *Energy & Buildings*, Elsevier B.V., 202, 109384.

Romojaro, P., Álvarez-Velarde, F., and García-Herranz, N. (2019). "Sensitivity methods for effective delayed neutron fraction and neutron generation time with summon." *Annals of Nuclear Energy*, Elsevier Ltd, 126, 410–418.

Sánchez, A. I., Villanueva, J. F., Carlos, S., and Martorell, S. (2018). "Uncertainty analysis of a large break loss of coolant accident in a pressurized water reactor using non-parametric methods." *Reliability Engineering and System Safety*, Elsevier Ltd, 174, 19–28.

Setiono, R., and Hui, L. C. K. (1995). "Use of a Quasi-Newton Method in a

Feedforward Neural Network Construction Algorithm." *IEEE Transactions on Neural Networks*, 6(1), 0–4.

Sharma, B., and Venugopalan, P. K. (2014). "Comparison of Neural Network Training Functions for Hematoma Classification in Brain CT Images." *IOSR Journal of Computer Engineering*, 16(1), 31–35.

Solomatine, D., and Ostfeld, A. (2008). "Data-Driven Modelling: Some Past Experiences and New Approaches approaches." *Journal of Hydroinformatics*, 10(1).

Sug, H. (2010). "The Effect of Training Set Size for the Performance of Neural Networks of Classification." *WSEAS Transactions on Computers*, 9(11), 1297–1306.

Tamimi, N., Samani, S., Minaei, M., and Harirchi, F. (2019). "An Artificial Intelligence Decision Support System for Unconventional Field Development Design." (2015).

Thakkar, J. G. (1975). "Correlation of Theory and Experiment for the Dynamics of a Pressurized Water Reactor." University of Tennessee.

Uhrig, R. E. (1993). "Use of neural networks in nuclear power plants." *ISA Transactions*, 32, 139–145.

U.S. NRC. (2017). *Acceptance criteria for emergency core cooling systems for light-water nuclear power reactors*.

Varuttamaseni, A. (2011). “Bayesian Network Representing System Dynamics in Risk Analysis of Nuclear Systems.” Ph.D. Thesis, University of Michigan.

Xu, S., and Chen, L. (2008). “A Novel Approach for Determining the Optimal Number of Hidden Layer Neurons for FNN’s and Its Application in Data Mining.” *5th International Conference on Information Technology and Applications*, 683–686.

Zhang, J., Wang, F., Wang, K., Lin, W., Xu, X., and Chen, C. (2011). “Data-Driven Intelligent Transportation Systems : A Survey.” *IEEE Transactions on Intelligent Transportation Systems*, 12(4), 1624–1639.

Zimmerman, S. G., Brittingham, J. C., Reed, M. L., Bandera, R. P., and Crawley, P. F. (1999). *PWR Reactor Physics Methodology Using CASMO-4/SIMULATE-3*. Arizona Public Service Company.

Table 5-1 Different transients employed in the present study

Transient description	Max.	Min.	Increment
Transient 1: Changing the reactivity	-0.006	+0.006	0.0015
Transient 2: Changing the steam generator-steam valve coefficient	-20%	+20%	5%
Transient 3: Changing the reactor core inlet temperature	-20^{o}F	+20^{o}F	5^{o}F
Transient 4: Changing the steam generator inlet temperature	-20^{o}F	+20^{o}F	5^{o}F

Table 5-2 Results of the PWR-NN for different training function

Algorithm	Training function	Description	n_h	Average number of epochs	R (T_f)	R (P_s)	*MSE* (T_f) $^oF^2$	*MSE* (P_s) psi^2	CPU time (s)
Gradient Descent	*traingd*	Gradient descent back propagation	did not converge						
	traingdm	Gradient descent with momentum back propagation	did not converge						
	trainrp	Resilient back propagation	4	879	0.9854	0.9985	201	22	11
			8	894	0.9886	0.9989	157	16	13
			11	904	0.9893	0.9991	147	14	15
Conjugate Gradient	*trainscg*	Scaled conjugate gradient back propagation	4	276	0.9844	0.9990	215	15	6
			8	303	0.9876	0.9991	171	13	8
			11	301	0.9881	0.9991	164	13	9
	traincgp	Conjugate gradient back propagation with Polak-Ribiére updates	4	270	0.9843	0.9991	217	14	12
			8	294	0.9874	0.9992	174	12	15
			11	332	0.9884	0.9992	159	12	21
	traincgf		4	264	0.9851	0.9991	206	13	12

		Conjugate gradient back propagation with Fletcher-Reeves updates	8	389	0.9892	0.9994	150	9	20
			11	431	0.9900	0.9994	138	8	28
Quasi-Newton	*trainbfg*	Broyden-Fletcher-Goldfarb- Shanno (BFGS) quasi-Newton back propagation	4	1000	0.9797	0.9949	279	77	65
			8	1000	0.9777	0.9926	306	112	78
			11	1000	0.9783	0.9937	298	95	95
	trainlm	Levenberg-Marquardt back propagation	4	265	0.9904	0.9995	132	7	17
			8	250	0.9934	0.9996	91	5	22
			11	336	**0.9940**	**0.9997**	**83**	**4**	38

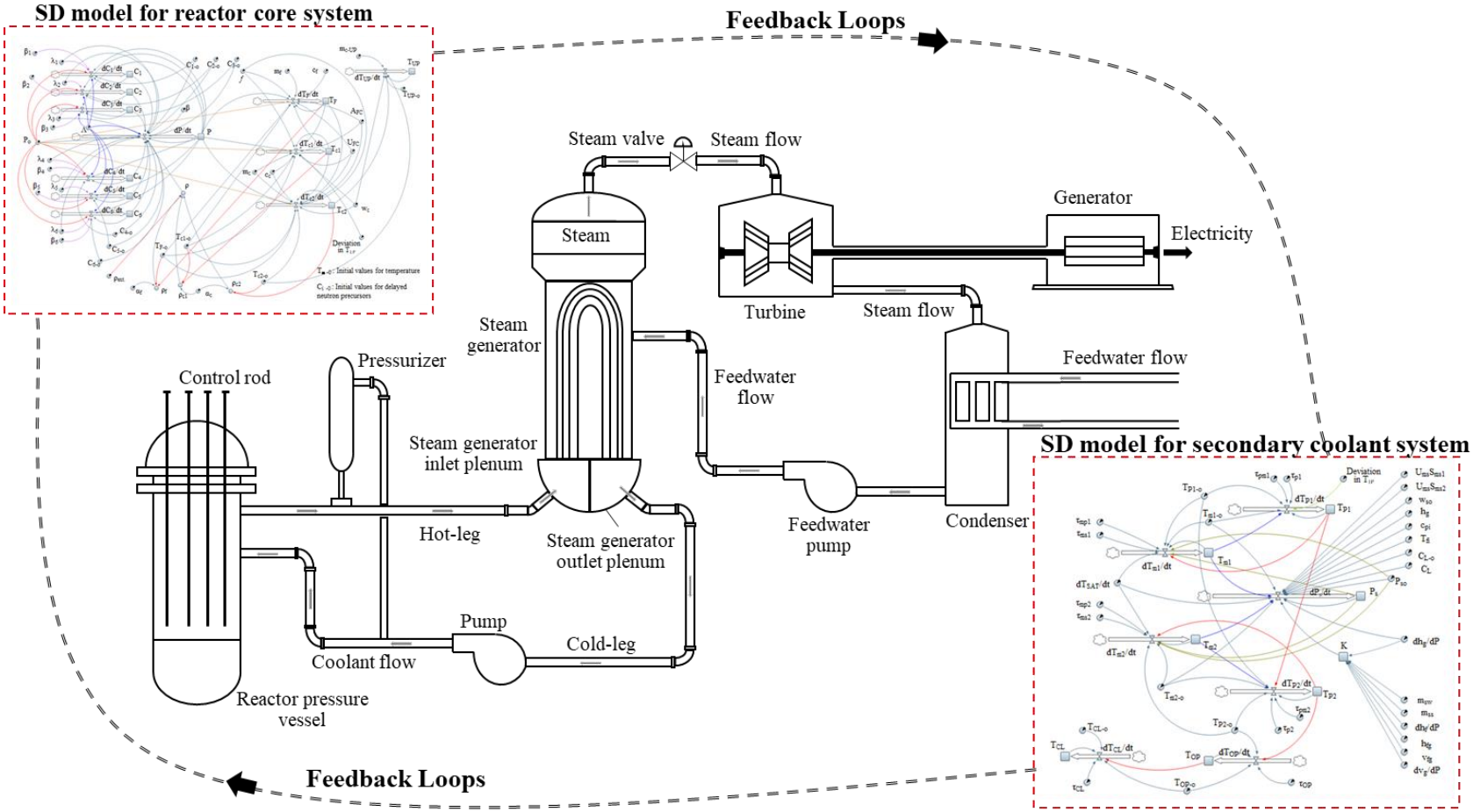

Figure 5-1: Schematic diagram of a typical PWR (El-Sefy et al. 2019).

a.

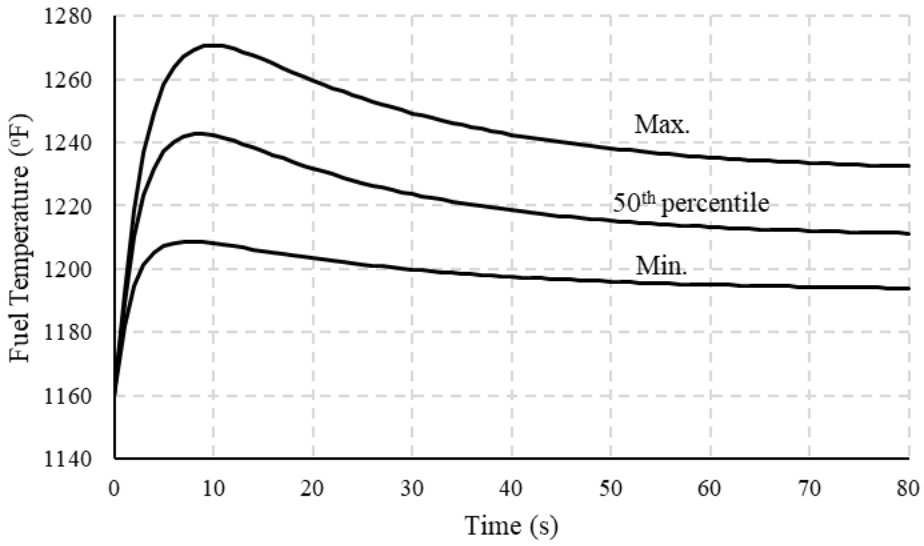

b.

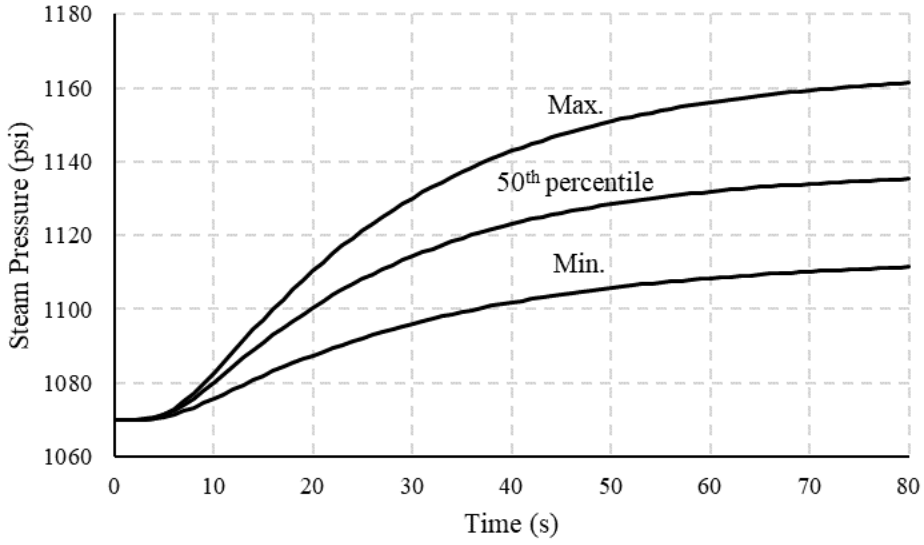

Figure 5-2: **a.** Sample of SD estimates of T_f due to reactivity transient of +0.0015. **b.** Sample of SD estimates of P_s at the same transient level.

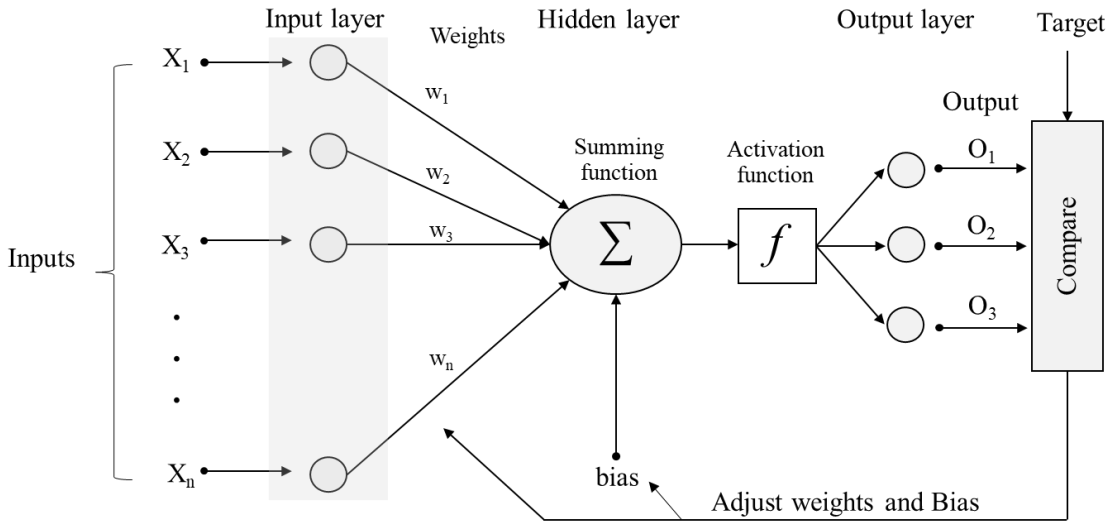

Figure 5-3: Schematic diagram of the feed forward back propagation neural network with single hidden layer.

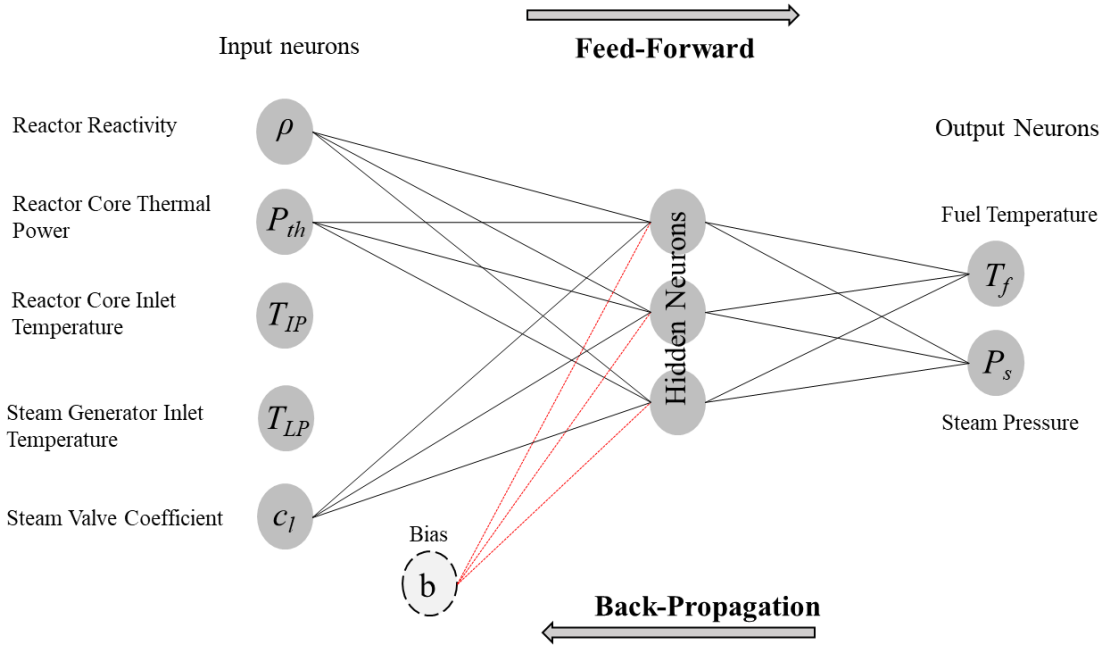

Figure 5-4: Schematic Diagram of ANN employed in the present study to simulate the dynamic behavior of a PWR.

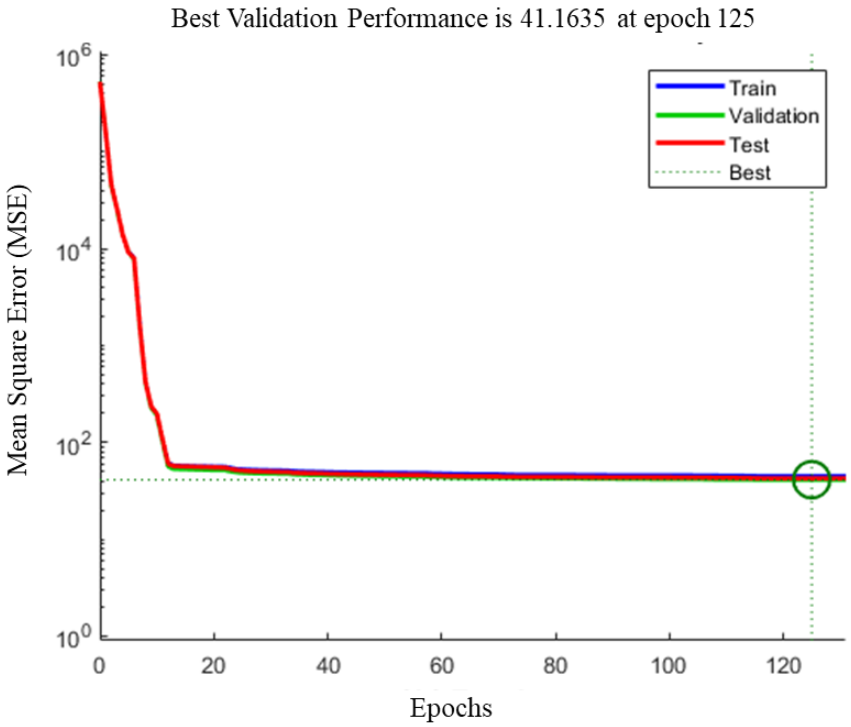

Figure 5-5: MSE values under the *trainlm* training function and over the different training iterations.

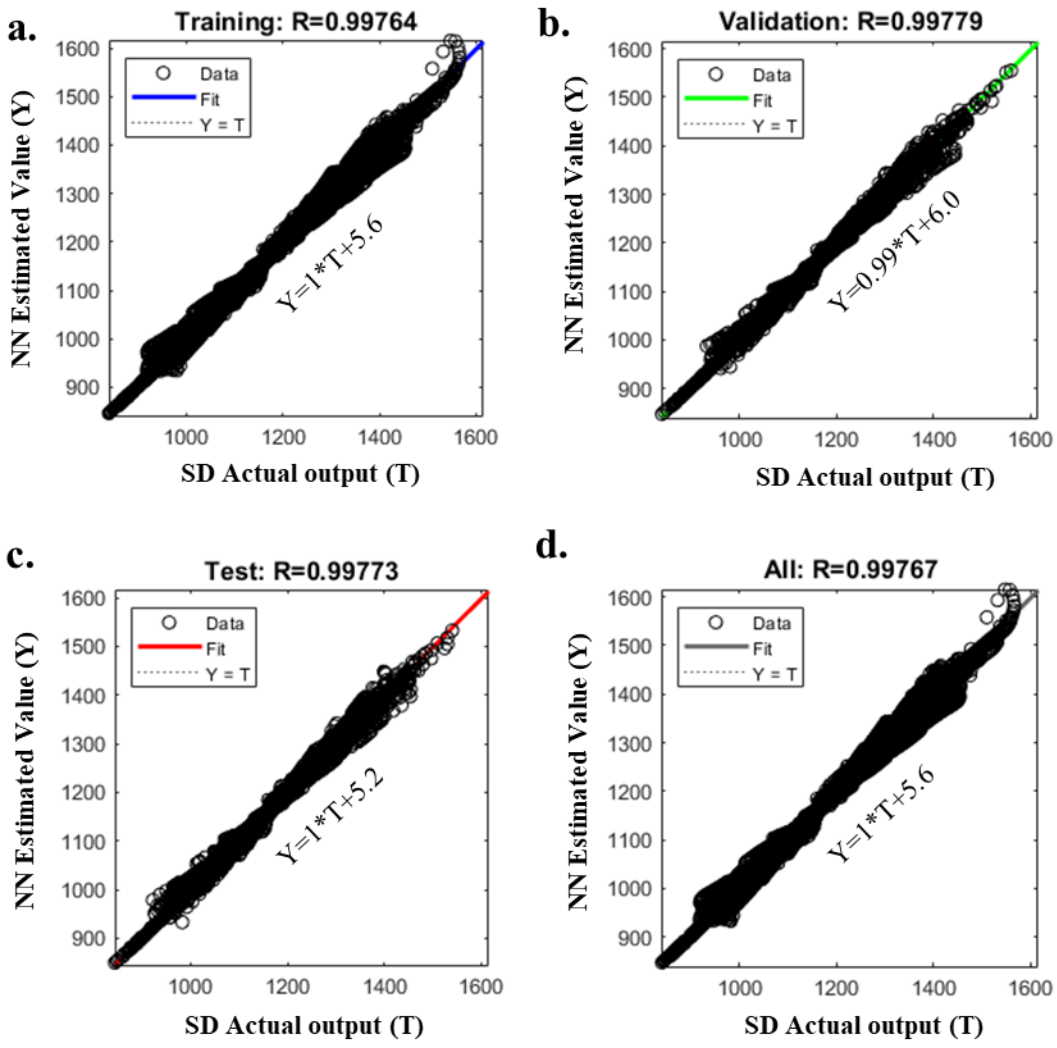

Figure 5-6: Regression values of the ANN with 11 hidden layer neurons under the *trainlm* training function for: **a.** Training subset, **b.** Validation subset, **c.** Testing subset, and **d.** All subsets combined together.

a.

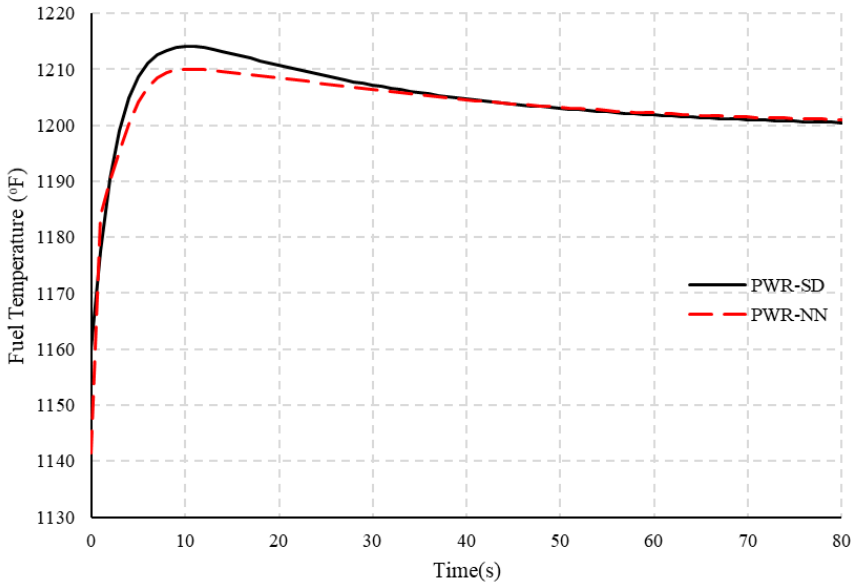

b.

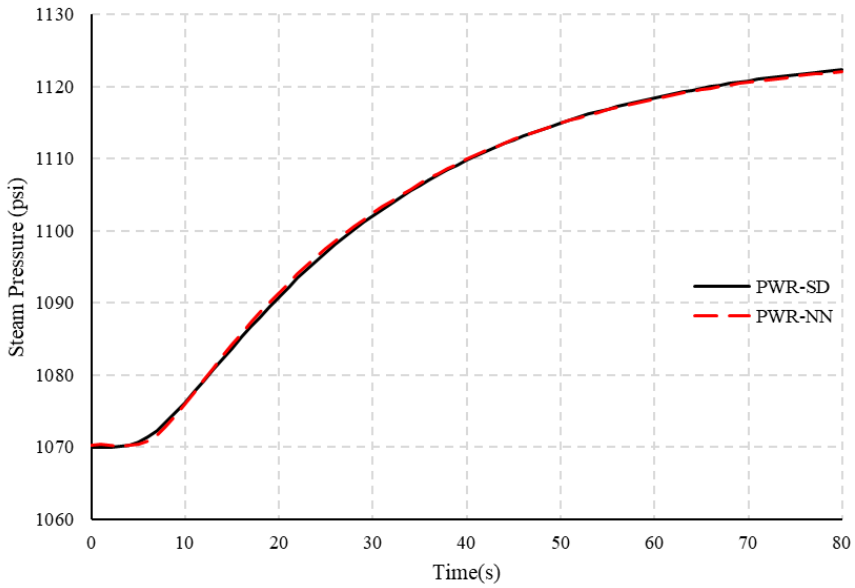

Figure 5-7: **a.** Comparison between NN prediction and SD estimate of fuel temperature due to an increase in reactivity level by +0.001 (Transient 1). **b.** Comparison between NN prediction and SD estimate of steam pressure at the same transient level.

a.

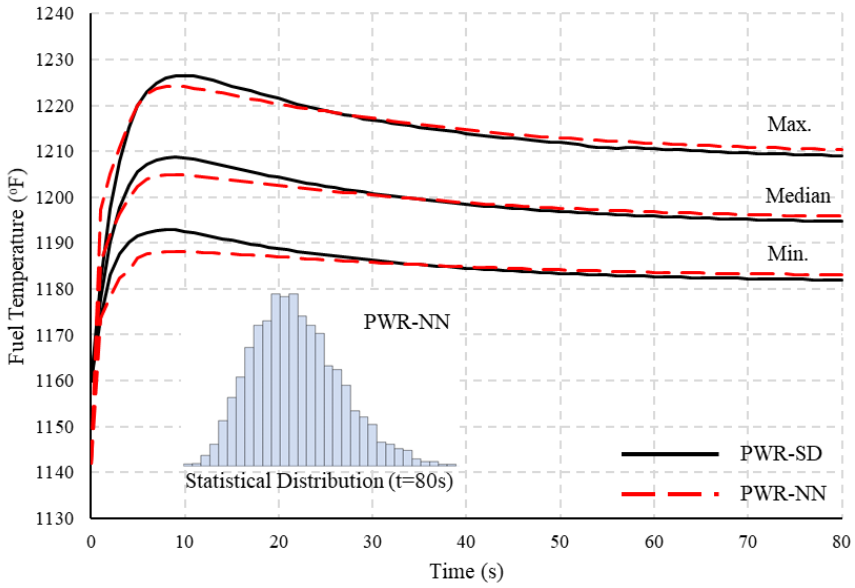

b.

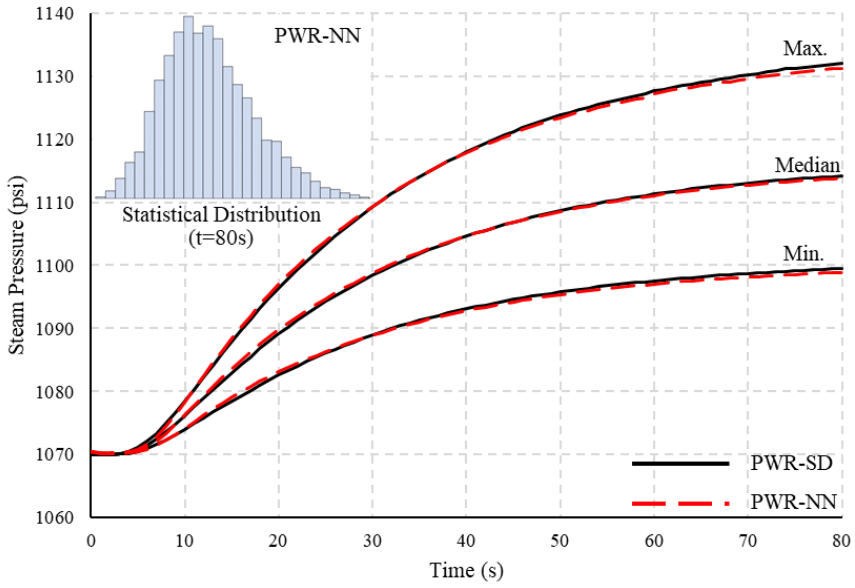

Figure 5-8: **a.** Comparison between NN predictions and SD estimates of uncertain fuel temperature due an increase in reactivity level by +0.001 (Transient 2). **b.** Comparison between NN predictions and SD estimates of uncertain steam pressure at the same transient level.

a.

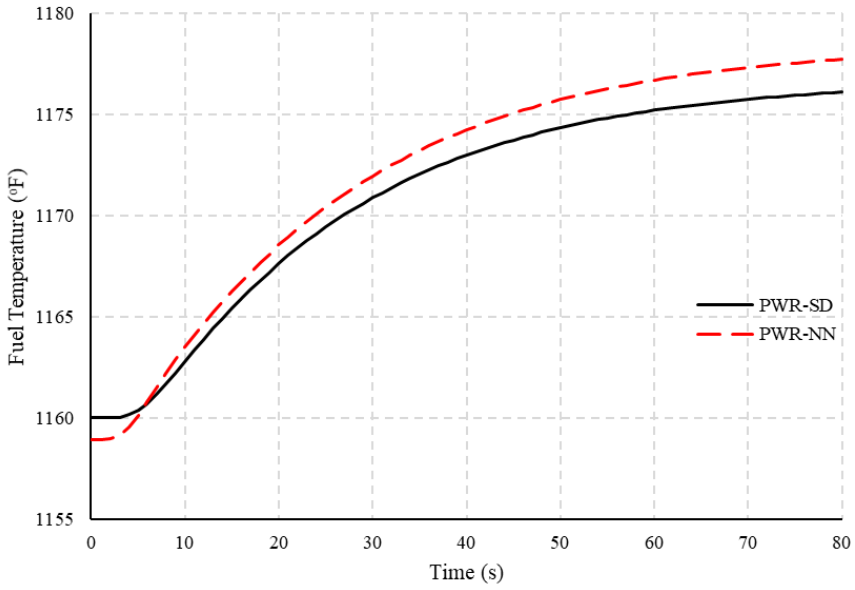

b.

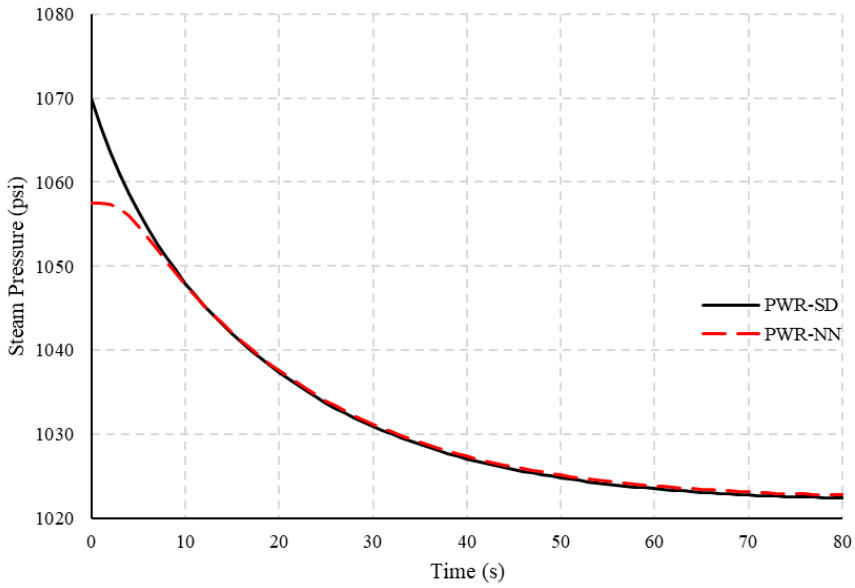

Figure 5-9: **a.** Comparison between NN prediction and SD estimate of fuel temperature due to an increase in steam valve coefficient by +7.5% (Transient 3). **b.** Comparison between NN prediction and SD estimate of steam pressure at the same transient level.

a.

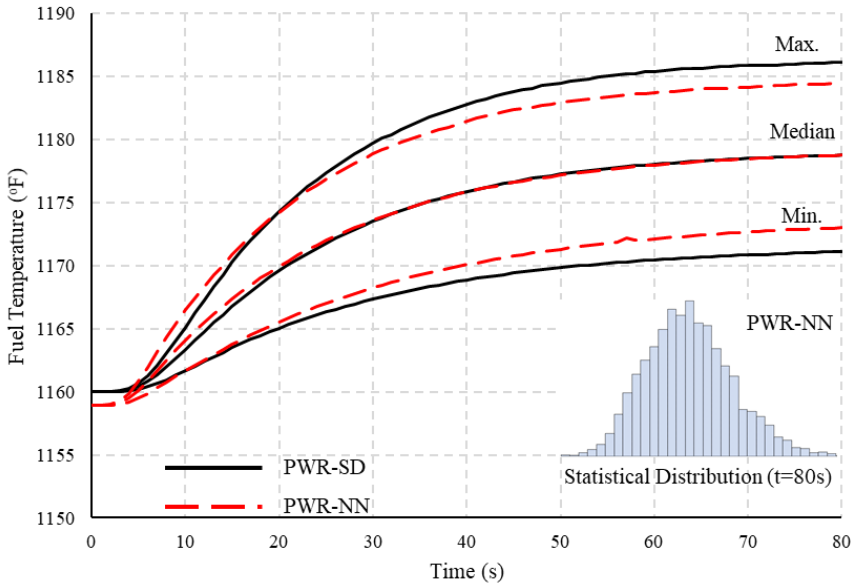

b.

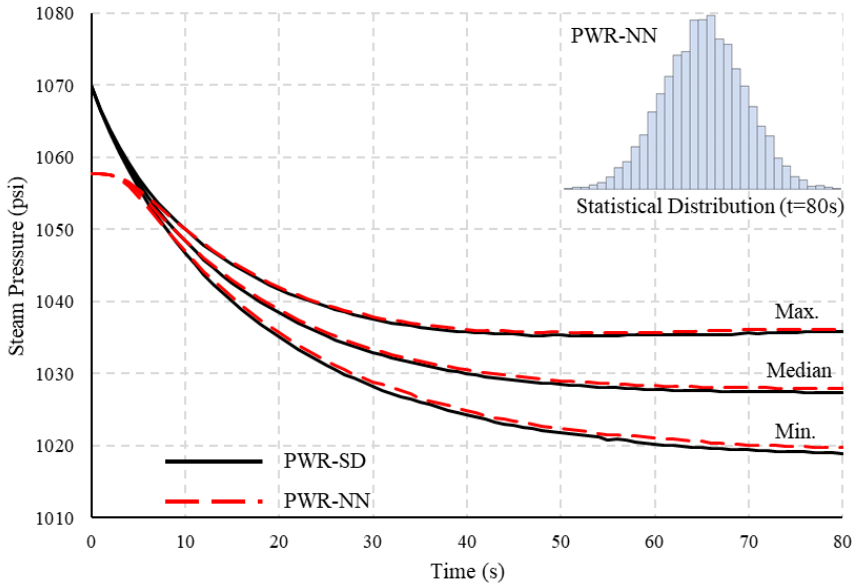

Figure 5-10: **a.** Comparison between NN predictions and SD estimates of uncertain fuel temperature due to an increase in steam valve coefficient by +7.5% (Transient 4). **b.** Comparison between NN predictions and SD estimates of uncertain steam pressure at the same transient level.

a.

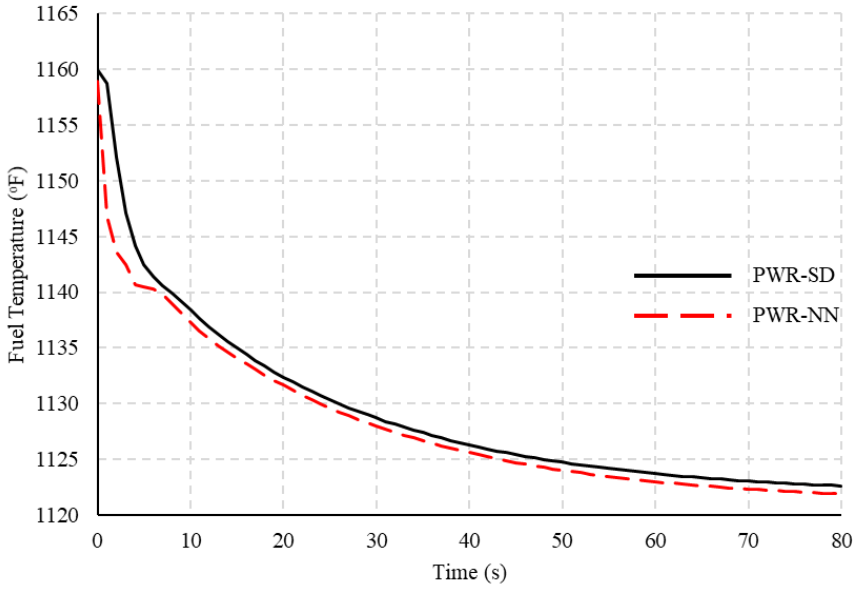

b.

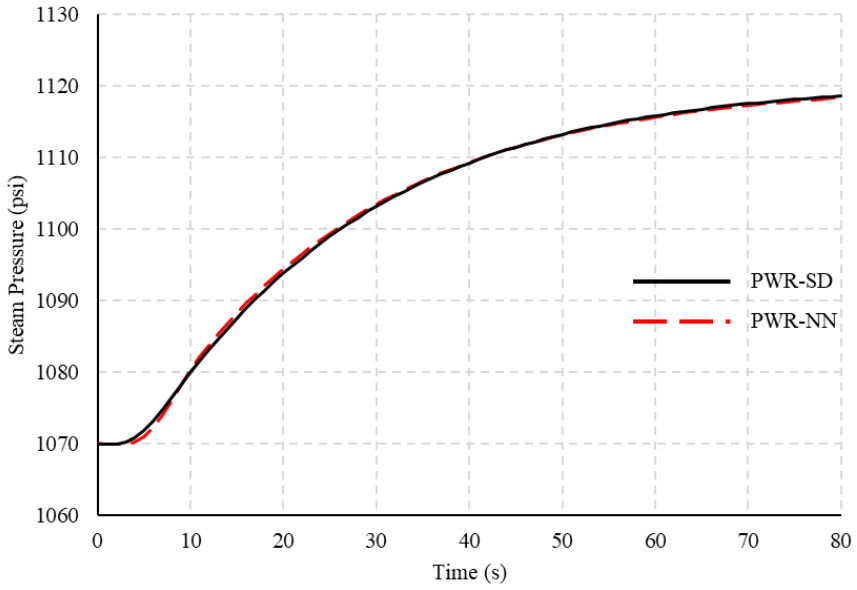

Figure 5-11: **a.** Comparison between NN prediction and SD estimate of fuel temperature due to an increase in the reactor core inlet temperature by +7.5°F (Transient 5). **b.** Comparison between NN prediction and SD estimate of steam pressure at the same transient level.

Chapter 6 : SUMMARY, CONCLUSIONS, AND RECOMMENDATIONS

6.1. SUMMARY

The overarching goals of this dissertation were to enhance the safety of nuclear power plants (**NPPs**) and overcome the challenges facing the existing DPRA approach through developing a physics-based system dynamics (**SD**) platform for dynamic probabilistic risk assessment (**DPRA**) of NPPs, as well as a data-driven early warning decision tool to empower rapid emergency response planning and risk mitigation strategies. As a first step in this endeavour, Latent Dirichlet Allocation (**LDA**) topic modelling and N-Gram text classification were utilized to identify the main trends in the current DPRA methodologies based on a total of 387 articles published in 50 different journals and conferences between 1981 and 2019. The evolution of DPRA simulation and graphical methodologies were accordingly presented and discussed. A qualitative literature review was subsequently performed to identify the main challenges facing current DPRA approaches.

Next, SD was utilized to deterministically simulate the dynamic interaction between the large and complex systems of a pressurized water reactor (**PWR**). In this respect, the developed model was used to simulate the thermal dynamics processes between different PWR systems. The model was validated using previously published results and was then used to predict system response under new reactor core and secondary coolant system transients.

The probabilistic nature of the PWR system parameters was subsequently coupled with the developed SD model, resulting in a DPRA platform, by considering the uncertainties associated with the plant's physical parameters and operating conditions. The DPRA platform was developed by integrating both the SD simulation technique and Monte Carlo simulations in conjunction with a triangular probability density function for the average fuel temperature in order to estimate the temporal probability of core damage. In this respect, the statistical behavior of 26 behavior governing parameters was represented by normal distributions, whereas seven other parameters were conservatively assumed to follow uniform distributions. The developed DPRA platform was subsequently used to estimate the temporal changes in fuel temperature and the probability of core damage under different transients considering the uncertainties of the PWR system. Moreover, a global sensitivity analysis was carried out to determine the parameters that significantly impact the average fuel temperature.

Finally, an artificial neural network (**ANN**) was developed to predict the nonlinear dynamic behavior of the critical PWR parameters (i.e., average fuel temperature and steam pressure of secondary cooling systems) in a fast, accurate, and intelligent fashion in order to avoid the computational overburden of physics-based models. The developed ANN was trained using a real-time dataset corresponding to 32 different transients and was subsequently tested under new

transients in order to evaluate its efficacy in predicting the response of the PWR system.

6.2. CONCLUSIONS AND CONTRIBUTIONS

The research in the present dissertation introduced a physics-based simulation platform for NPP DPRA that considers the dynamic interactions between large complex systems inside the NPP. The developed DPRA platform has the capability of simulating the complex feedback mechanisms among different systems including the reactor core, primary and secondary cooling systems, hot and cold legs, reactor core inlet and outlet plenums, and steam generator inlet and outlet plenums. In addition, this research demonstrates the ability of the developed platform to evaluate the temporal probability of core damage under different transients considering the uncertainties in the plant's physical parameters and operating conditions. Moreover, global sensitivity analysis demonstrated that the fuel coefficient of reactivity, the coolant temperature coefficient of reactivity, the heat transfer coefficient from fuel to coolant, and the total delayed neutron fraction are the primary controllers of the fuel temperature variability under the different transients considered. In summary, this research contributes to enhancing NPP safety by overcoming the challenges facing PRA approach for simulating large complex systems. In particular, the developed DPRA platform provides substantial advantages compared to current DPRA tools in terms of both computational time and data storage. Finally, this research introduced an artificial intelligence-based

early warning tool that can support the plant operators with rapid and accurate predictions of the system behavior. The developed data-driven model can accurately predict the nonlinear dynamic behavior of PWR critical parameters (i.e., average fuel temperature, steam pressure) under different transients. In addition, the statistical distributions of these parameters using ANN are compatible with the corresponding distributions from the SD simulation model (physics-based) when the uncertain system physical parameters and operating conditions are considered. The developed ANN also provides a computationally efficient alternative compared to SD models, especially when considering uncertainties. As such, the developed AI tool enables the development of effective risk mitigation strategies under unexpected operating conditions and can therefore serve as a rapid decision support system for plant operators and managers.

In light of the research findings reported in this dissertation, the following sections present the conclusions and contributions for Chapters 2 to 5.

6.2.1. CONCLUSIONS AND CONTRIBUTIONS FROM CHAPTER 2

Quantitative analysis of DPRA publications identified seven topics related to DPRA simulation and six topics related to graphical methodologies. The discrete dynamic event tree was found to be the most common approach for DPRA simulation methodologies. Afterward, qualitative literature reviews were performed to investigate the main challenges facing the DPRA approach. The main conclusions and contributions from Chapter 2 are:

- Static PRA methods have numerous limitations that can result in an inadequate assessment of the risk associated with complex dynamic systems such as NPPs.
- DPRA methodologies have a significant impact on enhancing the safety of NPPs by overcoming the limitations of static PRA methods, and there is a growing trend in the number of articles published on DPRA of NPPs because it is vital to consider the dynamic behavior of the system for risk assessment.
- Dynamic Logic Analytical Methodology (**DYLAM**), Markov/Cell-to-Cell Mapping Technique (**Markov/CCMT**), The Accident Dynamics Simulator paired with the Information, Decision, and Action in a Crew context cognitive model (**ADS-IDAC**), Monte Carlo Dynamic Event Tree (**MCDET**), Analysis of Dynamic Accident Progression Trees (**ADAPT**), and Reactor Analysis and Virtual Control Environmental (**RAVEN**) are the DPRA simulation methodologies most frequently employed in previous studies, while Go-Flow, Petri Net, dynamic fault tree, dynamic flowgraph method, extended event sequence diagram, and dynamic Bayesian network are the most frequently used DPRA graphical methodologies.
- RAVEN, ADAPT, and DBNs exhibit a growing trend in the publications related to DPRA and are considered promising methodologies for assessing the safety of dynamical systems.

- ADS-IDAC and DFM have significantly contributed to the publication of DPRA simulation and graphical methodologies, representing approximately 25% and 30% of the published articles, respectively.
- Further qualitative review highlights the limited applications of the DPRA approach in simulating large complex systems within NPPs, multi-unit risk assessment, and computational expensive of currently employed DPRA methodologies.
- The Fukushima Daiichi nuclear accident demonstrated the importance of assessing the risk of multi-unit NPPs; however, the application of DPRA in such systems is still in its infancy.
- The results from this chapter demonstrate the importance of enhancing and/or developing new DPRA tools that are capable of simulating the dynamic interaction between large complex systems within NPPs.

6.2.2. CONCLUSIONS AND CONTRIBUTIONS FROM CHAPTER 3

Three SD models were developed to simulate the thermal dynamic processes inside the reactor core, secondary coolant system, and the complete PWR system, respectively, in a deterministic way. The main conclusions and contributions from Chapter 3 are:

- The developed models were validated using the results of a previous study, and evaluated under different transients, such as adding a positive reactivity and increasing the reactor core inlet temperature.
- The developed SD models are able to simulate the nonlinear dynamic response of the PWR parameters under single and multiple transients, thereby indicating their ability to efficiently capture fluctuation in system behavior.
- The results of the SD model demonstrate the capability of the SD modelling approach to simulate the dynamic interactions between different large complex systems within the PWR.
- The developed SD model has significant advantages from both time and data storage perspectives compared to more complex NPP simulators.

6.2.3. CONCLUSIONS AND CONTRIBUTIONS FROM CHAPTER 4

Uncertainties associated with the NPP physical parameters and operating conditions were incorporated in the deterministic SD model developed in Chapter 3. The SD model is embedded within a Monte Carlo framework to enable the development of a NPP DPRA platform. The DPRA platform was subsequently used to predict the temporal probability of core damage under different transients. The main conclusions and contributions from Chapter 4 are:

- Uncertainties associated with the plant physical parameters and operating conditions significantly impact the average fuel temperature and probability of core damage.
- The developed DPRA platform is able to consider the dynamic interaction between several large systems including the reactor core, primary and secondary cooling systems, hot and cold legs, reactor core inlet and outlet plenums, and steam generator inlet and outlet plenums.
- The developed DPRA platform demonstrates the ability to assess the safety of NPPs by evaluating the temporal probability of core damage under single and multiple transients at a relatively low computational cost.
- The fuel temperature coefficient of reactivity, coolant temperature coefficient of reactivity, heat transfer coefficient from the fuel to coolant, and total delayed neutron fraction are the primary parameters governing the fuel temperature variability.
- The primary coolant mass flow has a considerable impact on the fuel temperature during the transients associated with a change in the inlet coolant temperature for either the reactor core or the secondary coolant system.

6.2.4. CONCLUSIONS AND CONTRIBUTIONS FROM CHAPTER 5

A data-driven model was developed to predict the dynamic response of the critical PWR parameters. A feed-forward backpropagation ANN model was trained based

on 32 transients to model the interaction between different systems. Eight training functions were employed during the training stage, in which the mean squared error (**MSE**) was utilized to select the most appropriate training function. The main conclusions and contributions from Chapter 5 are:

- The Levenberg-Marquardt backpropagation "*trainlm*" training function combined with eleven hidden-layer neurons showed the best performance compared to other considered training functions.
- The results of the training stage demonstrate the ability of the developed ANN model to successfully learn from the dataset despite the complex and dynamic nature of the underlying system.
- The developed ANN model was tested under new transients, including perturbations in reactivity, steam valve coefficient, and core inlet temperature. The obtained results demonstrate the capability of the developed ANN model to predict the PWR critical parameters (i.e., the average fuel temperature and steam pressure inside the secondary coolant system) with a lower computational cost compared to physics-based models.
- Uncertainties associated with the PWR system parameters are captured using the developed ANN model.
- The developed ANN model can provide the plant operators with rapid and accurate predictions of the system behavior without overburdening the model with the underlying complex physical interactions.

- The ANN-based model represents an intelligent early warning decision tool that can aid in the development of effective risk mitigation strategies under abnormal conditions, and can therefore serve as a rapid decision support system for NPP operators and managers.

6.3. RECOMMENDATIONS FOR FUTURE RESEARCH

The research presented in this dissertation contributes to DPRA simulation methods for NPPs by providing an integrated Monte Carlo-SD platform that can be employed to effectively predict the temporal probability of core damage in a PWR. Furthermore, the ANN-based model developed in this study represents an intelligent early warning decision tool that can support the plant operators with quick and accurate predictions of PWR critical parameters, which can enhance the safety of NPPs under abnormal conditions. In light of findings/results presented in this dissertation, this section presents possible research extensions that can be carried out to expand the developed DPRA simulation platform.

- The developed DPRA platform can include other PWR systems such as pressurizer, emergency coolant system, and emergency diesel generators to provide a digital twin of operational NPP.
- The SD model can be coupled with those representing external systems (e.g., power grid) in order to investigate the dynamic interaction between the PWR and such systems under natural or anthropogenic hazards.

- In light of the Fukushima Daiichi accident, DPRA of multi-unit NPPs has become more essential than ever before. The feedback loops in the SD modeling technique can simulate the dynamic interaction associated with multi-unit sites, thereby providing a comprehensive DPRA platform.
- Artificial intelligence-based techniques can be trained using real plant operation data in different systems to cover all possible operational transients and accident scenarios that can occur during NPP normal or abnormal operating conditions.